SECRETED MICRORNAS AND THEIR ROLE IN CANCER PROMOTION AND

DETECTION

by

Christopher TD Dickman

B.Sc., The University of British Columbia, 2009

M.Sc, The University of Western Ontario, 2012

A THESIS SUBMITTED IN PARTIAL FULFILLMENT OF

THE REQUIREMENTS FOR THE DEGREE OF

DOCTOR OF PHILOSOPHY

in

THE FACULTY OF GRADUATE AND POSTDOCTORAL STUDIES

(Experimental Medicine)

THE UNIVERSITY OF BRITISH COLUMBIA

(Vancouver)

April 2017

Abstract

Oral squamous cell carcinoma (OSCC) is the most common form of head and neck cancer. Although there have been improvements in detection and treatment with the development of targeted therapies, OSCC has a low five-year survival rate which has shown little improvement in recent history. OSCCs are known to secrete extracellular vesicles (EVs) into the extracellular space including into the blood stream. These EVs contain a wide variety of different molecules capable of effecting cancer processes including mRNAs, miRNAs, and proteins. By performing an in depth analysis we will gain a better understanding on how OSCC secreted miRNAs are capable of acting as messages between cancerous and stromal cells. Additionally, I have presented data on how these miRNAs can be exploited for their ability to act as biomarkers.

In this thesis I first described which miRNAs are altered in patients with oral cancer or carcinoma *in situ* and determined that this altered expression is capable of predicting cancer status. After validating the suitability of cell lines as an OSCC model, I examined if altered serum miRNAs overlap with miRNAs which are selectively secreted from oral cancer cell lines. Follow-up functional analysis was performed for miR-142-3p and it was determined that this miRNA was being secreted in order to remove it's tumor suppressive effect within the cancer cell and additionally to transfer a tumor promoting signal to endothelial cells of the tumor stroma. To confirm that this was not an isolated phenomenon I examined the function of miR-142-3p when secreted from lung cancer cells and noticed a similar effect in endothelial cells and an additional effect on fibroblasts. Effected fibroblasts underwent changes associated with wound healing and tumor promotion.

These data taken together provide a comprehensive analysis of the alterations of secreted miRNAs in OSCC and provide insight in the ability of some miRNAs to serve a dual role both

within the tumor cells and cells of the tumor stroma. It is possible these results could lead to the

creation of a diagnostic test with possible future applications to the diagnosis of oral cancer.

Preface

All research described in this thesis was conducted with the ethics approval of the University of British Columba Research Ethics Board (Certificate number: H10-02846)

Chapters 1, 3, 4, 5, and 6 were co-authored for publication. The full author lists are as follows:

A version of Chapter 1 will be published as:

Dickman, C. T. D., & Garnis, C. (In Preparation). The Role of Secreted miRNAs in Head and Neck Cancers.

I wrote and co-edited the manuscript. CG, provided guidance and co-edited the manuscript.

A version of Chapter 3 will be published as:

Dickman, C. T. D., MacLellan, S.A., Towle, R., Huang, Y., Chen, J., Poh, C. F., & Garnis, C. (Pending). The Identification and Validation of a Serum miRNA Based Biomarker for the Detection of Oral Cancer.

I wrote the manuscript, conducted most of the experiments, performed some of the data analysis and interpreted the results. SAM assisted with study design, RT assisted with data collection, YH and JC developed the statistical analysis protocol, CFP provided clinical samples and gave insight on clinical utility, CG assisted with study design, and supervised the research.

A version of Chapter 4 has been published as:

Dickman, C. T. D., Towle, R., Saini, R., & Garnis, C. (2015). Molecular Characterization of Immortalized Normal and Dysplastic Oral Cell Lines. Journal of Oral Pathology & Medicine, 44(5), 329-336.

I wrote the manuscript, conducted experiments, performed data analysis and interpreted the results. RT and RS assisted with conducting experiments, CG conceived of the project and provide supervisory insight. Permission for reprinting was obtained from John Wiley and Sons.

A version of Chapter 5 has been published as:

Dickman, C. T. D., Lawson, J., Jabalee, J., MacLellan, S. A., LePard, N. E., Bennewith, K. L., & Garnis, C. (Online ahead of print). Selective extracellular vesicle exclusion of miR-142-3p by oral cancer cells promotes both internal and extracellular malignant phenotypes. OncoTarget, DOI: 10.18632/oncotarget.14862

I wrote the manuscript, conducted most of the experiments, performed data analysis and interpreted the results. JL, JJ, SAM and NELP assisted with data collection, KLB assisted with planning *in vivo* experiments, CG assisted with planning, and interpretation of results; and provided supervision. Permission for reprinting is granted under the Creative Commons Attribution License.

A version of Chapter 6 will be published as:

Dickman, C. T. D., Lawson, J., Garnis, C. (In Preparation). Secretion of miR-142-3p in Lung Cancer Induces Angiogenesis and Fibroblast Activation.

I wrote the manuscript, conducted most of the experiments and performed data analysis. JL assisted with data collection and CG assisted with study design and provided supervision.

Table of Contents

List of Tables

List of Figures

List of Abbreviations

AUC	Area under the curve
BAC	Bacterial artificial chromosome
BCA	Bicinchoninic Acid
BCCRC	British Columbia Cancer Research Centre
BrdU	Bromodeoxyuridine
CAF	Cancer associated fibroblast
CGH	Comparative genomic hybridization
CIS	Carcinoma *in situ*
CT	Cycle threshold
CT	Computed tomography
DMEM	Dulbecco's modified Eagle's medium
DNA	Deoxyribonucleic acid
EBV	Epstein–Barr virus
ECL	Enhanced chemiluminescence
ENT	Ear, nose and throat
EV	Extracellular vesicle
FBS	Fetal bovine serum
FITC	Fluorescein isothiocyanate
FIV	Feline immunodeficiency virus
FV	Fluorescence visualization
GEO	Gene Expression Omnibus
GFP	Green fluorescent protein
HC	Healthy controls
HMEC1	Human microvascular endothelial cell 1
HNSCC	Head & neck squamous cell carcinoma
HPV	Human papillomavirus
HPV	Human papillomavirus
HRL	High-risk lesion
KEGG	Kyoto Encyclopedia of Genes and Genomes
LASSO	Least absolute shrinkage and selection operator
LMP	Low melting point
LNA	Locked nucleic acid
LNSCC	Laryngeal squamous cell carcinoma
miRNA/miR	microRNA
MRI	Magnetic resonance imaging
MTT	3-(4,5-dimethylthiazol-2-yl)-2,5-diphenyltetrazolium bromide
MV	Microvesicle
NPC	Nasopharyngeal carcinoma
NSCLC	Non-small cell lung cancer
OPSCC	Oropharyngeal squamous cell carcinoma
OSCC	Oral squamous cell carcinoma
PBS	Phosphate buffered saline
PCR	Polymerase chain reaction

PIMO	Pimonidazole
PVDF	Polyvinylidene difluoride
qRT-PCR	Quantitative real time PCR
RCF	Relative centrifugal force
RIPA	Radioimmunoprecipitation assay
RNA	Ribonucleic acid
ROC	Receiver operating characteristic
RPMI	Roswell Park Memorial Institute
SEV	Small extracellular vesicle
SCC	Squamous cell carcinoma
SCID	Severe combined immunodeficiency
SMRT	Sub-megabase resolution tiling
SST	Serum-separating tube
SV40T	Simian Vacuolating Virus 40 large T antigen
TCGA	The Cancer Genome Atlas
TEM	Transmission electron microscopy
TGFBR1	Transforming growth factor beta receptor I

Acknowledgements

I would like to offer my enduring thanks to all those who have supported me during my research at UBC.

Cathie Garnis, deserves a special acknowledgement for her guidance and advice, and giving me the opportunity to study in her lab. I am also grateful to my supervisory committee members, Dr. Catherine Poh, and Dr. Calum MacAulay who have provided great assistance and invaluable insight into my project.

I would also like to thank the past and present members of the Garnis lab, all of whom have provided useful insights and constructive edits to this thesis. I would also like to thank my colleagues at the British Columbia Cancer Research Center, and the Experimental Medicine Program.

This work would not have been possible without generous funding from the Canadian Institutes of Health Research, and the Pacific Otolaryngology Foundation.

Dedication

I dedicate this thesis to my family

Chapter 1: Introduction

Epithelial tissues, line the external surfaces of the body as well as internal cavities, and tubes (1). Epithelial cells generally take the shape of squamous, columnar or cuboidal cells, arranged into stratified layers with cell junctions connecting cells (1). Epithelial cells are separated from blood vessels and other tissues by basement membrane (1). The term carcinoma refers to cancer deriving from epithelium, and results when a mass of neoplastic cells penetrate the basement membrane.

Prior to the development of an invasive carcinoma, cells transform along a spectrum of normal to cancerous tissue with initial low grade alterations being referred to as hyperplasia characterized by an increase in cells with a normal morphology (2). Intermediate alterations are referred to as dysplasia and involve alterations to cell morphology where as advanced alterations to morphology involving the full thickness of the epithelium are referred to as carcinoma *in situ* (CIS), which is usually, considered a precancerous lesion as there is no invasion (2). CIS progresses to carcinoma when the cells are no longer constrained by the basement membrane, which may involve invasion of nearby and distant tissues (2).

Worldwide there are over half a million new cases of head and neck squamous cell carcinoma (HNSCC) reported annually with the highest incidence in Southern and Eastern Asia (3). HNSCC consists of cancers in the oral cavity as well as less common sites such as the oropharynx, nasopharynx, hypopharynx, larynx and the trachea. The primary modifiable risk factors are tobacco and alcohol use as well as HPV infection (3). On aggregate, individuals with HNSCC have a poor outcome, especially in individuals with HPV negative tumors, with two-year survival rates of ~58%. This is partially due to the high rate of recurrence and late stage at diagnosis (4). HPV positive HNSCC cases in the oropharynx have a much better survival rate of

~94% with progression free survival at ~85% (4). This effect however is site specific with HPV being a positive prognostic indicator in the oropharynx yet a negative indicator in the oral cavity (5). Outcomes for all HNSCC cases, regardless of etiology, are substantially improved by early diagnosis especially if detection is made at the precancerous stage (6). Interventions such as targeted therapies have enhanced the efficacy of cancer treatment and improved cancer patient survival, building on successes from standard care involving surgery, radiation, and chemotherapy. Nonetheless, there remains a clear need to develop new approaches for treating this disease. Additional knowledge of HNSCC cancer biology is needed to identify new druggable tumor cell processes.

MiRNAs are ~22bp non coding RNAs capable of regulating the expression of protein coding genes and are highly deregulated in a wide variety of cancer types including HNSCC (7). In recent years there has been substantial interest on miRNAs secreted from cancer cells into the extracellular space, where the miRNAs can be found in the blood as well as saliva (7-10). The excreted miRNAs are believed to be released from cancer cells via extracellular vesicles (EVs) as well as a part of protein and lipoprotein complexes (10-12). It remains unclear what proportion of miRNAs are secreted via each pathway. Some groups have proposed that the vast majority of miRNAs are encapsulated within EVs (10) while others have found the opposite and shown that most miRNAs are associated with circulating proteins (11,12).

Initially the discovery of nucleotides in the extracellular space was thought to be debris from the cell. However, some sequences of RNAs were shown to have higher concentration in vesicles than in cells leading to the belief that secretion could be selective (13). Many of the EV enriched RNAs have been shown to have a biological role and can have their function transferred from one cell to another (14). Particular interest has been given towards secreted miRNAs which

have tissue specific function, and are capable of inhibiting the translation of a wide variety of genes (15). There has been interest into the functional role these miRNAs may have in promoting or inhibiting cancer. MiRNAs secreted by tumors have been found to induce angiogenesis (16), inhibit immune cell activity (17) and prime pre-metastatic niches (18).

There has also been great interest in the use of circulating miRNAs, i.e. secreted miRNAs present in the blood, as biomarkers as circulating miRNAs are protected from degradation in the blood. When synthetic miRNA is added to the blood it is rapidly degraded due to the presence of RNase enzymes (19); however native miRNA is not, due to its associations with EVs and protein complexes (20). Secreted miRNAs have been reported as potential biomarkers in several cancer types (21-23), including HNSCC.

Herein is an overview of the known roles that secreted miRNAs play in HNSCC. We discussed the current state of biomarker research in HNSCC, looking at both blood and saliva based markers. Diagnostic and non-diagnostic biomarkers will be mentioned. We then presented what is known about the functional role that these secreted miRNAs play, and how they affect HNSCC oncogenicity.

1.1   Isolation and Quantification of Secreted miRNAs

The majority of biomarker research on secreted miRNAs examines miRNA isolated from whole saliva, serum or plasma. When performing functional analysis on secreted miRNAs, it is common to isolate EVs from serum or plasma, and to a lesser extent saliva (24-26). Whole blood is rarely used in either context due to the presence of miRNAs from the blood cells themselves. If the researcher desires to examine blood or salivary EVs in isolation they will generally be isolated by centrifugation or commercially available reagents (27). Further purification may be

3

performed to isolate sub populations of vesicles such as exosomes or microvesicles and remove

non-vesicular contaminants. This can be done using sucrose gradient separation or antibody

based methods (28). Circulating miRNAs, may be associated with proteins such as Ago2 as well

as lipoproteins which may be isolated using chromatography or immunoprecipitation (11).

Follow up analysis may be performed on miRNAs secreted into cell culture medium. After

selecting which fluid and EV isolation procedures are appropriate miRNAs can be extracted

from samples using phenol or spin column based methods, which may lead to variation in the

quantities of miRNAs extracted (29). After isolation by either phenol or spin column based

methods, of which there are several, miRNAs are generally quantified using standard methods

such as qRT-PCR, nanostring n-counter, microarray or sequencing. Due to the balance of cost,

accuracy, and throughput, the most common method used to search for miRNA biomarkers is an

initial screen using microarrays, then performing verification analysis to confirm that identified

miRNAs remain differentially expressed using qRT-PCR, as it is a more precise method (30).

The selection of a sample type as well as the quantification method may lead to differences in the

observed miRNAs.

1.2   MiRNAs as Biomarkers

1.2.1   Diagnostic Biomarkers

1.2.1.1   Salivary miRNAs

Salivary miRNAs have been found in EVs as well as a component of desquamated

epithelial cells (31), and collection methods aimed at detecting desquamated cells may show

similar miRNA levels when compared to standard saliva collection as was shown by Wiklund *et

al.*'s comparison of miR-375 and miR-200a-3p in the saliva and oral rinse (with cells) of OSCC

patients (32). Due to the direct contact between the oral cavity and saliva the majority of research on salivary miRNAs has focused on OSCC (Table 1.1). This is based upon the assumption that any cancer associated salivary miRNA originates from tumors in direct contact with the saliva. There is however potential for other cancers of the head and neck, which are not in direct contact with the saliva, to alter salivary miRNAs, as the miRNAs may be secreted into the blood stream causing alterations to miRNA releasing cells in the salivary glands as was seen with cancers as distant as the pancreas (33).

Table 1.1 Overview of salivary miRNA biomarker studies

References	Sample Type	Patients	Technique	miRNAs	AUC
(34)	Saliva	50 OSCC 50 HC	qRT-PCR array with select miRNA qRT-PCR verification	miR-200a-3p	0.65
				miR-125a-5p	0.62
(35)	Saliva	20 OSCC 40 PMD 20 RAS 20 HC	qRT-PCR with miRNAs chosen from literature	miR-21-5p	0.73 (OSCC vs HC)
				miR-145-5p	0.68 (OSCC vs HC)
				miR-184	0.86 (OSCC vs HC)
(36)	Saliva	9 OSCC 8 Remission 8 OLP 9 HC	Nanostring array with qRT-PCR verification	miR-27b-3p	0.96 (OSCC vs HC) 0.88 (OSCC vs Remission) 0.98 (OSCC vs OLP)
				miR-136-5p	0.97 (OSCC vs HC) 0.90 (OSCC vs Remission)
(37)	Saliva	45 OSCC 10 Leukoplakia 24 HC	qRT-PCR with miRNAs chosen from literature	miR-31-5p	0.82 (OSCC vs HC) 0.71 (OSCC pre-op vs post op)
(38)	Saliva	61 HNSCC 61 HC	qRT-PCR array with select miRNA qRT-PCR verification	miR-191-5p	0.98
				miR-134-5p	0.74
				miR-9-5p	0.85
(32)	Oral Rinse and Saliva	15 OSCC 7 HC	qRT-PCR with miRNAs chosen from tissue analysis	miR-375, miR-200a-3p	NA
(39)	Saliva	30 OSCC 20 HC	qRT-PCR with miRNAs chosen from literature	miR-31-5p	NA
(40)	Saliva	25 OSCC 25 HC	Microarray with qRT-PCR verification	miR-139-5p	0.81

HC: healthy controls, PMD: potentially malignant disease, RAS: recurrent aphthous stomatitis, OLP: oral lichen planus

In 2010 Park *et al.* profiled the saliva of 12 healthy controls (HCs) for 314 miRNAs using qRT-PCR to determine which miRNAs were highly expressed. This led to the creation of a smaller panel of 4 miRNAs to analyze between oral squamous cell carcinoma (OSCC) and HC samples, and it was discovered that miR-200a-3p and miR-125a-5p were down regulated, with ROC analysis showing an AUC of 0.65 and 0.62 respectively (34). A similar design of using a large initial screen was attempted by Salazar *et al.* whereby a panel of 84 miRNAs was used as an initial screen on 2 samples with saliva combined from 5 HNSCC patients or 5 HCs. This led to the selection of 5 miRNAs for analysis on the remaining samples, ultimately leading to the identification of miR-191-5p as a candidate miRNA with an AUC of 0.98. This is the highest AUC of the experiments we examined, however it is concerning in light of the fact that other researchers have reported that miR-191-5p is consistent across salivary samples, to the point that it can be used as an endogenous control (32,36).

 The largest initial screen was performed by Duz *et al.* who utilized a microarray containing a larger set of 2006 probes including miRNAs that are generally less reported in the literature. These researchers however ended up selecting the commonly reported miR-139-5p (40) as a candidate biomarker in patients with tongue squamous cell carcinoma.

Nanostring n-counter can also be used as an initial screen as demonstrated by Momen-Heravi *et al.* examining 700 miRNAs in 32 samples, this study then performed qRT-PCR verification on the same initial samples, as a 'validation' albeit not on an independent test set. This method led to the discovery that salivary miR-27b-3p was capable of differentiating between not only OSCC and HCs but also between OSCC and oral lichen planus; and individuals with OSCC from former OSCC patients in remission (36). Other researchers have also gone beyond comparisons between individuals with and without cancer and miR-21-5p, a

7

commonly reported oncomiR (41-43) is also capable of differentiating between healthy

individuals and individuals with dysplastic and non-dysplastic pre-malignant lesions. Mir-21-5p

however is not capable of differentiating HCs from individuals with non-cancer related diseases

such as recurrent aphthous stomatitis (RAS) (35). In a similar fashion researchers reported that

that miR-31-5p could differentiate between OSSC and leukoplakia or OSSC and HC, but not

leukoplakia and HC (37,39).

1.2.1.2   Circulating miRNAs

The majority of research on circulating miRNAs in has been performed using plasma

(7,44-52), with fewer studies utilizing serum (8,53) as shown in Table 1.2. This is despite reports

that miRNA quantification is more reproducible in serum (54), possibly due to incomplete

sequestering of the platelets to the buffy coat (55). There has been comparatively limited focus

on whole blood (56). Measurements of circulating miRNAs in individuals with HNSCC began in

2008 when the plasma of 30 patients with OSCC and 38 controls were profiled for miR-184

using qRT-PCR after it was determined the miRNA was deregulated in OSCC tissue. The

miRNA was found to be significantly different in the plasma of OSCC patients with the levels

returning to normal after treatment (57).

Table 1.2 Overview of circulating miRNA biomarker studies

References	Sample Type	Patients	Technique	miRNAs	AUC
(57)	Plasma	30 OSCC; 38 HC	qRT-PCR with miRNAs chosen from tissue analysis	miR-184	NA
(7)	Plasma	33 OSCC; 10 HC	qRT-PCR with miRNAs chosen from tissue analysis	miR-24-3p	0.82
(44)	Plasma	43 OSCC; 21 HC	qRT-PCR with miRNAs chosen from literature	miR-31-5p	0.82
(45)	Plasma	39 OSCC; 12 HC	qRT-PCR with miRNAs chosen from literature	miR-181a-5p, miR-181b-5p	0.89
(46)	Plasma	54 OSCC; 31 HC; 7 PMD	qRT-PCR with miRNAs chosen from cell line analysis	miR-10b-5p	0.93 (OSCC vs HC) 0.96 (PMD vs HC)
(53)	Serum	160 NPC; 143 HC	qRT-PCR array with select miRNA qRT-PCR verification	miR-17-5p, miR-20a-5p, miR-29c-3p, miR-223-3p	NA
(8)	Serum	16 OSCC; 14 *CIS*; 26 HC	qRT-PCR array	miR-338-3p	0.82
				miR-29a-3p	0.82
				miR-223-3p	0.81
				miR-16-5p	0.84
				Let-7b-5p	0.82
(47)	plasma	217 NPC 73 NPI	qRT-PCR with miRNAs chosen from literature	miR-21-5p, miR-24-3p, miR-155-5p, miR-378-3p	0.91
(48)	plasma	90 OSCC; 16 PMD 53 HC	qRT-PCR with miRNAs chosen from cell line analysis	miR-196a-5p; miR-196b-5p	0.96 (OSCC vs HC) 0.85 (PMD vs HC)
(49)	plasma	20 LSCC; 44 HC	qRT-PCR array	miR-331-3p; miR-603; miR-1303, miR-660-5p, miR-212-3p	NA
(50)	plasma	89 NPC; 18 Other Cancer; 28 HC	qRT-PCR with miRNAs chosen from cell line analysis	miR-BART7-3p; miR-BART13-3p	0.9
(51)	plasma	31 OSCC 31 HC	Microarray with qRT-PCR verification	miR-223-3p	0.73
(52)	plasma	50 HNSCC; 36 HC	qRT-PCR with miRNAs chosen from literature	miR-21-5p	NA
(56)	blood	57 OSCC; 33 HC	Microarray with qRT-PCR verification	miR-186-5p	0.69
				miR-3651	0.72
				miR-494-3p	0.82

NPI: nasopharyngitis, *CIS*: carcinoma *in situ*, LSCC: laryngeal squamous cell carcinoma

Subsequent studies have attempted to ascertain the predictive value of circulating miRNA deregulation. For example, Researchers' noticed that miR-24-3p, miR-181a-5p and miR-181b-5p were increased in the tissue of patients with OSCC, and it was theorized that these miRNAs act on p57 and other unknown genes to increase cancer cell growth, invasion and migration. The authors then examined the concentration of these miRNAs in the plasma, noticing an increase, that was believed to be a passive consequence of increased cellular concentration rather than selective secretion (7,45). Similarly Liu *et al.* chose miR-31-5p as a potential candidate biomarker in OSSC from literature reports demonstrating its increased expression in the tissue of several cancers types, with qRT-PCR profiling showing an AUC of 0.82 (44). These tissue based approaches for selecting miRNAs to analyze are in contrast to Tachibana *et al.*'s use of a microarray for an initial screen of plasma miRNAs, ultimately leading to discovery of miR-223-3p as a single qRT-PCR based marker for verification analysis (51), which had a lower AUC of 0.73 despite the greater number to miRNAs to choose from.

The majority of research in OSCC examined the different miRNA profiles between healthy individuals and those with cancer. After conducting an examination of cell lines and xenografts, Lu *et al.* noticed that miR-10b-5p levels in plasma could not only distinguish between OSCC patients and HCs with high precision (AUC 0.93) but also between non-dysplastic leukoplakia patients and HCs with an improved AUC of 0.96 (46). This suggests the miRNA is secreted early on in the development of a malignancy, and could assist with the detection of more treatable early stage disease. Later analysis on miR-196a-5p and miR-196b-5p showed that these plasma miRNAs could distinguish between patients with pre-cancerous lesions including, hyperkeratosis and hyperplasia from healthy individuals, but with reduced accuracy then when compared to identifying OSCC (AUC of 0.96 vs 0.98). When examining more

advanced potentially malignant diseases including dysplasia and carcinoma *in situ* (*CIS*) MacLellan *et al.* demonstrated that the serum miRNAs from patients with pre-malignant diseases were more similar to the serum from OSCC patients if the lesion was more advanced. With this knowledge and the knowledge that *CIS* like OSCC is regarded as an indication for excision the authors combined these samples into one group and were still capable of identifying 5 separate miRNA biomarkers that could differentiate these lesions from HCs (8). This study is also notable due to its consideration of the effect of haemolysis which other studies did not account for.

Serum and plasma miRNAs are vulnerable to contamination from blood cell derived miRNAs and so care must be taken to either eliminate samples effected by haemolysis, or during analysis account for the contamination of specific miRNAs (58-61). This is concerning considering identified candidate miRNAs may originate from blood cells and owe their differences to inconsistencies in blood sample processing. For example miR-21-5p and miR-223-3p have been associated with haemolysis (61) and therefore it makes it more difficult to interpret studies which examine these miRNAs (8,47,49,51-53). Possibly serving to highlight this concern when Ries *et al.* performed biomarker analysis on whole blood they were still able to identify the candidate biomarkers: miR-186-5p, miR-3651 and miR-494-3p but with lower accuracy, possibly due to the masking effects of cellular miRNA (56).

In contrast to salivary miRNAs, which are mostly studied by researchers focusing on OSCC and other oral diseases circulating miRNAs have received attention in other head and neck sites including the larynx and nasopharynx. Ayaz *et al.* examined the plasma of 20 patients with laryngeal squamous cell carcinoma (LSCC) and identified 5 miRNAs which were neither expressed in HCs or in literature reports of any other disease state at the time. This would be

expected to give the biomarkers increased specificity, however later research has found these

miRNAs to be expressed in non LSCC plasma (62).

Circulating miRNAs have also been examined in nasopharyngeal carcinoma (NPC). Liu

et al. performed an analysis on a panel of 21 miRNAs that they chose because of a known

deregulation in NPC tissue and high expression in plasma (47). This pre-selection allowed for

higher throughput analysis on 217 patients and 73 controls, an impressive number of samples

considering the rarity of NPC even when considering the increased incidence in Southern China

where a great deal of NPC research occurs (3). With a similar sample size Zeng *et al.* profiled

plasma miRNAs on a large sample set of 160 NPC patients and 143 HCs. Initial screens with

large qRT-PCR panels were used to narrow down the examined miRNAs to miR-17-5p, miR-

20a-5p, miR-29c-3p, and miR-223-3p. These miRNAs were then analyzed in a training set of 30

cancer and 30 control samples in which the detection threshold was set, i.e. the combined CT

values necessary to be called as a cancer sample. The researchers then used an independent test

set of 57 control and 74 cancer samples to determine that the model had a sensitivity of 97 and a

specificity of 96 (53). The results of these two studies are notable for their association between

NPC, and enrichment in miR-21-5p and miR-223-3p which have been found in the plasma of

patients with other cancers (52), and therefore may reduce the potential specificity of the

biomarker. This downside may be uniquely addressed in NPC due to the disease commonly

being caused by infection with Epstein Barr-Virus (EBV) which encodes its own unique

miRNAs. Zhang et al discovered a subset of these miRNAs, miR-BART7-3p an miR-BART13-

3p have utility in distinguishing not only the serum of patients with NPC from controls, but also

individuals with other cancer types (50).

1.2.2   Prognostic and Other Non-Diagnostic Biomarkers

Prognostic biomarkers are intended to predict patient outcomes including the chance of recurrence. As with most cancers the main prognostic factor predicting HNSCC outcome is stage with metastatic disease having poor outcomes (4) and extracapsular spread among neck lymph nodes also being a negative indicator (63), whereas HPV status is a know positive indicator (64) although it is site specific (5). Secreted miRNAs as prognostic biomarkers in HNSCC are comparatively rare.

In a study using 15 individuals with low-grade dysplasia, 8 of them later progressed to OSCC, it was discovered that miRNAs: miR-10b-5p, miR-145-5p, miR-99b-5p, miR-708-5p, and miR-181c-5p were significantly different between the two groups (65). This could be an incentive to remove likely progressing lesions, as many low-grade dysplasias are merely monitored for progression. There have only been a few more studies on circulating miRNAs and similarly the work has been preliminary with samples sizes too small to properly measure predictive power with 1-4 cases being examined in each study (52,66-68).

However there are indications that circulating secreted miRNAs may be suitable for predicting tumor recurrence (52,66). Mir-21-5p was found to be up-regulated in the plasma of individuals with OSCC tumors and after resection the miRNA level returned to normal, except in patients who later died from recurrence. A later study showed both plasma miR-21-5p, and miR-223-3p were up-regulated in patients with HNSCC, prior to surgery with levels returning to normal in non-progressors after surgery, however miR-223-3p but not miR-21-5p remained elevated in an individual suffering a recurrence. As these are miRNAs identified as a potential diagnostic biomarkers by others (8,51), it is possibility the miRNA was secreted from occult tumor burden at the time of resection, however it raises the question of the why certain

biomarker miRNAs remain elevated but not others (66). MiR-155-5p, miR-146a-5p, and miR-15a-5p were found to be lower in the blood of individuals with more advanced HNSCC (67,68), suggesting their potential utility in aiding with prognosis. As these miRNAs are lower in the blood of individuals with larger tumors this suggests that they do not originate from the tumor, and may be secreted from blood cells or the surrounding tissues. Additionally, as these are generally regarded as tumor suppressive miRNAs it could be that their absences from the blood allows for the cancer to progress in a yet to be identified mechanism (67,68). Taken together these prognostic biomarkers are a potential indicator for more aggressive adjuvant therapy.

In addition to prognosis, biomarkers can be used to measure response to treatment. EBV, the main cause of NPC, encodes miRNAs not otherwise present in humans. Examination of EBV miRNAs secreted from NPC tumors has improvements over examining EBV antibodies in monitoring tumor burden, as antibody levels can be expected to remain in the blood after the removal of the tumor. EBV miRNAs miR-BART7-3p and miR-BART13-3p were also shown to decrease in response to decreases in tumor burden and therefore have potential to track disease progression and may be useful in determining the benefit of continued adjuvant therapy (50).

1.2.3 Common Themes Among miRNA Biomarkers

When examining saliva and blood one would expect there to be miRNAs that are secreted into both fluids. When we examined HNSCC biomarker studies we saw that there is overlap among miR-31-5p (37,39,44), and, miR-184 (35,57) being identified in both saliva and blood as potential HNSCC biomarkers. Notably secreted miR-21-5p was found to be indicative of not only HNSCC in saliva and blood (35,47,52) but has also been named as a possible biomarker for other cancer types including lung (41), colorectal (42), and breast (43). This suggests that miR-

21-5p may have a higher potential in follow up studies due to its association with many cancer types, implying miR-21-5p's detection is a more robust result. This, however, may potentially reduce the specificity of any clinical test as it may be difficult to refine a search for a specific tumor.

With both salivary and blood based biomarkers, researchers have gone past comparisons between individuals with and without HNSCC, but have also examined individuals who have premalignant lesions. This is important for potential clinical applications, as those at high risk for HNSCC, and therefore the likely population to be tested, are more likely than the general public to have non-cancerous diseases of the head and neck. When included in biomarker studies pre-malignant lesions are still distinguishable from HNSCC, but it becomes more difficult the further the lesion has progressed (8,35-37,48). This comparison is uncommon partially because individuals with pre-malignant lesions may not be referred to specialty care, making inclusion of these patients in research more difficult. This is unfortunate as the molecular alterations which occur in these tissues may mask more serious disease, and decrease real world specificity of a miRNA test.

Another reason to give consideration to the test population is that the group at highest risk for HNSCC are those who have been previously been diagnosed. Oral squamous cell carcinoma (OSCC) and oropharyngeal squamous cell carcinoma (OPSCC) have a 20-fold increase in the risk of a second head and neck primary tumor (69). In individuals with early-stage disease who have undergone primary treatment, there is a 24% chance of recurrence within 5 years (69). Initial treatment involving radiation or surgery can make visual diagnosis of a recurrence or second primary much more difficult. Detection of a local recurrence could be hampered due to scar tissues formation and altered anatomy which would hamper visual

inspection even with the aid of toluidine blue vital stain (70). HNSCC recurrence will frequently

be detected distantly as a regional or distant metastasis in the lung or neck without a

corresponding local tumor. This generally leads to a dismal outcome (69). A non-invasive

biomarker capable of detecting disease recurrence before it is otherwise clinically evident could

positively impact life expectancy. It would therefore be highly beneficial if a miRNA biomarker

could be capable of detecting HNSCC in a population that has already received treatment.

Examination of secreted miRNAs in individuals with HNSCC both in saliva and blood showed

that after resection of the tumors, circulating miRNA profiles largely return to normal

(36,40,47,52,57). This suggests that comparisons between individuals with and without HNSCC

may be applicable to a test group that has already been treated (36). Future research will need to

examine what effects primary treatments have on miRNA profiles.

There are several statistical challenges to overcome with all types of biomarker research

in HNSCC. With few exceptions (53) the majority of biomarker tests described above likely

represent a best case estimate of those test's ability to perform. The next step for a clinically

usable biomarker of secreted miRNAs would involve a large sample size with improved

statistical analysis involving independent validation. The creation of a statistical classifier is

biased when the samples that were used to create the classifier were also used to determine its

accuracy, as there is the possibility for a model to be analyzing background noise. A model must

be validated on an independent test set of patients whose data were not used to influence which

miRNA(s) are being tested or what values were determined to be indicative of cancer (71). To

further build upon this a clinical trial would be required to determine if a biomarker was useful in

a clinical setting where diagnosis is unknown and to see if that translates into an improvement in

patient outcome (72).

Demographic matching between experimental groups is important to ensure that any observed changes in miRNA are due to the pathology of the disease and not underlying risk factors. Notably the most common risk factor associated with HNSCC is smoking status which may affect both salivary and circulatory miRNAs. Tobacco use is known to cause alterations in saliva production (73), it would therefore be interesting to determine if this contributes to salivary miRNA differences independently of cancer status. Circulating miRNA profiles of the same individual before and after smoking have shown that smoking does not create an immediate effect on miRNA makeup (58) however comparisons between long term smokers and never smokers have shown a difference (74).

Depending on the method of quantifying secreted miRNAs it is common to use an endogenous control to normalize samples during data analysis. The ideal endogenous control has a consistent quantity in the blood and saliva of all the patients in the study, and there is no universally accepted miRNA for this purpose. Best practice is to choose an endogenous control that is suitable in the sample set being examined rather than relying upon literature values (38). Concerns are raised when an one group identifies an appropriate endogenous control, that is then picked out as a candidate classifier by another group as happed with miR-191-5p (36,38).

1.3   Functional Analysis of Secreted miRNAs

There has been a substantial amount of research in the last decade demonstrating the functional role of secreted miRNAs, however; there is comparatively little information that has been conducted in the context of HNSCC. The most common hypothesis for the function of secreted miRNAs is in cell-to-cell communication. Although the majority of extracellular miRNA may not be associated with EVs (11) the majority of functional research has focused on

17

vesicular miRNA due to the perceived potential of EVs to deliver miRNA with function retained, to the receiving cell (75). In 2007 research in mast cells demonstrated that EVs and their miRNAs can be transferred between cells and the hypothesis was made that transferred miRNAs regulate the expression of a wide variety of mRNAs (76). This was later confirmed with salivary miRNAs (77). It is difficult to isolate the functional role solely of secreted miRNAs as EVs are known to carry mRNA and protein as well. Functional studies have linked HNSCC EVs to tumor vascularity (Chapter 5) and immune system modulation, through contact with T-cells and dendritic cells (24-26). Studies linking function to specific miRNAs have been more limited.

It is possible to examine the effects of individual miRNAs through over-expression of miRNAs of interest in xenografts. It has been shown that OSCC EVs are capable of transferring miR-142-3p to endothelial cells, which can serve to increase tumor vascularity and decrease hypoxia. This process was found to serve a dual role as the act of ridding the cancer cell of mir-142-3p also removes the tumor suppressive effect that the miRNA is known to have in epithelial cells (Chapter 5). The prognostic biomarker candidates miR-146a-5p and miR-155-5p show decreased expression in the blood of patients with aggressive HNSCC and the inhibition of these miRNAs can increase proliferation and migration in cancer cells (68). While it is currently speculative it is possible that the suppressive effect of these miRNAs is being eliminated by alterations in cancer cell transcription, with resulting decreases in the blood, or it may be possible that circulating miR-146a-5p and miR-155-5p if present in the blood, is transferred to HNSCC tumors, causing tumor suppression and explaining the decreased aggressiveness of tumors in individuals with high concentrations of these miRNAs in the blood (68). This raises the possibility that immune cells may be modifying the cancer cells, as was also reported in hepatocellular carcinoma (78).

It is easier to link changes in cellular phenotype to a specific miRNA in the context of NPC due to the presence of unique miRNAs encoded by EBV. It is therefore possible to analyze the effect of these miRNAs independently of endogenous miRNAs. NPC tumors are known to secrete EVs enriched for the EBV BART miRNAs (79) leading to an enrichment of BART miRNAs in the blood (80). NPC EVs are capable of transferring BART miRNAs between cells (81), where it is possible that through regulation of genes in the wnt signaling pathway including APC and WIF1 (82) they remove inhibitory effects on cell growth, metastasis and angiogenesis (83). Additionally when the EBV specific miRNA: miR-BHRF1-3 is taken up by dendritic cells there is a dose dependant reduction in CXCL11 (9) a previously confirmed target (84) and a cytokine used to recruit activated T-cells (85). Additionally in NPC the secreted miRNAs miR-24-3p, miR-891a, miR-106a-5p, miR-20a-5p, and miR-1908 are known to modulate T-cell activity by acting upon the MARK1 signaling pathway (17). Taken together the data suggest a major role of secreted EVs in evading potential immune responses.

1.4   Conclusions

Secreted miRNAs are promising avenues for biomarkers for HNSCC both in the blood and the saliva. It will be important to increase the number of patients included in trials as well as establish common methods of miRNA isolation and analysis to allow comparison between studies. Multiple groups are proceeding with potential miRNA signatures across several different HNSCC subtypes. Subsequent studies will require validation of candidates on independent samples preferably at independent labs.

Continued functional analysis of secreted miRNAs will give insight into tumor biology and will help give insight in to how tumors interact with the stroma and potential metastatic sites.

This opens up the possibility of several targetable pathways with upcoming nucleotide based treatments. The available literature is quickly expanding and with it the notion of increased clinical utility. The long-term decrease in the cost of sequencing will likely improve reliability with far-reaching implications for use in personalized medicine.

Chapter 2: Thesis Theme and Rationale

2.1   Goals and Rationale

OSCC and non-small cell lung cancer (NSCLC) are cancers with dismal survival rates that have shown limited improvement in recent decades. If we gain a better understanding of the molecular mechanisms that control carcinogenesis we may be able to identify potential treatment and management options of these cancers. My work examined the ability of miRNAs to differentiate between individuals with and without OSCC or *CIS*. This could lead to the development of biomarkers capable of detecting recurrence, and determining which pre-cancerous lesions have a higher risk of progression. Work described here and elsewhere shows that circulating miRNAs can be accurate biomarkers for cancer; however there is still a limited understanding of which miRNAs are undergoing selective secretion and what purpose these miRNAs have in promoting carcinogenesis. The overall goal of my thesis was to investigate miRNAs that are selectively released in OSCC and NSCLC and determine what biological roles they play with regards to tumorigenesis. This information will give insights into cancer biology and determine how cancer cells communicate with their tumor stroma using miRNAs. The information gained here can potentially lead to the identification of drug targets which can lead to an improvement of outcomes for theses two diseases which retain overall poor rates of survival.

2.2   Hypotheses

The hypotheses and questions examined were:

1: Is there a subset of serum miRNAs that are capable of differentiating between individuals with and without oral cancer or *CIS*?

2: Are MiRNAs being selectively excluded from OSCC cells when doing so will confer a carcinogenic advantage? This may occur both by the removal of tumor suppressive miRNAs and also by promoting a supportive tumor microenvironment by the secretion of cell-to-cell communicating miRNAs.

3: The tumor promoting activity of miRNAs identified in 1 & 2 will not be unique to OSCC but will also affect other cancer types including NSCLC.

2.3   Specific Aims

Aim 1: <u>Identify which miRNAs are capable of differentiating between individuals with and without oral cancer</u>

Chapter 3 discusses the use of a genome wide panel of miRNAs to profile the serum of individuals with OSCC or *CIS* in comparison to a demographically matched group of non-cancer controls. We used this information to create a statistical model capable of predicting the cancer status of the individuals included in the study. To ensure the rigor of the analysis method we used this statistical model to query an independent set of serum samples that had no influence in the creation of the model. This work represents the first attempt to identify serum miRNA biomarkers for oral cancer that are capable of functioning in a large independent sample set.

Aim 2: <u>Characterize oral cell lines for their suitability to act as an analog of human tissue</u>

Previous scientists in the Garnis lab have characterized oral cancer cell lines for DNA mutations and alterations in mRNA expression. This provided a useful reference for researchers conducting *in vitro* analysis on oral cancer. Building upon this knowledge I believed that it

would be beneficial to characterize normal and dysplastic cell lines for DNA mutations as well as alteration to both mRNA and miRNA expression. It is known that the growth of cells in culture is capable of causing molecular alterations to all of these features. Experiments performed using these cell lines can be performed with full knowledge of the limitations in comparing between *in vitro* and *in vivo* studies. This information is discussed in Chapter 4, and provides insight into the interpretation of the results obtained in Chapter 5.

Aim 3: Identify the miRNAs that are selectively excreted from OSCC cell lines in culture via EVs.

Before conducting functional analysis of the miRNAs which are different between individuals with and without OSCC it is important to determine if these miRNAs are being selectively secreted from the cancer cells themselves. This step is necessary as there are many cells capable of secreting miRNAs into the serum of cancer patients and identification of their source is important to elucidating the role of the secreted miRNAs. In Chapter 5 of this thesis, I examined a panel of 4 OSCC cell lines and 1 oral dysplasia cell line and profile them for the same panel of miRNAs described in Aim 2. By comparing the miRNAs present in the cell to the miRNAs that are in the EVs I can determine which miRNAs are undergoing selective excretion rather than having alterations due to changes in total miRNA expression. This is based off of the prediction that selected miRNAs are more likely to have a functional role in promoting cancer growth when compared to other miRNAs which may be secreted.

Aim 4: Determine the function of the EV miRNAs discussed in Aim 3 with regards to OSCC

In a panel of OSCC cell lines the exosomal secretion pathway was altered through the use of shRNAs, and of the miRNAs identified in Aim 3, miR-142-3p was found to be the most

responsive to these changes. Chapter 5 examined the functional role that miR-142-3p plays within the cancer cell to give insight into what selective benefit there is to eliminating it from the cell. To also explain why this miRNA was not merely altered through changes in gene transcription, we explored the possibility that this miRNA was acting as a cell-to-cell communicator, a possibility demonstrated by others. We examined the ability of this miRNA to act upon endothelial cells of the tumor stroma, both by inducing increased expression in the endothelial cells and by transferring miRNA by way of EVs to more accurately mimic natural processes. Mouse models were also utilized to demonstrate that the observed phenotype was not a unique artifact of the cell culture environment, a crucial warning from chapter 4.

Additionally, we sought to characterize the mRNA target of this miRNA in an effort to provide a more complete explanation of the miRNA's activity.

Aim 5: Identify to what degree there is similarity in the function of miRNAs that are secreted in the EVs of OSCC compared to NSCLC

Chapter 6 examined the possibility that the functional pathway of miR-142-3p described in Aim 4 is broadly applicable to other forms of cancer. The functional role of miR-142-3p originating from lung cancer cell lines is examined using similar methodology to chapter 5. Assessing multiple ways that secreted miRNAs communicate with the tumor stroma is important for building a complete picture of EV transfer. And therefore there is additionally an examination of the miRNA's role upon cancer associated fibroblasts (CAFs), with assays used to determine if fibroblasts are induced to express markers which have been associated with a tumor promoting niche.

Chapter 3: The Identification and Validation of a Serum miRNA Based Biomarker for the Detection of Oral Cancer

3.1 Introduction

Oral squamous cell carcinoma (OSCC) is the most commonly diagnosed form of head and neck cancer and the 8th most common cancer worldwide (86).The disease has a poor prognosis and overall survival rates for the disease have seen little improvement despite recent advances in care. A partial cause of the high mortality is due to the late stage at diagnosis when the disease is more difficult to treat with surgical resection (87). There is also a high rate of recurrence, and second primary (87). There is potential to greatly increase the survival rates for individuals with oral cancer if a method is developed that allows earlier detection.

An ideal biomarker would be one that is obtainable non-invasively such as from blood or urine and there has been recent interest into the evaluation of circulating miRNAs which have been found to be stably expressed in the blood (20) with non-random variance in the miRNA profiles between individual with different diseases including oral squamous cell carcinoma (OSCC)(7,8,88). These facts taken together show the potential for miRNAs to provide utility in the early detection of OSCC.

Profiling of miRNAs for the purpose of identifying biomarkers is normally done on serum or plasma to avoid the large contribution of RNA from blood cells masking miRNAs which are possibly secreted by tumor cells (89). Serum has the benefit of being easier to collect and process and is also more available. Plasma has also been shown to have more variable expression when performing technical replicates (54) which could be due to varying

contributions of platelet miRNAs (55). A weakness of serum and plasma is that it is known to be affected by haemolysis of the blood sample which could lead to inconsistent contributions of red blood cell miRNA to the miRNA profile (90). The options to eliminate this effect are first to exclude from analysis any sample which has hemoglobin detectable over a certain threshold, and second to exclude from analysis miRNAs that are known to be affected by haemolysis (58). The rejection of haemolysed samples provides the ability to analyze more miRNAs, the rejection of haemolysis affected miRNAs provides more potential clinical utility as repeated blood draws would not be needed from individuals prone to haemolysis. This method therefore has the potential of a faster processing time and a decreased number of patient visits.

Several previous researchers have attempted to develop a circulating biomarker for OSCC by examination of blood, serum and plasma, yet have not been able to show high accuracy in large independent sample sets (7,34,51,56,66,91). This chapter details an effort to build upon previous studies into circulating oral cancer biomarker detection through an increase in sample size and a more stringent statistical analysis to create, select and validate a test that can differentiate between individuals with and without oral cancer. We decided to group OSCC and *CIS* together for our analysis as the high rate of progression to OSCC (92) has lead to an understanding that these lesion must be removed (93,94). Inclusion of these individuals assists in the analysis of a biomarker's potential to detect early stage disease.

3.2   Materials & Methods

3.2.1   Sample Acquisition

Serum samples were collected from patients with either *CIS* or OSCC (collectively high-risk lesions or HRLs) undergoing curative resection treatment. Control serum samples from

individuals without cancer were demographically matched for sex, age, and smoking history. The non-cancer control samples were obtained from a pan-Canadian study on the early detection of lung cancer. A comparison of demographic information can be seen in Table 3.1.

All blood samples were collected in SST vacutainer tubes then allowed to clot for 30 min at room temperature. Samples were then centrifuged a room temperature for 15 min at 1500 RCF and frozen in aliquots at -80°C within 2 hours.

Table 3.1 Demographics of the study cohort

	HRL	Control	HRL	Control	HRL	Control
	SYBR		TaqMan Training		TaqMan Validation	
Total Patients	48	51	48	49	29	24
CIS	18	NA	18	NA	14	NA
SCC	30	NA	30	NA	15	NA
Age mean	62	63	62	63	56	65
Age range	35-93	50-75	35-93	50-75	23-79	55-75
Males	35	29	35	29	21	10
Females	13	22	13	20	8	14
Former smokers	24	30	24	30	0	10
Current smokers	14	21	14	19	29	14
never smokers	10	0	10	0	0	0
pack-year mean	21	47	21	47	33	45
pack-year range	0-156	30-80	0-156	30-80	0-73	17-63

3.2.2 RNA Extraction

We extracted RNA from 200 µl of serum with a miRNeasy Mini Kit (Qiagen) using the manufacturer's protocol with the addition of 1.25 µl of MS2 carrier RNA (Roche Applied Science) which was added to QIAzol Lysis Reagent prior to the addition of serum. After purification RNA was suspended in 50 µl of RNase free water and stored at -80°C.

3.2.3 qRT-PCR

Initial qRT-PCR analysis was performed using Exiqon's LNA based platform, with the profile of 30 HRL and 26 control samples being previously described (8). Additional samples were also profiled to bring the total to 51 control samples and 48 cancer samples. CDNA was made using a miRCURY LNA Universal cDNA synthesis kit on 19.2 µl of serum RNA. CDNA was then quantified using SYBR Green master mix and miRCURY LNA Universal RT miRNA PCR Human Panel I and II, according to the manufacturer's recommendations. This allowed for the quantification of 742 miRNAs, although 10 of these miRNAs have been removed from miRBase (www.mirbase.org) due to the possible detection of other RNAs. All assays were examined for distinct melting curves and samples with multiple melting temperatures (Tm) or CT>35 were excluded from analysis.

In order to demonstrate that the observed results were not merely an artifact of the Exiqon platform subsequent analysis was performed using the Thermo Fisher TaqMan system using custom pre-spotted plates with each assay run in triplicate. This was performed on a subset of promising miRNAs determined through statistical analysis described below. RNA was quantified using a Qubit 3.0 (Thermo Fisher) using the RNA HS reagents. 150ng of RNA was

run to make cDNA using TaqMan miRNA reverse transcription kits, for qPCR, Universal Master Mix II was used, according to manufacturer's recommendations.

3.2.4   Data Analysis

For SYBR qRT-PCRs, miRNAs were excluded from analysis if they were not expressed with a in at least half of the control group or half of the disease group. We excluded 162 miRNAs present on Human Panel I and II that had been shown to have altered detection dependant on sample haemolysis (58).

For SYBR and TaqMan analysis expression was normalized to an endogenous control miR-23b-3p chosen based upon its value using the geNorm algorithm showing it was the least variable miRNA across samples (95). CT values for miRNAs that were not detected were set to the threshold of detection (35 for SYBR and 37 for TaqMan). To normalize the CT of potential candidate miRNAs the CT value was subtracted from the CT of the chosen normalizing miRNA; this was done for each sample. CT values represent a logarithmic scale therefore data were first linearized using the formula $CT_{linear} = 2^{(-CT\ normalized)}$. During the creation of a statistical model the linearized value was used as well as its root and square, as the relationship between miRNA level and disease state may not be linear. To allow the inclusion of all possible exponents would increase the computational demands.

3.3   Results

3.3.1   Preliminary SYBR Analysis

We analyzed miRNA concentration in 99 serum samples from 48 individuals with HRLs and 51 control individuals. Of the 742 miRNAs that were queried by qRT-PCR, 162 were known to be effected by haemolysis and were excluded from further analysis (58). Of the remaining

miRNAs 415 were detected in at least one serum samples with only 14 miRNAs being detected in every sample. In order to focus attention on miRNAs which are likely to be informative and to reduce computational requirements we limited further analysis to the miRNAs which were expressed in at least 50% of the HRL group or 50% of the control group. After this selection 106 miRNAs remained. Analysis of the miRNAs and their CT values identified miR-23b-3p as having the least variability among all samples as determined by the geNorm algorithm (95).

An attempt to use logistic regression alone to create a statistical model analyzing all of the remaining 106 miRNAs would likely lead to over fitting and poor predictive performance (96). Therefore our goal was to choose a subset of miRNAs to be included in the statistical model. This was done using a LASSO penalty which creates a disincentive to the inclusion of miRNAs that give little information to the classification of the serum samples (97). As the penalty is decreased the number of miRNAs included in the model changes this change is referred to as an 'action'. An action can increase the number of miRNAs in the model, but if miRNAs included in the model at a later step provide superior attributes in combination, an action may remove miRNAs as well. The miRNAs selected and the order they were included in or excluded from the model is shown in Table 3.2.

Table 3.2 LASSO selection of miRNAs for analysis of SYBR qRT-PCR with the inclusion of linearized CT values as well as their squares and roots

Order	Action	miRNA	Exponent
1	Add	hsa-miR-23a-3p	0.5
2	Add	hsa-miR-346	0.5
3	Add	hsa-miR-342-3p	1
4	Add	hsa-miR-205-5p	0.5
5	Add	hsa-miR-145-5p	2
6	Add	hsa-miR-342-3p	0.5
7	Add	hsa-miR-33a-5p	0.5
8	Add	hsa-miR-125b-5p	1
9	Add	hsa-miR-142-3p	0.5
10	Add	hsa-miR-616-3p	0.5
11	Add	hsa-miR-10a-5p	1
12	Add	hsa-miR-550a-5p	2
13	Add	hsa-miR-200c-3p	1
14	Add	hsa-miR-10a-5p	0.5
15	Add	hsa-miR-125b-5p	0.5
16	Add	hsa-miR-200c-3p	0.5
17	Remove	hsa-miR-10a-5p	1
18	Remove	hsa-miR-200c-3p	1
19	Add	hsa-miR-28-3p	0.5
20	Remove	hsa-miR-125b-5p	1
21	Add	hsa-miR-497-5p	0.5
22	Add	hsa-miR-543	0.5
23	Add	hsa-miR-29b-1-5p	2
24	Add	hsa-miR-29b-1-5p	0.5

Before moving on to validation in an independent test set it was our wish to estimate the potential accuracy of our statistical model relative to the number of miRNAs included. This was done via bootstrapping; samples were randomly split into groups with 2/3rds of HRLs and 2/3rds of controls forming a training set and the remainder forming a validation set. LASSO analysis and logistic regression was performed. The selection of miRNAs and their influence on the probability calculation (their weight) was done only on the training set. This was done to not create an optimism bias towards the inclusion of miRNAs which are only informative in the validation set. The accuracy, sensitivity and specificity was calculated for each action, and then repeated 10000 times for alternate splits between training and validation groups. Figure 3.1 shows that the average accuracy that a model has in the validation set, is dependent on the number of LASSO actions performed. The average accuracy in the validation set increases to a plateau with the inclusion of approximately 15 LASSO actions, roughly equivalent to the number of miRNAs in the model.
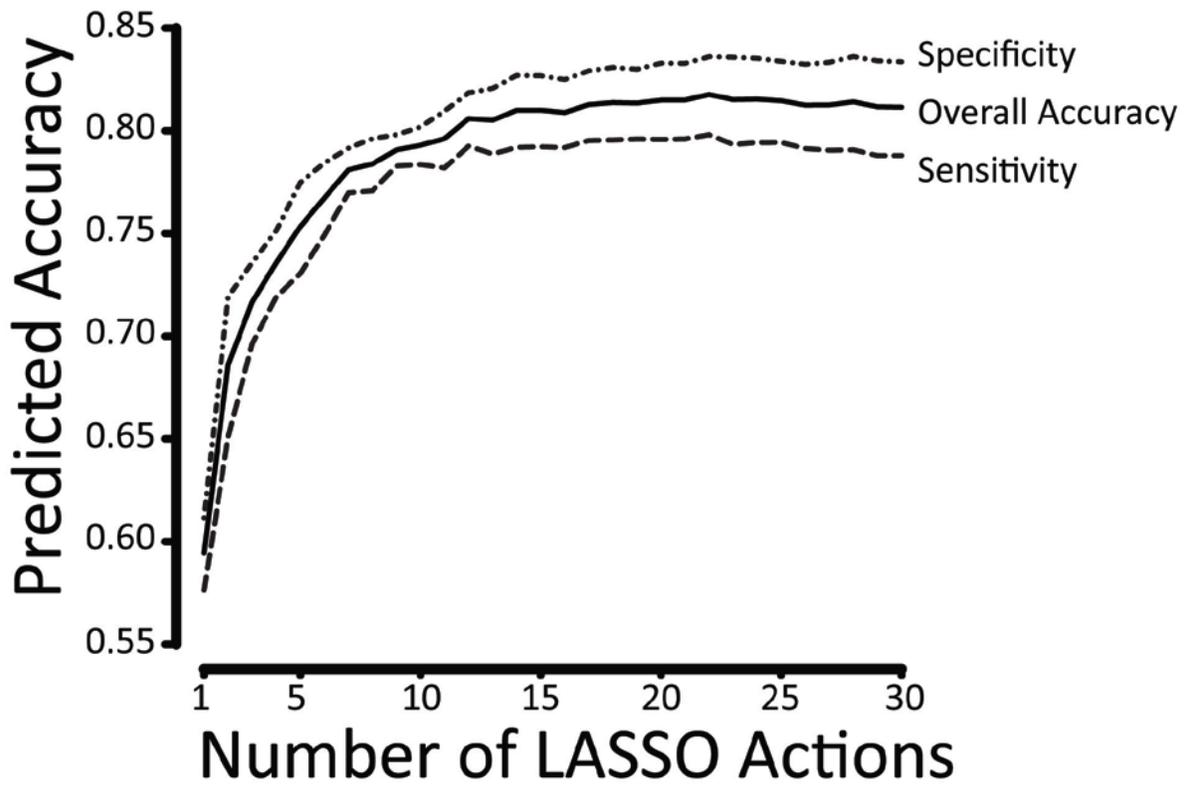
Figure 3.1 Average accuracy for preliminary SYBR analysis. This graph shows the average sensitivity, specificity and overall accuracy in determining oral cancer status per LASSO action while examining randomly partitioned validation sets of miRNA expression. Resampling was performed 10000 times and therefore the averages shown are based off of models with the inclusion of different miRNAs under examination.

3.3.2 TaqMan Training Analysis

Attempts to test the statistical model described above were made difficult by the re-formatting of Exiqon's SYBR platform which led to a requirement to regenerate the original statistical model. We used this as an opportunity to confirm that the observed results were a function of underlying trends in the miRNAs rather than, platform specific artifacts and further analysis was performed using TaqMan reagents. We chose to conduct verification analysis with the 14 highest ranked miRNAs from Table 3.2, as well as the endogenous control miR-23b-3p, due to the plateau in accuracy as well as the space requirements on the custom 384 well plates. On the TaqMan platform we were unable to detect miR-346 at the levels present in serum and therefore it was excluded from further analysis. Of the original 99 serum samples 2 controls were excluded due to an insufficient quantity of RNA. Profiling proceeded on the remaining 97 serum samples.
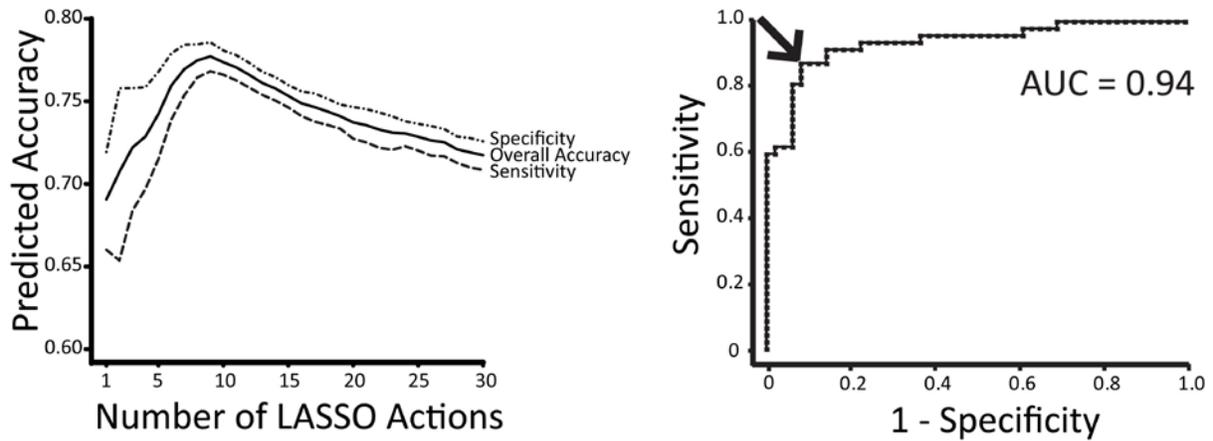
Figure 3.2 Accuracy of TaqMan analysis training set. A: shows the average sensitivity, specificity and overall accuracy when comparing across resampled data sets (accuracy is recorded on the validation set). B: shows an ROC curve when the regression is performed on the 6 miRNAs chosen after 9 LASSO actions performed on the entire set without segregation into training and validation sets. Those miRNAs are listed in Table 3.3. The arrow shows the point on the curve we believe has optimal sensitivity and specificity, and led to a threshold in the probability calculation that would be used to make calls in the independent test set.

The statistical model was regenerated using the same process as above. Figure 3.2 A

shows the predicted accuracy of the model by analysis in a bootstrapped validation set. It is clear

that the model reaches peak accuracy when there are 9 LASSO actions. If the analysis is

performed on the entire 97 samples in the training set, 9 LASSO actions lead to the inclusion the

6 miRNAs in Table 3.3. A comparison between Tables 3.2 and 3.3 shows that with the exception

of miR-346 which was excluded from the TaqMan analysis, the 6 most relevant miRNAs are

consistent across groups. Figure 3.2 B shows the ROC curve created by regression of the

selected miRNAs with an AUC of 0.94. Although the curve is likely over fit it is useful for

determining the threshold above which samples will be called as HRLs in the validation set. This

point is indicated by an arrow (Fig. 3.2 B) and corresponds to a sensitivity of 0.87 and a

specificity of 0.92. Also of interest is the observation that miR-33a-5p, miR-23a-3p, and miR-

342-3p were found at higher levels in the control samples, with miR-145-5p, miR-205-5p and

miR-125b-5p being higher in the cancer samples.

Table 3.3 miRNAs selected after 9 LASSO actions on TaqMan training set data

miRNA	Exponent[a]
hsa-miR-125b-5p	1
hsa-miR-342-3p	1
hsa-miR-23a-3p	1
hsa-miR-205-5p	1
hsa-miR-145-5p	2
hsa-miR-33a-5p	1
hsa-miR-145-5p	1

[a] An exponent of 1 means that the LASSO action included the linearized CT value of a given miRNA, an exponent of 2 means that the square of the linearized CT was included
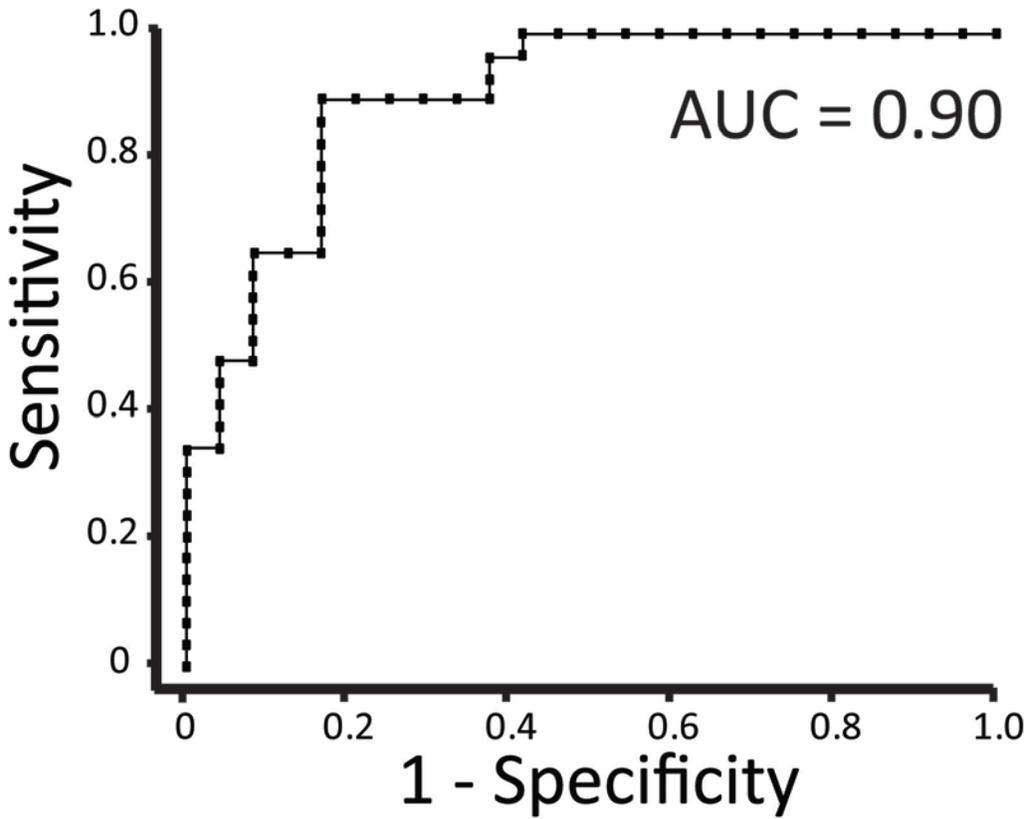
Figure 3.3 Accuracy of candidate miRNAs in an independent test set. This graph was generated by validating the 6 miRNA model described in figure 3.2B, on an independent test set.

3.3.3   TaqMan Validation Analysis

An independent test set of serum samples was profiled to test the identified statistical model without influencing its creation or selection. This set included 29 HRL samples and 24 control samples. Figure 3.3 shows the ROC curve has an AUC of 0.90, a minor decrease in accuracy when compared to the training set. However while using the same threshold that was identified in Figure 3.2B the sensitivity and specificity are 0.45 and 0.96. The overall likelihood of a sample being called as a cancer was decreased despite the format of the qPCR platform being the same.

We attempted to find an explanation for this variation. When performing replication experiments it was noticed that exact repeats could lead to a variation between technical replicates with a CT value difference of up to 0.5. Communications with the manufacturer revealed that this was within the acceptable parameters of the assay. In order to estimate the possible effect that this could have on a biomarker's performance we introduced random alterations to the raw CT values obtained in the validation analysis. A random number between 0.5 and 0.5 was added to each CT value prior to any processing. This was repeated 9 times, with the unmodified example leading to a set of 10. The sensitivity ranged from 0.38-0.55 with an average of 0.46 and the specificity ranged from 0.92-1.0 with an average of 0.92. This suggests that the qRT-PCR platform is reasonably robust to common variations in CT values, there is notably a decrease in the observed sensitivity compared to what was predicted in Figure 3.2 A, but an increase in specificity, likely due to reasons other than small variations in the qRT-PCR platform.

3.4 Discussion

There has been a substantial effort to examine secreted miRNAs both in saliva and blood, and to analyze their role in detecting oral HRLs. Examination of salivary miRNAs started in 2009 (34) and circulating miRNAs in 2008 (57). In order to not limit biomarker analysis to those that have been identified as deregulated in tissue, Maclellan *et al.* conducted the first global analysis of a large number of miRNAs (8). Several other researchers have conducted follow-up analysis providing useful information for ongoing research (51,56,66,91). These studies generally contained fewer than 100 research subjects and lacked validation of their analysis on an independent test set that had no influence on the selection or creation of their statistical model. Ongoing research in biomarker discovery has established that independent validation is a necessary follow up prior to the utilization of any biomarker in cancer (98), and may help alleviate the observation that most biomarkers do not achieve clinical utility.

Analysis of biomarkers in individuals with oral cancer or carcinoma *in situ* can be used to more effectively stratify patients and improve disease outcome. By analyzing serum miRNAs from 152 individuals with or without oral HRLs we have been able to identify 7 miRNAs that are deregulated, and are capable of distinguishing between these patients with a high AUC, and specificity but an unreliable sensitivity. This means that the statistical test has a validated ability to separate the HRL and control groups, but the ability to make calls is affected by a bias towards a decreased probability of cancer. This will need to be addressed to increase confidence in a diagnostic test with clinical applications. It is speculative to say what the cause of this bias is, however there are some possibilities. The training samples were analyzed at an earlier date then the test samples, it is possible that there were changes over time in the thermal cycler's performance. It is also possible that the reagents used degraded over time. An analysis of the CT

41

values however does not show a change in total expression over time. Future analysis would be improved if the separation into training and test sets occurred after all samples were run and then randomized relative to the date the samples were quantified.

It is important to discuss the possible applications of a test with a low sensitivity and high specificity. Such a test is not an absolute bar to clinical applications as there is still benefit to a subset of individuals. Specificity is generally more relevant when deciding to perform an invasive or costly procedure however when designing a screening test on a broad population a high sensitivity is generally preferable allowing for more discerning methods to be used to confirm diagnosis later on (99). A determination of acceptable test parameters must be made in collaboration with clinicians and would be specific to the population examined.

By removing miRNAs that are known to be affected by haemolysis we decrease the vulnerability of our assay to differences in sample collection. This partially improves upon a meta analysis including over 900 participants that have been tested for either circulating, tissue or salivary miRNAs which could discriminate between oral cancer and controls with a higher sensitivity at 0.75 but a lower specificity at 0.77 (100). Our more focused approach yielded an AUC of 0.90, a sensitivity of 0.45 and a specificity of 0.96 while at the same time using a more discerning analysis method.

The current standard for detecting oral cancer is visual inspection of the oral cavity as tumors are often visually apparent (101). Visual examination may also discover precancerous and non-cancerous lesions as well as true cancers and often follow up testing is necessary to confirm diagnosis. Detection of oral cancer is made much more difficult during a recurrence as primary treatment usually involves surgery with or without radiation which can cause major changes to the anatomy of the mouth. Recurred tumors are often only detected when they are

large enough to cause pain even when examinations include the use of diagnostic aids such as an FV scope or toluidine blue vital stain (70). A biomarker capable of distinguishing between individuals with and without oral cancer may help overcome these difficulties. Future research would need to analyze a large number of individuals after treatment while monitoring for recurrence. There is cause for optimism as previous studies have demonstrated that post treatment miRNA profiles are similar to non-cancer profiles (36). This potentially could alleviate a concern that there may be an effect of treatment on circulating miRNAs.

The observation that many of the candidate miRNAs are higher in the control samples (miR-33a-5p, miR-23a-3p, and miR-342-3p) suggests that the deregulated miRNAs originate from outside the tumor. This indicates there may be a global deregulation of miRNAs in individuals with oral cancer. While unusual this complements previous research that has demonstrated similar decreases of mIR-342-3p in leukemia (102), with other examinations of oral cancer also showing decreases of specific circulating miRNAs in the control group (56). Conversely our own research directly measuring the miRNAs secreted from OSCC and lung cancer cells has shown that miR-145-5p was the only miRNA that is enriched in the serum of individuals with OSCC and is also selectively exported into the extracellular space from cell lines (Chapter 5). In lung cancer secretion of miR-145-5p appears to be selected for, due to inhibition of the protein CamK1D when the miRNA is transferred to endothelial cells, with a pro-angiogenic effect (data not shown). MiR-125b-5p has shown to be increased in the serum of individuals with lung cancer and more aggressive forms of breast cancer (103,104). Conversely miR-125b-5p's decrease in oral tissue appears to be an indicator of progression (105), raising the question that the miRNA may be present in the serum due to disposal from the tumor, an idea recently proposed upon examination of extracellular vesicle secreted miRNAs (13).

In conclusion the expression of the miRNAs miR-125b-5p, miR-342-3p, miR-23a-3p, miR-205-5p, miR-145-5p, miR-33a-5p miR-145-5p and the endogenous control miR-23b-3p have been demonstrated and analytically validated on an independent test group to have a high AUC but with an unknown bias leading towards a modest sensitivity and a high specificity to discriminate between individuals with and without oral cancer or carcinoma *in situ.* This work will be applicable to future research on early detection of recurrence, and further analysis must be conducted to validate the clinical utility of the test in its ability to detect a subset of OSCC/CIS cases.

Chapter 4: Molecular Characterization of Immortalized Normal and Dysplastic Oral Cell Lines

4.1   Introduction

Cell models have yielded significant insights into cancer biology and remain a staple of oncology research; they are widely used to model the progression of disease and the response of human tissue to drugs, as a precursor to research in animals and humans (106-109). Cell lines, especially those derived from tumors, are known to exhibit significant molecular heterogeneity and previous work has shown that many molecular alterations can occur before malignant transformation (110). Analysis of genes that contribute to disease states can be hindered by the complex genetic background of many cell lines. For oral cancer, while there is extensive molecular characterization of cell lines derived from invasive disease tissues (111-115), there is limited molecular information available to complement analysis of commonly cited cell lines derived from normal or dysplastic oral tissues (116,117).

Normal and pre-malignant tissues generally exhibit less molecular complexity than cancerous cells (118), hence cell lines derived from such tissues are invaluable for the study of cancer progression and initiation. Unlike tumor cell lines, normal primary human cells can only carry out a finite number of replications before they undergo senescence (119), thus limiting the length of time cells may be grown in culture. To circumvent this issue, primary cell lines are often immortalized using a variety of methods including silencing tumor suppressor genes (such as p53 and K-Ras (120)) infection with viral oncogenes, such as SV40T (121) or E6 and E7 (122), or constitutive expression of hTERT (telomerase reverse transcriptase) (123). The ideal

immortalized cell is one that is genetically identical to the primary normal cells from which they were derived but also capable of infinite reproduction. In reality, the immortalization process and prolonged replication may introduce alterations to the cells (124,125). To use cell lines as a tool for modeling cancer initiation and progression or other diseases of the oral mucosa, it is vital to determine the genetic background of these cells. Commercially available normal oral cell lines (OKF4, OKP7, OKF4 TERT, OKF4 E6E7, OKF6 TERT1, OKF6 TERT2, OKF6 E6E7, and OKP7 bmi1 TERT); and oral dysplastic lines (POE9n TERT and DOK) have undergone some molecular characterization with regards to major oncogenes; however, they have yet to be molecularly characterized in a comprehensive manner (126-128). A Google Scholar search shows that the normal cell lines have been mentioned 298 times with the most commonly used being OKF6 TERT1, comparatively the dysplasia lines were mentioned 1110 times. Here, we report whole genome DNA copy number analysis and global expression profiling of both miRNAs and mRNAs for these oral tissue cell lines, generating a comprehensive molecular resource for all subsequent modeling work involving these cells.

4.2   Methods

4.2.1   Cell Lines and Tissue

Normal oral cells OKF4, OKP7 and cell lines OKF4 TERT, OKF4 E6E7, OKF6 TERT1, OKF6 TERT2, OKF6 E6E7, OKP7 bmi1 TERT and the oral dysplastic line POE9n/TERT were purchased from the Harvard Skin Disease Research Center Cell Culture Core (Boston, MA, USA). The dysplastic line DOK was obtained from the European Collection of Cell Cultures (Salisbury, UK). Cells were grown in Keratinocyte Serum Free Medium supplemented with L-Glutamine, bovine pituitary extract, and epidermal growth factor, and were passaged upon

46

reaching 30–40% confluency. DOK cells were grown differently; they were allowed to grow in Dulbecco's Modified Eagle Medium supplemented with 10% fetal bovine serum, and 5 μg/ml hydrocortisone. Dysplastic cells were passaged at 70% confluency. Table 4.1 summarizes information previously reported about these cell lines.

Table 4.1 Cell line pathology and status of common oncogenes

Cell line	Pathological status	Immortalization	p53 Status	pRb Status	p16 Status	p14 ARF	Source of tissue
OKF4 TERT[a]	Normal	Immortalized	Not expressed	Unknown	Unknown	Unknown	Floor of Mouth
OKF4 E6E7[a]	Normal	Immortalized	Deficient	Deficient	Unknown	Unknown	Floor of Mouth
OKF4[a]	Normal	Non-immortalized	Unknown	Unknown	Expressed (126)	Unknown	Floor of Mouth
OKF6 TERT1[a]	Normal	Immortalized	Not expressed	Unknown	Loss of Heterozygosity, Protein detected (127)	Loss of Heterozygosity, Protein detected (127)	Floor of Mouth
OKF6 TERT2[a]	Normal	Immortalized	Unknown	Unknown	Homozygous deletion (127)	Homozygous deletion (127)	Floor of Mouth
OKF6 E6E7[a]	Normal	Immortalized	Deficient	Deficient	Unknown	Unknown	Floor of Mouth
OKP7 bmi1 TERT[a]	Normal	Immortalized	Unknown	Unknown	Deficient	Deficient	Soft Palate
OKP7[a]	Normal	Non-immortalized	Unknown	Unknown	Unknown	Unknown	Soft Palate
POE9n TERT[a]	Severe Dysplasia	Immortalized	Deficient (126)	Deficient (127)	Homozygous deletion	Homozygous deletion	Floor of Mouth
DOK (128)	Moderate Dysplasia	Naturally Immortal	12 bp deletion and Increased expression (128)	Unknown	Expression of mutated form (129)	Functional	Tongue

[a] Obtained from the Harvard Skin Disease Research Center Cell Culture Core

Both DNA and RNA were extracted from each line when cells reached their maximum confluency, as described above. OKF4 and OKP7 Primary cells were used between passage 6 and 8. DNA from these cells was isolated using a standard phenol-chloroform extraction and treatment with RNase (130). RNA was isolated using the TRIzol (Invitrogen, Carlsbad, CA, USA)-chloroform extraction method (as per manufacturer's instructions). RNA used in miRNA profiling received DNase treatment using the DNA-free kit (Applied Biosystems, Foster City, CA, USA). Normal oral tissue adjacent to removed tumors was previously obtained and from 20 patients with a pathologist analyzing biopsies to confirm histopathological status, 18 samples were collected from the tongue and one each from the gingiva and the floor of the mouth (131). RNA extractions from clinical tissues contributing to the mRNA analyses in this work were previously described (131).

4.2.2 DNA Copy Number CGH Array

DNA copy number variation was analyzed using the SMRT v.2 whole genome tiling-path array (BC Cancer Research Centre, Vancouver, BC, Canada) (132-134). This array contains ~26,000 overlapping bacterial artificial chromosome (BAC) hybridization probes, spotted in duplicate, which cover the entire human genome. Cell line DNA was compared to a reference DNA sample from a healthy human male volunteer. The hybridization protocol has been previously described (135). Slides were scanned using a GenePix 4000B and images were converted to data files using SoftWorx Tracker software. Systematic biases were removed and the data were normalized using the software CGHNorm (136). Data were visualized using SeeGH software (137). DNA gains and losses were defined using the waviCGH program (138). DNA copy segmentation and probability calling was performed and all other settings were set as

defaults. Called gains and losses were visually inspected and were excluded if the call was based on a single outlying data point. Adjacent calls were consolidated when large segments were separated by small intervening segments that were not considered as gains or losses due to high variability. Array data have been made available (GEO Reference: GSE59238).

4.2.3   mRNA Expression Array

Extracted RNA was analyzed for mRNA expression using the Agilent Whole Human Genome Microarray Kit, 4x44K. Hybridizations were performed as per manufacturer's protocol (Agilent, Santa Clara, CA, USA). Scanning was performed on a GenePix 4000B microarray scanner. To perform clustering of expression data, missing values were excluded if the mRNA was not present in at least 30 of 35 samples tested. A total of 36,844 probes were included in the cluster analysis. Cluster analysis was performed using Genesis (Institute for Genomics and Bioinformatics, Graz University of Technology; Graz, Austria). Average hierarchal clustering was performed using a Pearson Correlation, with a heat map generated from resultant data (Supplemental Figure 4.1). Fold change expression data between OKF4 TERT/OKF4, OKF4 E6E7/OKF4, and OKP7 bmi1 TERT/OKP7 cells were calculated by dividing the array intensity value of the immortalized line by the intensity value of the primary line. Using KEGG pathway analysis (139) in the bioinformatic program Cytoscape (140) with the ClueGO plug-in (141), we determined which gene pathways exhibited significantly different activity between these pairs. All expression data are publicly available (GEO Reference: GSE59238).

4.2.4   miRNA qRT-PCR Panel

RNA was reverse transcribed using the Exiqon miRCURY LNA Universal RT microRNA PCR, polyadenylation and cDNA synthesis kit (142). The cDNA was used to complete a quantitative real-time PCR using a SYBR Green master mix for Exiqon's microRNA Ready-to-use PCR, Human panel I + II, V2.M. All steps were performed in accordance with manufacturer protocols (Exiqon A/S, Vedbaek, Denmark). These panels consist of two 384 well plates testing 742 unique miRNAs. Using the ViiA7 RUO software, results were analyzed to remove data from wells that had multiple Tm peaks and lacking linear amplification plots. MiRNA data were then imported into the GenEx program (MultiD Analysis Göteborg, Sweden). Interplate calibration was performed using the data from included spike-ins, and wells with CT values >35 were excluded. Data were normalized to the mean expression value of the miRNAs that were expressed in each cell line (143). Cluster analysis was performed as with mRNA and a heat map was generated (Supplemental Figure 4.2).

4.3   Results

4.3.1   Detection of Copy Number Alterations

Figure 4.1 shows an overlay of the genomic profiles for each of the immortalized normal and dysplastic cell lines OKF4 TERT, OKF4 E6E7, OKF6 TERT1, OKF6 TERT2, OKF6 E6E7, OKP7 bmi1 TERT, DOK, and POE9n TERT. DNA Copy number analysis showed that each of the cell lines harbored DNA copy number alterations. The cell line with the highest percentage of its genome altered was not a dysplastic line, but rather one of the hTERT immortalized normal lines (OKF4 TERT). Table 4.2 shows the total amount of the genome that experienced an alteration, either a gain or a loss, for each cell line. No genomic alterations were observed across

all cell lines. The largest areas gained in a subset of cases were entire gains of chromosome 5 in

OKF4 TERT and OKF6 TERT1, and a gain of the entire chromosome 5q arm in OKF6 E6E7.

Supplemental Table 4.3 shows a breakdown of the regions exhibiting a gain or a loss, with DOK

having the highest number of DNA copy number changes called by waviCGH. The OKF4-

derived cell lines (from the same primary cells but immortalized by different methods) showed

no overlapping copy number alterations with each other; however, each of the OKF6-derived cell

lines exhibited a gain at the distal end of chromosome 5 (from bp 130 350 388 to 180 844 590).
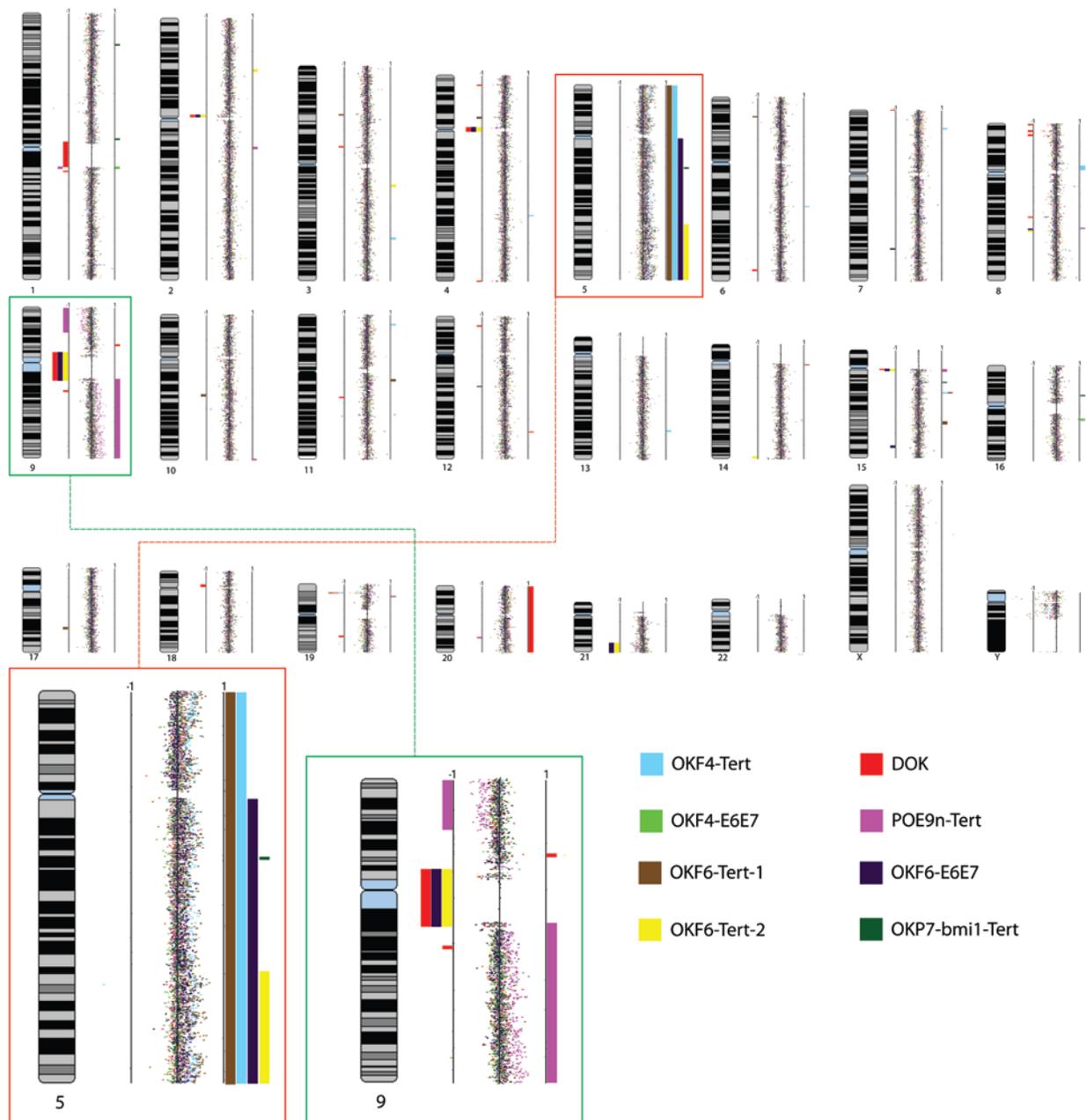
 Figure 4.1 Overview of copy number variation in eight normalized or dysplastic cell lines. Each BAC clone on the CGH array is represented by a single dot, shifts to the right represent a gain whereas shifts to the left represent a loss, the farther a clone is shifted the greater the number of copies gained or lost. Called gains and losses have been highlighted with a colored bar. Each of the eight cell lines tested are represented with a different color. Chromosomes 5 and 9 have been enlarged to show increased detail.

Table 4.2 A list of the total number of base pairs in genomic areas affected by a gain or a loss

Cell line	Total lost base pairs	Total gained base pairs	Total affected base pairs
OKF4 TERT	167 062	190 743 294	190 910 356
OKF6 TERT1	3 181 063	185 342 799	188 523 862
OKF6 E6E7	40 126 051	130 215 260	170 341 311
DOK	64 376 856	64 571 931	128 948 787
POE9n TERT	25 201 924	75 585 026	100 786 950
OKF6 TERT2	39 222 265	51 468 927	90 691 192
OKP7 bmi1 TERT	406 516	5 708 431	6 114 947
OKF4 E6E7	NA	2 445 872	2445 872

4.3.2   Genome-Wide Gene Expression Profiles

Gene expression results for 19 596 genes were obtained for each studied cell line. To determine how closely the normal and dysplastic lines resembled their parental lines—and each other—a clustering analysis was performed (Fig. 4.2). Non-immortalized primary cells did not cluster together. Immortalized cell lines did not appear to cluster with the primary cells they were derived from nor did the hTERT-immortalized cells; however, cell lines immortalized with E6 and E7 showed expression patterns very similar to each other. Additionally, clustering did not seem to be linked to i) the location in the oral cavity from which a given cell line was derived or ii) p53 mutational status.
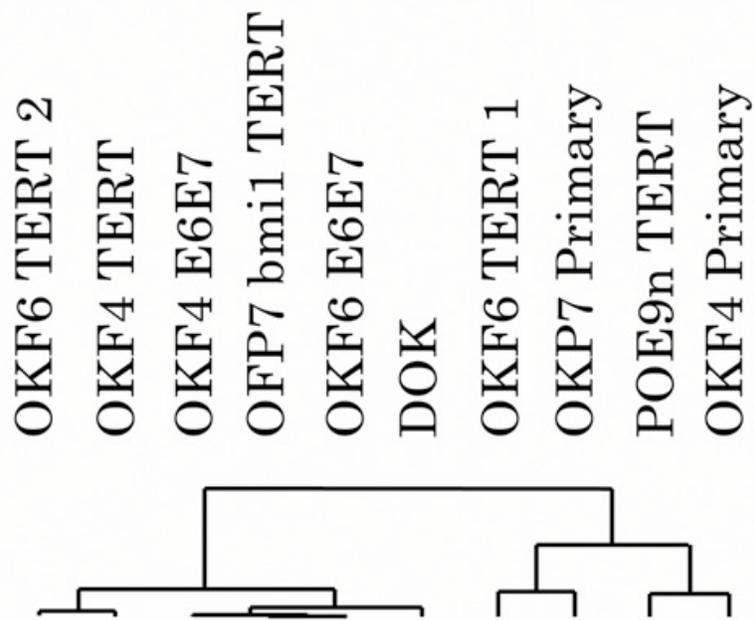
Figure 4.2 Hierarchal cluster tree for mRNA expression. The data was generated using 10 cell lines.

E6 and E7 proteins cause post-translational silencing of pRb and p53. DOK, the non-artificially immortalized dysplasia line, was known previously to have a 12 bp deletion in p53 (128). The post-translational silencing and deletion of p53 in these lines would not be expected to affect expression values. We examined the expression of p53 in the remaining cell lines to determine if cells could be bypassing cell cycle checkpoints by reducing p53 expression. The average expression of p53 in cells not known to have a p53 silencing mechanism was 64% of what it was for DOK and the E6E7 immortalized cells (which had normal levels of p53 expression when compared to normal oral tissue profiled previously [GEO reference: GSE46802] (131). This difference was not significant ($P = 0.13$). The lower p53 expression in all cell lines compared to all tissues was deemed significant by t-test ($P = 0.021$), with normal tissue having the highest average expression. A similar difference was not observed for the expression levels of pRb, which showed no consistent pattern of expression. HTERT expression is also necessary for immortalized replication and cell lines had lower levels of hTERT relative to normal tissues ($P < 0.001$). The cell line expressing the least amount of hTERT, OKF6 E6E7, expressed 52% more hTERT than was detected on average for normal oral tissue samples. Table 4.3 shows the relative expression of each cell line.

Table 4.3 The expression of telomerase reverse transcriptase in cell lines, expression is displayed in fold change relative to the average expression of normal oral tissues.

Cell Line	Fold Change TERT Expression
OKF6 E6E7	1.520381
POE9n TERT	1.531946
OKF7 bmi TERT	1.664808
OKF4 E6E7	1.680977
OKF4 TERT	1.73545
OKF6 TERT2	1.735488
DOK	1.91229
OKF4	1.982372
OKF6 TERT1	2.044107
OKP7	2.06332

Fold change analysis of mRNA expression between OKF4 TERT/OKF4, OKF4 E6E7/OKF4, and OKP7 bmi1 TERT/OKP7 cells showed 102 genes with higher expression in all three of the immortalized cells relative to the cell line they were derived from and 65 genes expressed in greater quantity in the primary lines (Supplemental Table 4.1). A large number of the deregulated genes play a role in cell cycle control, including BUB1, CCNB1, CCNB2, CDK1, MCM6, PTTG1, TGFB2, and TTK (141). Also of note were the genes related to p53 signaling: CCNB1, CCNB2, CDK1, and PMAIP1 (141). KEGG pathway analysis showed the genes from these pathways were significantly overrepresented in the list of genes dysregulated by more than 2 fold (P = 0.0001 and 0.003, respectively).

4.3.3   miRNA Expression Analysis

QRT-PCR of 742 miRNAs showed that 123 miRNAs were expressed in all cell lines and 379 miRNAs were expressed in at least one of the evaluated cell lines. The cell lines expressed an average of 260 miRNAs with a range of 147 miRNAs for OKP7 bmi1 TERT to 301 miRNAs for OKP7. Cluster analysis of miRNA expression data showed the relationship between miRNA expression for each sample (Fig. 4.3). Figure 4.3 shows that the miRNA expression was most similar between the two primary cell lines. Also of note is that the two dysplasia cell lines did not form a cluster distinct from normal cell lines.
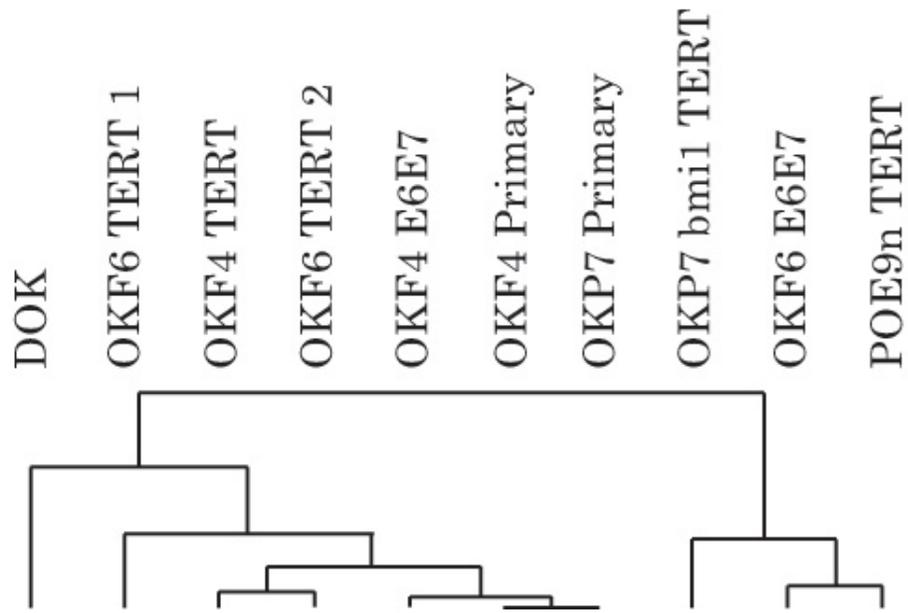
Figure 4.3 Hierarchal cluster tree for miRNA expression in the 10 cell lines tested.

To determine whether there were any similarities between miRNA expression of the immortalized cell lines and the primary lines, fold change of miRNA expression was calculated between OKF4 TERT/OKF4, OKF4 E6E7/OKF4, and OKP7 bmi1 TERT/OKP7. MiR-210 and miR-34a were down-regulated in the immortalized cell lines in all three of the pairs. MiR-200c-5p, miR-25-3p, miR-29b-1-5p, miR-877-5p, miR-93-3p, and miR-934 were all up-regulated in the immortalized lines.

4.4   Discussion

Normal cell lines are used in a large variety of laboratory applications for modeling transformation from healthy to disease states (144) and as a control for experiments examining cancer cell lines (113). Normal and dysplastic cell lines can be challenging to establish in culture as they often become senescent after a few generations (119). Consequently, fewer of these cell lines have been thoroughly characterized relative to cancer lines. One way to mitigate some of the issues facing these cell lines is immortalization; however, this may introduce alterations to the cells. It is important to note that immortalization is not the only cause of alterations in the cell lines. The OKF6 derived cell lines share a common gain in chromosome 5 (Fig. 4.1, Supplemental Table 4.2) this would suggest that the mutation was present in the primary cell line.

The cell lines OKF4 E6E7 and OKF6 E6E7 examined in this study have been immortalized with the genes E6 and E7 from the oncovirus HPV type 16 which are known to circumvent senescence and increase proliferation (145). The E6 and E7 proteins are known to post-translationally inactivate the tumor suppressors p53 and pRb (Table 4.1)(146). Previous work has shown that p53 and pRb are commonly regulated post-transcriptionally in HPV

61

negative cancers as well (147). When present, p53 and pRb can halt cell division at the G1/S division and are responsible for eliminating uncontrolled cell growth; both proteins also function to reduce and eliminate DNA damage and the elimination of these proteins can lead to increased mutation. To be able to replicate indefinitely in cell culture, one would expect all immortalized cell lines to have developed a mechanism to bypass cell cycle check points between the G1 and S phase. Our data show that regardless of immortalization method the cell lines have a mechanism for bypassing these cell cycle checks by reducing expression of p53, as well as expression alterations of other genes involved in cell cycle control for example BUB1 (Supplemental Table 4.1) which undergoes a decrease in expression in pre-senescent cells but not in immortalized lines (148). MiRNAs play an important role as well in the bypassing of theses check points. Reduced expression of miR-34a has previously been shown to impact p53 pathway signaling (149) and we detect it as down-regulated in this work as well. Conversely, the immortalized cell lines we analyzed show an increase in expression of miR-25 which is known to be increased in oral tumors (150) and to down-regulate the p53 pathway, which could also aid in the immortalization of these cell lines (151).

The ability to overcome senescence caused by telomere loss with each division is also necessary for cells to persist in culture. Five of the lines in this study were immortalized through the addition of hTERT, an enzyme subunit responsible for lengthening telomeres (123) and commonly up-regulated in germ cells, stem cells, and many cancers (152). Table 4.3 also shows that hTERT is more highly expressed in all of our primary and immortalized cell lines than it is in tissue. This demonstrates the selective pressure toward maintaining telomere length. Immortalization with hTERT has been previously shown to cause genomic alterations including gains of entire chromosomes and losses of chromosomal arms (124), but has also been shown to

increase genomic stability in tissues that are deficient for p53 (153), where p53 itself can lead to genomic instability (154). Even without large genomic alterations, hTERT is capable of inducing changes in the expression of many oncogenes and tumor suppressors (155,156). Previous work has shown that cultured keratinocytes have altered expression of genes for keratins and differentiation proteins due to differences in the local microenvironment (157,158). In contrast to our results in Table 4.2, previous literature has shown the rate of genomic mutation appears to be higher in cells that have been immortalized with E6 and E7, with karyotyping revealing ring chromosome formation and changes in ploidy status (125). This could explain the dysregulation of several cell cycle proteins in cell lines infected with E6 and E7 (159).

Also of interest is that the immortalization method used to derive a given line was not a predictor of how closely cell lines would cluster together in terms of mRNA or miRNA expression (Figs 4.2 and 4.3). MiRNA expression did seem to cause clustering based upon whether or not the cells were immortalized, regardless of method, but contrary to what would be expected this was not seen in mRNA expression. Clustering also did not appear to be due to the progenitor primary line. Clustering of gene and miRNA expression also did not appear to be based upon the site within the oral cavity that these cells derived from; this is interesting as previous work on both normal and malignant oral tissue has shown differences in the expression of mRNAs (160-162) and miRNAs (163). This emphasizes the role of micro-environment on molecular characteristics of the cells, an observation not evident when the cells are grown in the same culture environment. This would suggest that there is either an unknown factor responsible for the majority of the changes in gene expression or that many of the expression changes are random, possibly the result of changes in DNA dosage, epigenetics, or mutation in transcription factors.

A better understanding of oral cancer initiation and progression is necessary to reduce mortality rates and model systems afford an excellent means for characterizing these processes. This study identifies several molecular alterations that can be seen in immortalized and dysplastic oral cell lines. Our data suggest that cell culture derivation processes may account for a large portion of the changes in mRNA and miRNA expression we observed—and possibly a small portion of DNA alterations as well—a finding that must be considered when drawing conclusions based on using these systems. This reality should not negate the use of these systems to model disease. Rather, the results of this first-ever comprehensive molecular analysis of normal and dysplastic oral cell lines should instead be used to improve study design for work that involves these cell models.

Chapter 5: Selective Extracellular Vesicle Exclusion of miR-142-3p by Oral Cancer Cells Promotes Both Internal and Extracellular Malignant Phenotypes

5.1   Introduction

Extracellular vesicles (EVs) are a heterogeneous group of small membrane bound vesicles that include exosomes, microvesicles, apoptotic blebs and large oncosomes (164-167). Those vesicles which are smaller than 150 nm regardless of origin are referred to as small EVs (SEVs) (167). SEVs are known to contain various cargo including proteins, mRNA, and miRNAs (168). A single miRNA can alter the protein expression of several genes and has been linked to numerous disease processes, including cancer (169-171). SEVs are increasingly being evaluated as biomarkers for delineating clinical disease states (172-174), as therapeutic targets (175), and as drug delivery vehicles (176). Further, tumor-derived SEVs have also been reported to act on distant lymph nodes prior to metastasis, creating favorable conditions for angiogenesis and extra-cellular matrix changes that can prime a pre-metastatic niche that promotes subsequent metastatic tumor growth (177,178).

Packaging of miRNAs into SEVs has been reported by many as selective rather than indiscriminate (76,179,180); the mechanisms governing this process are not well understood, though they may involve protein binding to distinct sequence motifs (181-184). Small RNAs can be enriched in SEVs, with some miRNAs exhibiting much higher enrichment in SEVs as compared to the cells that produced the them (which may not contain detectable intracellular levels of a given miRNA) (76,179,180). MiRNA content in SEVs also varies based on cell type

and cell state, with miRNA content in SEVs isolated from normal cells in particular differing from miRNA content in dysplastic and cancer cells (172,185,186).

The selective packaging of specific miRNAs into SEVs in tumors implies a biological role and can be driven by selection for conditions that promote or inhibit malignancy. Significantly, some SEV-packaged miRNAs have exhibited oncogenic activity, while others demonstrate tumor suppressive functions; for example, mir-24-3p, miR-891a, miR-106a-5p, miR-2a-5p, and miR-1908 secreted from head and neck cancer cells can decrease T-cell response in the tumor stroma by targeting the Mark1 signaling pathway (17). SEV secreted miRNAs: miR-150-5p, miR-214-3p, miR-92a-3p and miR-210-3p have been shown to have pro-angiogenic roles (14,16,187,188). Alternatively healthy cells may attempt to attenuate a tumor as demonstrated by immune cells such as macrophages which can secrete growth inhibitory miR-142-3p and miR-223-3p which target Hepatocellular carcinoma cells (78).

While studies have typically focused on the role of SEV-released miRNAs in cell-cell communication, miRNAs may also be selectively packaged for SEV-mediated release as a means of eliminating a tumor suppressive factor from the cancer cell as has been reported with the miRNAs let-7 and miR-23b-3p (13,89). It is also possible that a given miRNA might have a dual role in facilitating malignant processes both locally and via cell-cell communication as these miRNAs promote angiogenesis when expressed in endothelial cells (189,190).

This thesis reports the miRNAs which are selectively secreted from oral cancer cell lines. Follow up with one of these miRNAs: miR-142-3p found that secretion of this miRNA from oral cancer cell lines promotes growth of the cancer cell by eliminating the miRNA's tumor suppressive effect. MiR-142-3p also promotes angiogenesis which in tumor xenografts leads to

decreased hypoxia. Both of these actions are mediated by the protein TGFBR1 a direct target of miR-142-3p.

5.2   Materials and Methods

5.2.1   Cell Lines

The oral cancer cell lines Cal27, SCC-4, SCC-9, and SCC-25 were obtained from ATCC and the oral dysplastic line DOK was obtained from the European Collection of Cell Cultures. Cell lines were maintained according to distributor recommendations. 293T and HMEC1 cells were received as a gift from Dr. Aly Karson and were cultured in Dulbecco's Modified Eagle's Medium supplemented with 10% fetal bovine serum (FBS) at 37°C. RNA was extracted from cells and SEVs using the miRCURY RNA Isolation Kit (Exiqon) per manufacturer instructions.

5.2.2   SEV Isolation

Cell lines were seeded into eight, 15 cm plates. Forty-eight hours before reaching 90% confluency, media was replaced with media containing 1% FBS without noticeably affecting growth. The FBS was depleted of SEVs by ultracentrifugation at 110,000g overnight in order to reduce contamination from bovine SEVs. Cells were allowed to excrete SEVs into media for 48 hours, after which the conditioned media was collected and subjected to multiple rounds of centrifugation as previously described (191). Dead cells and cellular fragments were removed from media at 4°C with centrifugation at 200g for 10 minutes, 2,000g for 30 minutes, and 10,000g for 60 minutes, with the precipitate being discarded at each interval. SEVs were precipitated using an ultracentrifuge at 110,000 g at 4°C for 70 minutes, after which the supernatant was removed and the pellet was rinsed with PBS. SEVs were re-precipitated with an

67

additional 110,000g spin for 70 min. RNA was extracted from both SEVs and cells from one of the plates excreting SEVs as described above. Previous researchers have suggested this method might lead to contamination from bovine miRNA not removed by SEV depletion (192,193), and therefore the SEV isolation procedure was performed on non-conditioned media with 1% depleted FBS. Supplemental Figure 5.1 demonstrates a decrease in miRNA below the threshold of detection. Transmission electron microscopy (TEM) images were prepared by absorbing a PBS-suspended sample on 200 mesh formvar-coated nickel grids, allowing the sample to dry, and then fixing the sample by floating the grid on a drop of 1% glutaraldehyde for 10 min. Negative staining was performed by floating the grid on a drop of 1% Uranyl acetate for 1 min. Grids were viewed on a Tecnai 12 microscope.

5.2.3   Western Blotting

Protein was collected through lysis with radioimmunoprecipitation assay (RIPA) buffer supplemented with 1:100 protease inhibitor (Life Technologies) and phosphatase inhibitor cocktail I & II (Sigma-Aldrich). Protein was quantified using a Bicinchoninic Acid Protein assay kit (Life Technologies). 10 µg of protein was separated using NuPAGE 4–12% Bis-Tris Gels (Life Technologies) and transferred to polyvinylidene difluoride membranes (Millipore). Membranes were blocked in 5% BSA, 1X TBS, and 0.1% Tween-20 at room temperature for 1 hour. Membranes were then incubated overnight at 4°C with the appropriate primary antibody: 1:1000 diluted anti-CD63 (EXOAB-Cd63A-1, System Biosciences), anti-TSG101 (ab83, Abcam) or anti-phospoSMAD2/3 (8828 Cell Signaling) antibodies or 1:2000 diluted anti-TGFBR1 (AF3025, R&D Systems).

After washing the antibodies were incubated with peroxidase-conjugated 1:2000 Anti-Rabbit (7074, Cell Signaling Technology), Anti-Mouse (NXA931, GE Healthcare), or Anti-Goat (6741, Abcam) antibodies. For TGFBR1, anti-GAPDH (1:4000) (2118, Cell Signaling Technology) was used as a loading control. Detection was performed using Amersham ECL Western Blotting Detection Kit (GE Healthcare). To quantitatively assess western blot images of TGFBR1 expression, the 'gel analysis' function in the ImageJ program (http://imagej.nih.gov) was used and normalized to GAPDH expression.

5.2.4   Real Time PCR

QRT-PCR was used to identify miRNAs differentially expressed in cells as compared with SEVs. Reverse transcription was performed on 40 ng of RNA using an Exiqon Universal cDNA synthesis kit, and qRT-PCR was performed using Exiqon's SYBR based microRNA Ready-to-Use PCR, Human Panel I+II V2.M as previously described (194) to test for the expression of 742 miRNAs. Verification analysis on individual miRNAs was performed on 100 ng of RNA using TaqMan miRNA reverse transcription kits and TaqMan Universal Master Mix II and MicroRNA assays for qRT-PCR (Life Technologies). All assays were performed in triplicate per manufacturer protocol. TaqMan High-Capacity cDNA reverse transcription kits, Gene Expression Master Mix, and Gene Expression Assays (Life Technologies) were used to assess impacts of SMPD3 and Rab27A knockdown.

5.2.5   Statistical Analysis of miRNA Data

Pre-processing of SYBR miRNA qRT-PCR data were completed as previously described (170). We performed a paired analysis to identify miRNAs that were differentially expressed

between SEVs and their parental cell lines (i.e. the cells that gave rise to them). MiRNAs were considered enriched if 1) a >4-fold difference in expression was noted between SEV and cellular fractions following normalization to the global mean of miRNA expression (143) or 2) a given miRNA was detected in one fraction (either cell or SEV) at a CT below 33 and not detected (at a CT below the threshold of detection: 35) in the matched fraction for all of the cell lines tested. For follow-up miRNA analysis, cellular miRNA quantification was normalized to the expression of U6. As there is no known endogenous control for SEV miRNAs, follow-up quantification was performed with expression normalized to the cel-miR-39 spike-in control (Qiagen). Analysis of knockdown efficiency of SMPD3 and Rab27A expression was normalized to GAPDH.

5.2.6 Over-expression and shRNA Vectors

Over-expression FIV lenti-vectors were purchased from GeneCopoeia for miR-142-3p (HmiR02082-MR01) and a scramble sequence control (CmiR0001-MR01) (hereafter miR-142 OE and OE Control). The miR-142 OE vector produces both 3p and 5p strands. Vectors were packaged using 293T cells and a GeneCopoeia Lenti-Pac FIV Expression Packaging Kit (FPK-LvTR) according to the manufacturer's recommendations. For knockdown of Rab27A, shRNA vectors were purchased from Dharmacon. Five vectors were purchased to determine knockdown efficiency (TRCN0000005294, TRCN0000005295, TRCN0000005296, TRCN0000005297, TRCN0000005298) the 2 vectors with the highest efficiency were used for ongoing analysis (TRCN0000005295, TRCN0000005296 hereafter 5295 and 5296 respectively). Empty pLKO.1 was used as a control. SEV staining vector pCT-CD63-GFP was purchased from SystemBio. For rescue experiments a TGFBR1 open reading frame (ORF) clone (TRCN0000488036) within a pLX_TRC317 vector as well as an empty vector control were purchased from Sigma Aldrich

(hereafter TGFBR1 ORF and Control ORF). Lentivirus was created using 293T cells with each shRNA, GFP or ORF plasmid, packaging plasmids VSVG and d8.91 using TransIT-LT1 transfection reagent (Mirus). For all vectors, virus-containing conditioned media was collected over 3 days post transfection and filtered using 0.45 μm filters and stored at -80°C. Cells were selected over 10 days using either 400 μg/mL G418 (over-expression lines) or 2 μg/mL puromycin (shRNA, ORF and GFP lines).

5.2.7   MTT Cell Proliferation Assay

Stably infected miR-142 OE cells and their controls were plated in 6 wells of five 96 well plates at a density of 1000 cells for DOK infected with either miR-142 OE, OE Control, or combined miR-142 OE/TGFBR1 ORF, or miR-142 OE/Control ORF. 500 Cal27 cells infected with the same vectors were plated with 500 cells per well. Cell viability was measured once a day for 5 days using Colorimetric thiazolyl blue tetrazolium bromide (Sigma-Aldrich) as previously described (195) with the highest and lowest value from each condition being discarded. Statistical significance was determined using Student's *t*-test on day 5 with a cutoff value of $P < 0.05$.

5.2.8   Soft Agar Colony Formation Assay

A 12-well plate was filled with a bottom layer of 0.5% low melting point (LMP) agarose. A layer made with 2000 cells from both Cal27 OE Control and Cal27 miR-142 OE lines in 0.37% LMP agarose was added on top of the bottom layer. After four weeks the number of colonies per well was counted for both lines. All experiments were performed in triplicate. Colonies which consisted of at least 15 cells were counted.

71

5.2.9 Tube formation Assay

HMEC1 cells were grown on a 96 well plate and upon reaching 50% confluency SEVs were added to the cell culture media. SEVs were isolated from one, 15mm plate of Cal27 CD63-GFP cells and diluted in 100µl of DMEM media. This was performed in triplicate. HMEC1 cells were grown in SEV containing media for 24 hours after which the media was replaced with un-modified DMEM. White and fluorescent images were taken using phase contrast on an Axiovert S1000 microscope. This was also performed with SEVs isolated from Cal27 miR-142 OE or Cal27 OE Control with RNA being extracted after 24 hours.

Tube formation assays were performed by the addition of 100 μL of growth factor reduced Matrigel (Corning) at 10 mg/mL to each well of a 24 well plate. The day before the assay HMEC1 cells were grown to 80% confluency then serum starved over night. Three wells of 4.56×10^3 HMEC1 cells were plated in 100 μL DMEM supplemented with 1% FBS on matrigel plates. SEVs isolated from one, 15mm plate of Cal27 miR-142 OE or Cal27 OE Control and diluted in 10µl of PBS were added to the cell culture medium. As a control 10µl PBS was also used. This was performed in triplicate for each treatment group. To test the effect of the miRNA in isolation HMEC1 miR-142 OE or HMEC1 OE Control cells were plated using the same conditions without the addition of SEVs. All tube formation experiments were repeated with 1×10^4 HMEC1 cells infected with TGFBR1 ORF or Control ORF vectors to determine the contribution of TGFBR1 to the observed phenotype. Images were taken after 16 hours using differential interference contrast. The average tube length among three replicates was calculated using the ImageJ macro 'Angiogenesis Analyzer'.

5.2.10 Tumor Xenografts

Immunocompromised NOD-SCID mice were bred and housed in the Animal Resource Center at the BC Cancer Research Center under pathogen free conditions. All experiments were performed in accordance with UBC and Canadian Council on Animal Care guidelines. Male mice were injected subcutaneously with 2 million Cal27 cells infected with either Rab27A shRNA (n = 7), Control shRNA (n = 8), miR-142 OE (n = 8) or OE Control (n = 7) vectors. After injection, caliper measurements of tumors were taken twice a week. Volume was calculated as a half ellipsoid using the formula length x width x height x $(4\pi/6)$. Mice were euthanized on post-injection day 33 (Rab27A shRNA and Control shRNA tumors) or day 35 (miR-142 OE or OE Control tumors). Ninety minutes prior to euthanasia, mice were injected with Intraperitoneal pimonidazole (PIMO) (100 mg/kg), which binds to hypoxic cells, and bromodeoxyuridine (BrdU) (90mg/kg), which incorporates into replicating DNA and 10 minutes prior to euthanasia with intravenous Hoechst 33342 (Hoechst) (25 µg/mouse) to demarcate perfused vasculature. Tumors were resected, weighed, and then bisected along the sagittal plane and frozen in Optimal Cutting Temperature compound.

5.2.11 Immunofluorescence

10 µm serial sections were taken from the center of each tumor. Sections were stained with endothelial cell marker 1:200 anti-CD31 (553370, BD Pharmingen) for 90 minutes followed by 1:100 Alexa Fluor 594 conjugated secondary antibody (A-11007, Thermo Fisher) for 30 min, and then 1:1000 FITC conjugated anti-PIMO (4.3.11.3, Hypoxyprobe Inc) for 90 min. Subsequent sections were incubated in 2M HCl/0.1% Triton X-100 for 10 min to denature DNA and expose BrdU, then triple stained in sequence with 1:100 anti-BrdU (ab6326, Abcam)

for 90 min, 1:100 Alexa Fluor 594-conjugated secondary antibody for 30 min, 1:1000 FITC-conjugated anti-PIMO for 90 min, and 0.1 µg/mL DAPI for 5 min. All slides were mounted with Vectashield (H-1000, Vector Laboratories). Acid washing removed Hoechst staining, and removed background green fluorescence, therefore perfusion was quantified from the first set of slides and hypoxic PIMO staining was quantified from the second set of slides. Whole cross-section tiling images were taken under 10X objective magnification with a Zeiss Imager Z1 using a QImaging Retiga 4000R camera with Northern Eclipse software and staining was quantified using ImageJ as previously described (196). Images were captured in black and white for each emission spectrum and then combined in false color.

5.3   Results

5.3.1   Identification of miRNAs Under Selection

To identify miRNAs that are selectively released and/or retained via SEVs in oral cancer and dysplasia cells, SEVs were collected from Cal27, SCC-4, SCC-9, and SCC-25 cancer cell lines and oral dysplasia cell line DOK by centrifugation (191). Western blots for known exosomal proteins CD81 and TSG101, as well as Histone H3 (which is not expected to be present in SEVs) were performed on all SEV extracts and compared to protein levels in donor cells (Fig. 5.1A) (197). TSG101 and CD81 were increased in the SEV fraction of all samples relative to donor cells, while H3 was strongly expressed in donor cell fractions and only detected at negligible levels in SEV fractions. This suggests that the isolated SEVs were enriched for exosomes with the possible inclusion of other similarly sized vesicles and particles. SEVs were further characterized using transmission electron microscopy (TEM) on isolates from SCC-4 and Cal27 cells (Fig. 5.1B and C), and NanoSight on isolates from DOK and Cal27 cells (Fig, 5.2A

and B, black lines), with both tests showing a largely homogenous population of vesicles of approximately 100 nm in diameter.
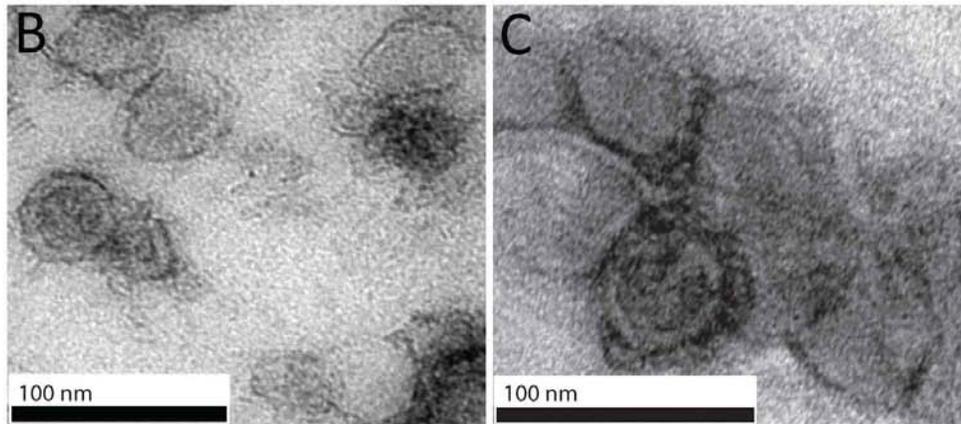
Figure 5.1 The isolation of SEVs. A: Western blot on 10ug of protein isolated from SEVs for exosome enriched markers TSG101 and CD81; and negative control Histone H3. (C refers to the cellular fraction and S to SEV). B, C: Uranyl acetate negative stained TEM images, of SEVs isolated from SCC-4 (B) and Cal27 cell lines (C).

There is substantial discussion on the correct nomenclature of SEVs and what is frequently referred to as 'exosomes' in experiments on their functional role, i.e. small EVs derived from ultracentrifugation, may not meet more strict definitions of exosome, in other words endosomally derived small vesicles which may share common protein markers with other vesicles (167,198). For the purpose of this thesis we will refer to ultracentrifuge derived vesicles as SEVs with the understanding that this is a mixed population of ~100 nm particles, that is enriched for category III EVs including exosomes as defined by Kowal *et al.* (167).

RNA was isolated from all cell lines, as well as matched SEV samples and analyzed using qRT-PCR. Donor cells exhibited expression of 27-34% of the 742 miRNAs examined, while SEVs expressed 27-39% of these 742 miRNAs. One hundred thirty-one miRNAs were detected in both the donor cell and SEV RNA populations from all five cell lines. Using a 4-fold expression difference threshold to determine enrichment in either donor cells or SEVs, each cell line had an average of ten miRNAs enriched in donor cells and 17 miRNAs enriched in SEVs. Top candidates were selected based on the frequency with which four-fold expression differences were noted. The miRNAs enriched in all SEV samples were: miR-142-3p, miR-150-5p, miR-451a, and miR-223-3p. In addition, miR-126-3p was enriched in 4/5 lines, while miR-126-5p, miR-144-3p, and miR-605-5p were enriched in 3/5 lines. Candidate miRNAs enriched in SEVs were not detectable in the cellular fraction in most instances. The only miRNA candidate enriched in all donor cells was miR-502-5p, which was not detected in any SEV fraction. MiR-197-3p was enriched in 3/5 donor cell fractions, though still detectable in SEVs. The majority of miRNAs detected were not enriched, and instead had similar levels in both the SEV and donor cell fractions (Supplemental Figure 5.2).

5.3.2 Inhibition of SEVs Excretion Increases Cellular miRNA Concentration

To determine if miRNA candidates were extracted from SEVs and not co-precipitating factors, we blocked exosome release and assayed for miRNA expression within cells. Multiple known pathways mediate exosome formation and release. One method involves transformation of membrane sphingomyelin to ceramide, creating a vesicle inside a multivesicular body. This pathway is catalyzed by SMPD3 (199). Downstream, Rab27A mediates transport of multivesicular bodies to plasma membranes and vesicle docking that drives extracellular release of their exosome content (200). SMPD3 was detectable in only one of the oral dysplasia/cancer cell lines by qRT-PCR (Supplemental Fig. 5.3 A), a finding that is consistent with our knowledge of SMPD3 expression in oral tumors (131). As Rab27A was highly expressed (Supplemental Fig. 5.3 A), we silenced it using two different lentiviral shRNAs. In Cal27 cells, knockdown efficiency for shRNA 5295 was 89% and for shRNA 5296 was 96%. In DOK cells, knockdown efficiency for shRNA 5295 was 94% and for shRNA 5296 was 95% (Supplemental Fig. 5.3 B). Knockdown of Rab27A led to a decrease in SEV secretion shown by NanoSight analysis, which also determined that vesicles from Rab27A knockdown and control cell lines were similar in size (Fig. 5.2A and B). Silencing Rab27A resulted in an increase in the intracellular content of all candidate miRNAs except for miR-451a, which was not detectable in the cells. Depending on the cell line and shRNA used, miR-150-5p and miR-223-3p exhibited variable increases in expression (Fig. 5.2C). MiR-142-3p was consistently increased >4-fold intracellularly in each cell line following treatment with both Rab27A shRNAs (Fig. 5.2C). SEVs from the Cal27 Rab27A knockdown lines were extracted and profiled for miR-142-3p expression. Knockdown of Rab27A decreased the amount of miR-142-3p excreted from cells by 50.8% and 50.3% with shRNA vectors 5296 (p=0.03) and 5295 (p=0.01) (Supplemental Fig. 5.3

C). With the exception of miR-451a these results suggest an association of the candidate miRNAs with exosomes. MiR-451a, may be associated with Rab27A independent exosomes or other vesicular or non-vesicular factors as suggested by others (11,12).
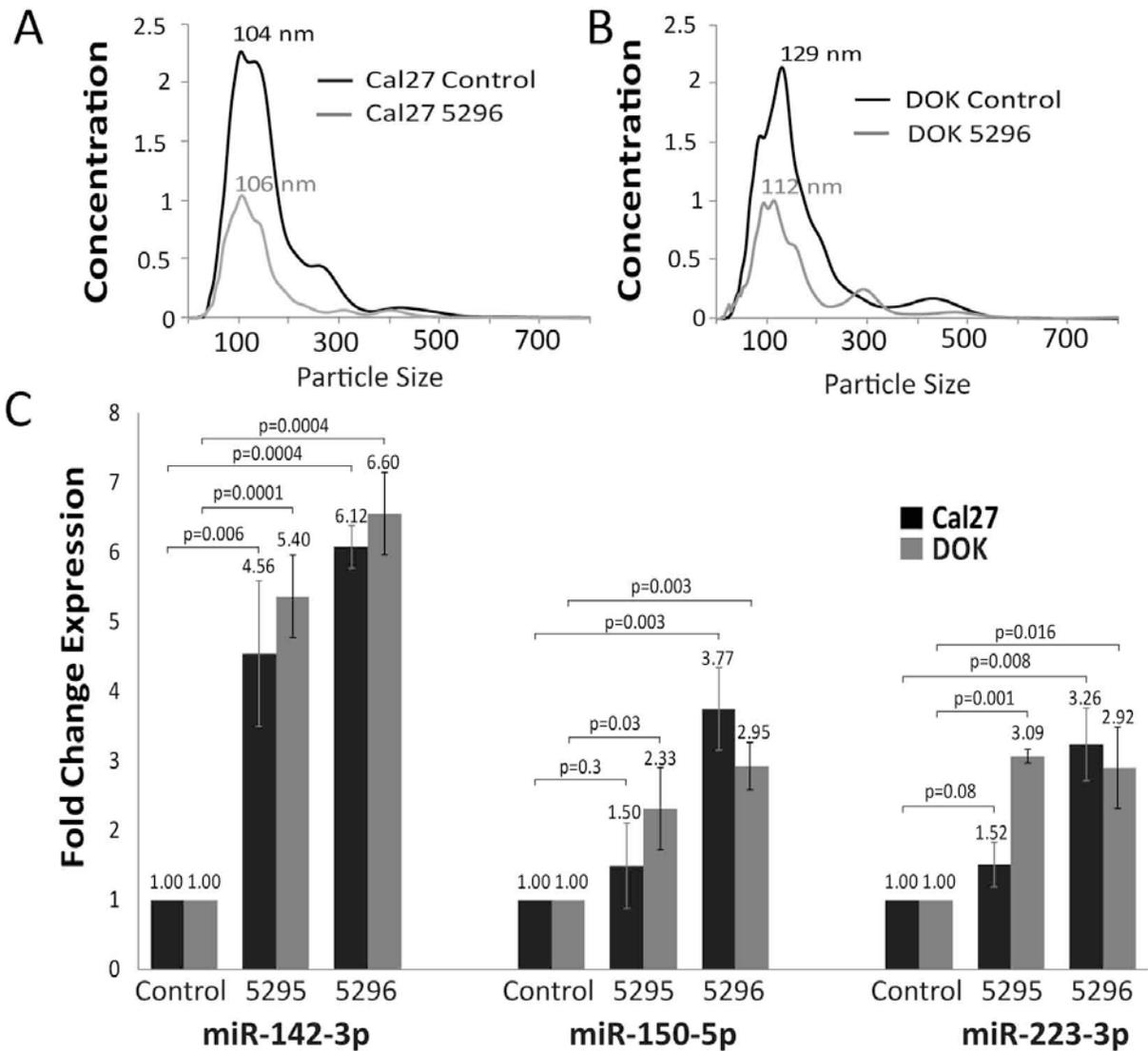
Figure 5.2 Result of exosome release inhibition. A, B: NanoSight determined size distribution of particles obtained during SEV precipitation in Cal27 (A) and DOK (B) cells with either a Control shRNA vector or Rab27A KD 5296 vector. Concentration represents 10^9 particles per ml. C: Cellular fraction fold change RT-PCR expression values of miR-142-3p, 150-5p and 223-3p in Cal27 and DOK cells after Rab27A knock down compared to control cell lines (n=3) error bars represent standard deviation and P values were determined by Student's t-test on delta delta CT levels.

5.3.3   TGFBR1 is a Target of miR-142-3p

A literature search for potential targets of miR-142-3p using PubMed and GeneRIF (201) revealed TGFBR1 as the only candidate that showed interaction with miR-142-3p in epithelial cancers (202) and has correlates with oral cancer progression (202,203). These findings are consistent with previous gene expression data showing a decrease in TGFBR1 expression in oral cancer cell lines compared to normal primary lines (111,194,204). Additionally it is well established that the 3'UTR of TGFBR1 is capable of binding miR-142 3p (202,205)

To determine if miR-142-3p targets TGFBR1 in OSCC, we stably over-expressed miR-142-3p in Cal27 and DOK cells (creating miR-142 OE lines). To confirm that increased miR-142-3p was excreted via SEVs, SEVs from Cal27 miR-142 OE and Cal27 OE Control cells were collected and qRT-PCR was performed on RNA collected from each cell type. This analysis demonstrated that miR-142-3p was increased 8.71 fold in SEVs collected from miR-142 OE cells as compared with OE Control cells (Supplemental Fig. 5.3 D). A western blot for TGFBR1 expression in these cells confirmed a decrease in TGFBR1 expression (Fig. 5.3A). Analysis of western blot results showed that miR-142-3p over-expression was associated with a decrease in TGFBR1 expression by 70.1% in DOK cells and 40.0% in Cal27 cells. This led to a decrease in the phosphorylation of downstream genes SMAD2 and SMAD3 (Supplemental Fig 5.3 E). Western blots on Cal27 Rab27A KD 5295 and DOK KD 5295 showed no effect (not shown) on TGFBR1 expression. Rab27A's known role is to traffic exosomes to the plasma membrane, this may suggest that miR-142-3p is sequestered within the cell.
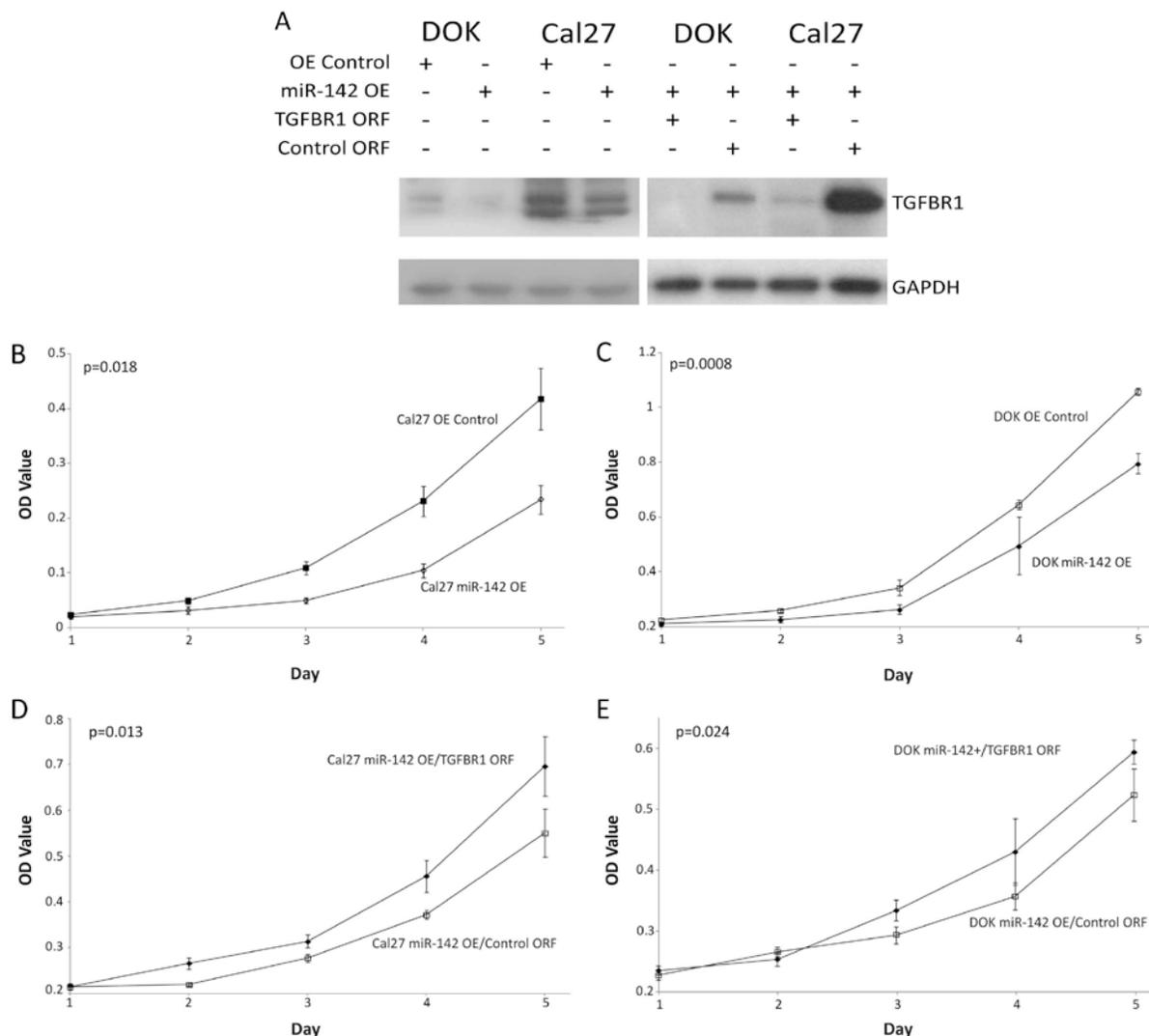
Figure 5.3 Effects of miR-142-3p over-expression. A: Western blot for TGFBR1levels in DOK and Cal27 with miR-142 OE or OE Control vectors, percent change values were calculated in ImageJ with levels normalized to GAPDH, and show a decrease in TGFBR1 expression of 70.1% in DOK and 40.0% in Cal27. Additionally Cal27 and DOK miR-142 OE cells were infected with TGFBR1 and Control ORF rescue vectors and shown at a lower exposure time. The growth of B,D: Cal27 and C,E: DOK by MTT proliferation assay, B and C demonstrating the effect of miR-142-3p over-expression and D,E demonstrating phenotypic rescue by the addition of TGFBR1 ORF vector. P values were determined by Student's t-test on the final day, error bars represent standard deviation.

5.3.4   MiR-142-3p Decreases the Growth Rate of Oral Cell Lines

Cal27 and DOK miR-142 OE and OE Control cell lines were tested for the effect of

increased miR-142-3p on cellular proliferation using an MTT assay (Fig. 5.3B and C). MiR-142-

3p had a significant inhibitory effect on the growth of DOK and Cal27, a finding that is

consistent with the known role of TFGBR1 (206). This effect was abrogated by the co-infection

of Cal27 and DOK miR-142 OE lines with TGFBR1 ORF clones lacking the 3'UTR binding site

of miR-142-3p (Fig. 5.3D and E). To analyze the effect of miR-142-3p increase on anchorage

independent growth a colony formation assay was performed on Cal27 cell lines with either the

miR-142 OE or Control OE vectors added (Supplemental Fig. 5.3 F). (DOK cells were excluded

from this assay as dysplastic cells do not form colonies). From three replicates, Cal27 OE

Control cells grew 2.8 fold more colonies on average compared to Cal27 miR-142+ (p = 0.002).

No differences in colony size were noted. Taken together, these data suggest that over-

expression of miR-142-3p in oral cancer and dysplasia cells is associated with reduced

carcinogenicity *in vitro* at least partially due to by decreasing TGFBR1 expression.

5.3.5   MiR-142-3p Induces Angiogenesis *in vitro*

CD63 is associated with intracellular vesicles and SEVs. Fluorescent SEVs from Cal27

cells expressing GFP-labeled CD63 were added to the media of HMEC1 cells growing in 96-

well plates and examined under a fluorescent microscope after 48 hours (Fig. 5.4A). Uptake of

fluorescent SEVs was observed in the HMEC1 cells in a perinuclear fashion.
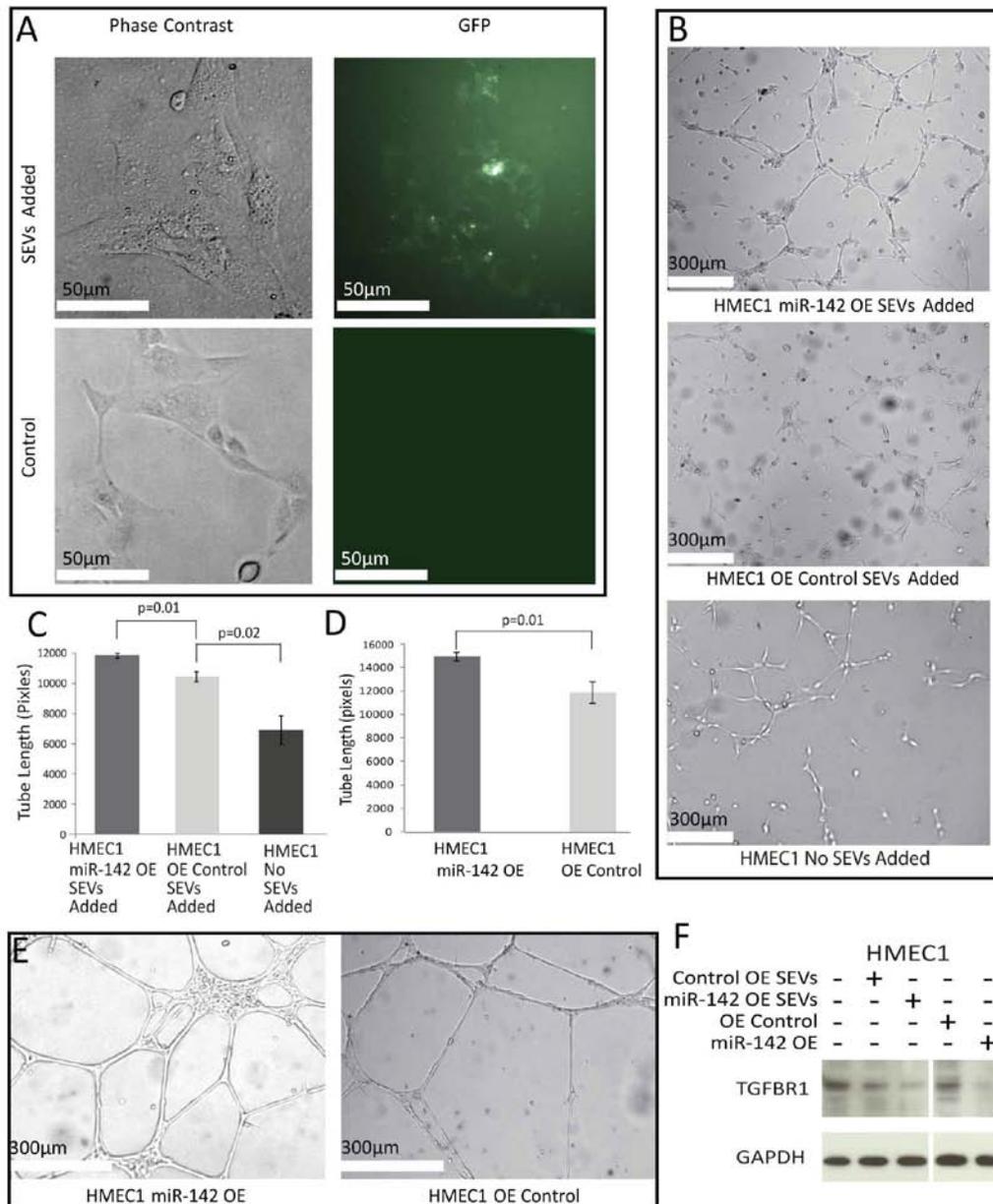
Figure 5.4 Effects of SEV Transfer. A: White light and fluorescent images of HMEC1 cells with and without the addition of CD63-GFP stained SEVs under phase contrast. All tube formation assay images were taken 16 hours after seeding. B: Tube formation assay on HMEC1 cells with the addition of SEVs from Cal27 OE Control and Cal27 142 OE. C,D: Average length of formed tubes, with SEV addition to HMEC1 cells (C) or over-expression of miR-142-3p (D). Averages were measured in three fields of view across three wells; error bars represent standard deviation and p values were determined by Student's t-test. E: Tube formation assay in HMEC1 cells over-expressing miR-142-3p or the OE Control vector. F: Western blot for TGFBR1 and GAPDH comparing the levels in HMEC1 cells after the addition of SEVs extracted from Cal27 OE Control or Cal27 miR-142 OE cell lines and HMEC1 cells expressing miR-142 OE or OE Control vectors. Percent change values were calculated in ImageJ with levels normalized to GAPDH; there was a decrease of 36% and 79% respectively in the levels of TGFBR1 between cells given OE Control SEVs and cells given miR-142 OE SEVs when compared to cells given no SEVs. There was a decrease of 78% TGFBR1 levels between HMEC1 OE Control cells and HMEC1 miR-142 OE cells.

When expression of TGFBR1 is lower in endothelial cells it has been shown to reduce apoptosis and increase proliferation (207). *In vitro* tube formation assays are a common surrogate of angiogenesis (208). To determine if SEVs and, more specifically, miR-142-3p within SEVs has an impact on angiogenesis, we added SEVs from Cal27 142 OE and Cal27 OE Control to the media of a tube formation assay performed on HMEC1 cells (Fig. 5.4B). All treatment groups were capable of forming tubes, with miR-142 OE SEVs stimulating development of tubes approximately 1.14 times longer than cells that received SEVs from OE control Cal27 cells. HMEC1 cells with OE Control SEVs added, developed tubes approximately 1.54 times longer than those observed in cells that were not exposed to SEVs (Fig. 5.4C). The difference in tube formation between HMEC1 cells with OE Control SEVs and no SEVs could be due to the transfer of the wild-type quantity of miR-142-3p, or could be due to the inclusion of other factors known to effect angiogenesis for example mIR-150-5p (14). To confirm that miR-142-3p was responsible for at least a proportion of the increase in angiogenesis, the experiment was repeated on HMEC1 cells expressing the miR-142 OE or OE Control vectors with no SEVs added (Fig. 5.4D and E). A similar trend was observed with miR-142-3p over-expression causing a significant 1.2-fold increase in tube length relative to HMEC1 cells receiving the OE Control vector. Taken together, these data suggest that miR-142-3p is one factor present in SEVs capable of inducing angiogenesis. The same target of miR-142-3p identified in oral cancer cells, TGFBR1, showed a decrease with the addition of miR-142-3p to endothelial cells both via over expression and the addition of SEVs (Fig. 5.4F).
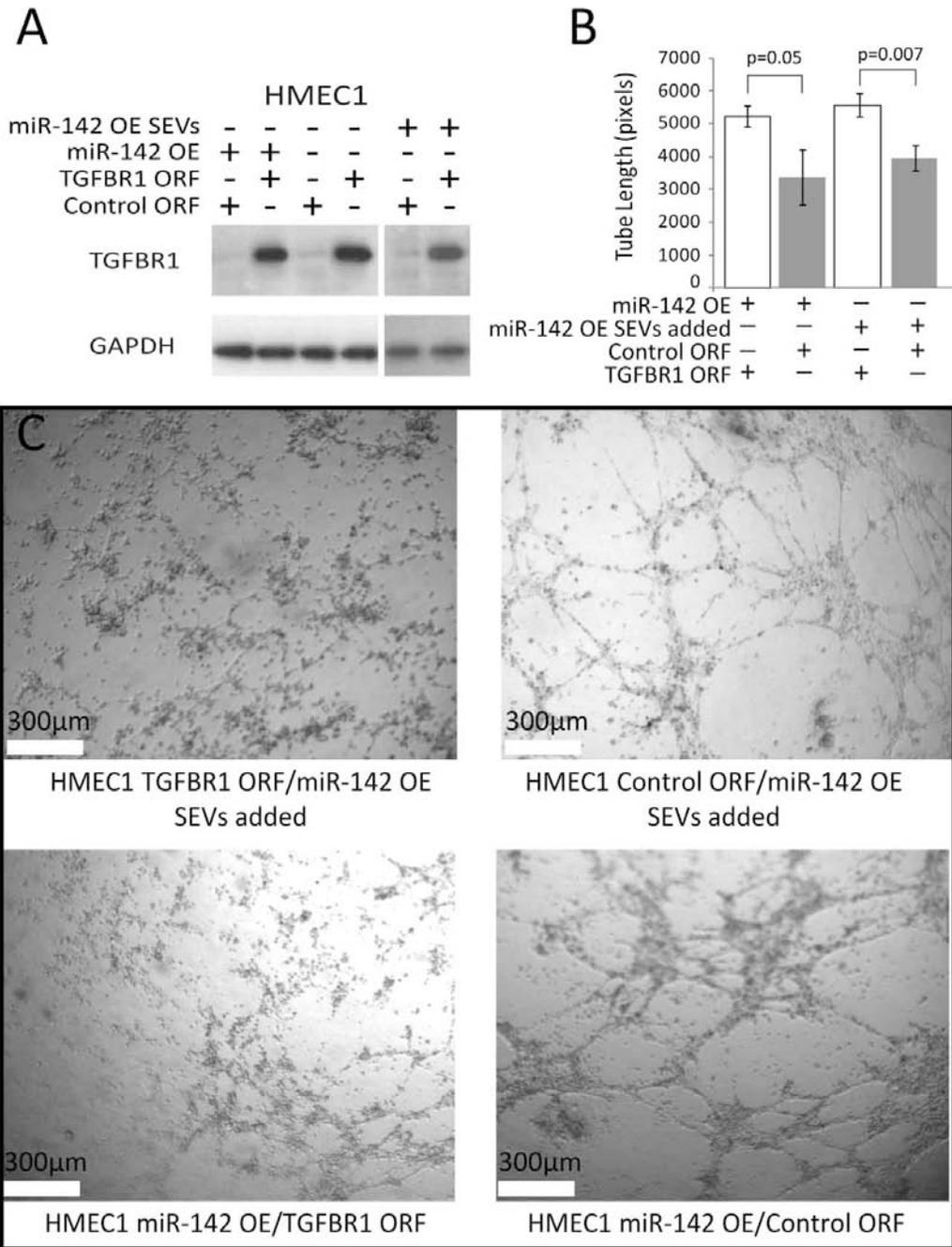
Figure 5.5 Tube Formation Phenotypic Rescue. A: Western blot for TGFBR1, compared to the loading control GAPDH, for HMEC1 cells expressing TGFBR1 ORF or Control ORF vectors, with the addition of miR-142-3p from direct over-expression or the addition of SEVs from Cal27 miR-142 OE. B: Average length of tubes formed in HMEC1 cells expressing TGFBR1 ORF or Control ORF rescue vectors, with either co-expression of miR-142 OE vector or addition of Cal27 miR-142 OE SEVs. Error bars represent standard deviation and P values were determined by Student's t-test. C: Tube formation micrographs of HMEC1 rescue lines.

In order to confirm that alterations to TGFBR1 expression were not incidental to the findings of alterations in tube formation a phenotypic rescue was performed by the addition of exogenous TGFBR1 with an altered 3'UTR, allowing for high TGFBR1 expression in the presences of miR-142-3p (Fig 5.5 A). TGFBR1 over expression caused a decrease in tube formation of 33% in HMEC1 cells over expressing miR-142-3p, and a decrease of 29% when SEVs from Cal27 miR-142 OE were added (Fig. 5.5 B and C).

5.3.6 Secreted miR-142-3p is Associated with Increased Vascular Density in vivo

We were interested in whether SEV secretion and miR-142-3p over-expression affected primary tumor growth and the solid tumor microenvironment. Attempts to inhibit the secretion of only miR-142-3p by MISSION miRNA inhibitors (Sigma-Aldrich) were unsuccessful as the inhibitory effect was not transferred into SEVs and donor cell expression of miR-142-3p was already low. To determine the effect of reducing SEV production on tumorigenesis, we subcutaneously implanted Rab27A knockdown cells (which reduced secretion of SEVs and as a result, global secreted miRNA content) in SCID mice. Rab27A knockdown tumors showed decreased growth, blood vessel density, and vascular function, and increased tumor hypoxia (Fig. 5.6 and 5.7).
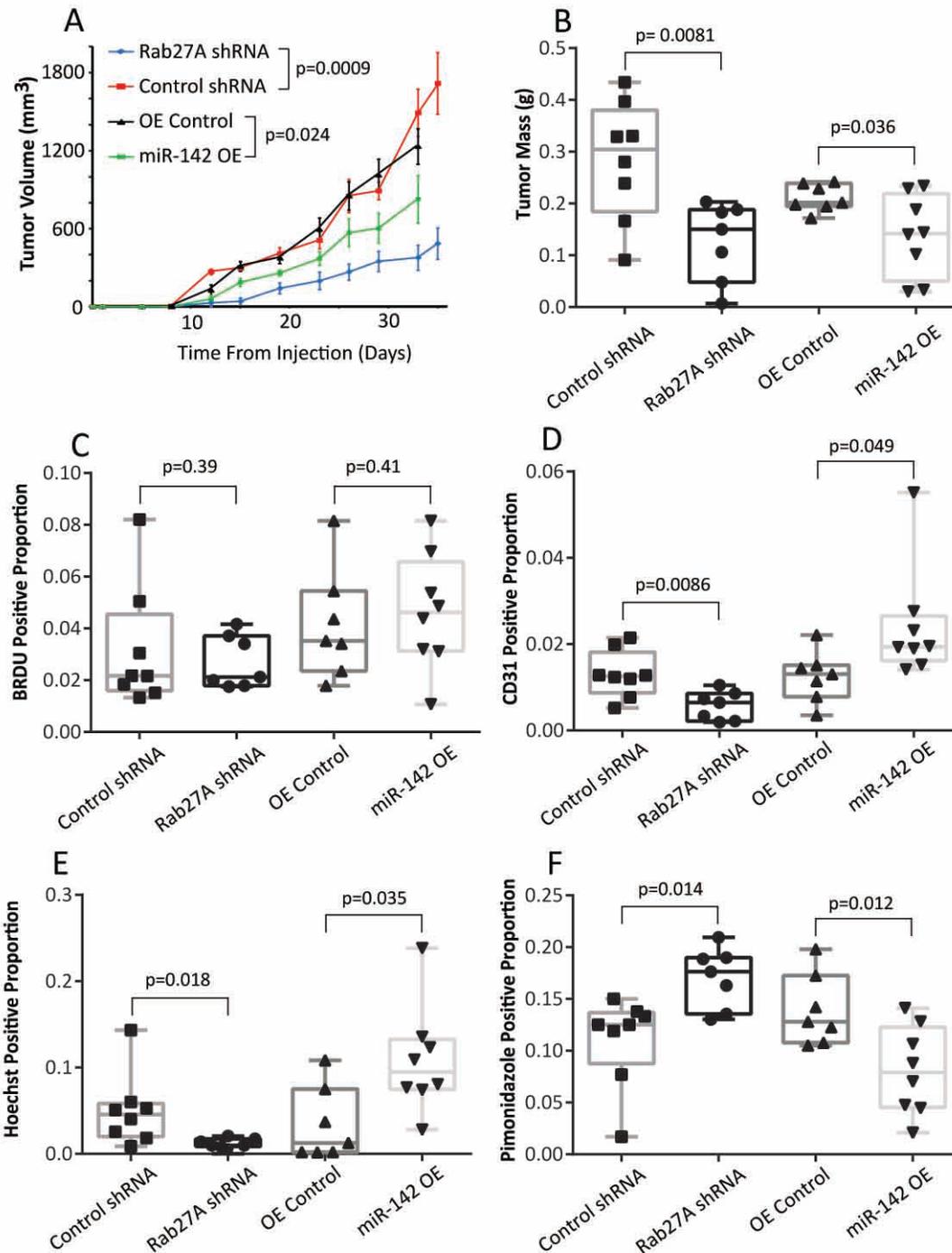
Figure 5.6 Tumor Xenografts. A: Average tumor volume over 35 days measured twice weekly in mice injected with 2 million Cal27 cells with Control shRNA (n=8), Rab27A 5296 shRNA (n=7); or the over-expression vectors OE Control (n=7) or miR-142 OE (n=8). Error bars represent standard error. B: Tumor mass taken upon excision on day 35 of Rab27A and Control shRNA tumors and on day 33 of miR-142 OE and OE Control tumors. Box plots showing BRDU positive nuclei relative to all nuclei (C); Blood Vessel CD31 staining (D) Hoechst perfusion staining (E) and Pimonidazole Hypoxia staining (F) relative to tumor area. A-F: All p values were calculated with Student's t-test.
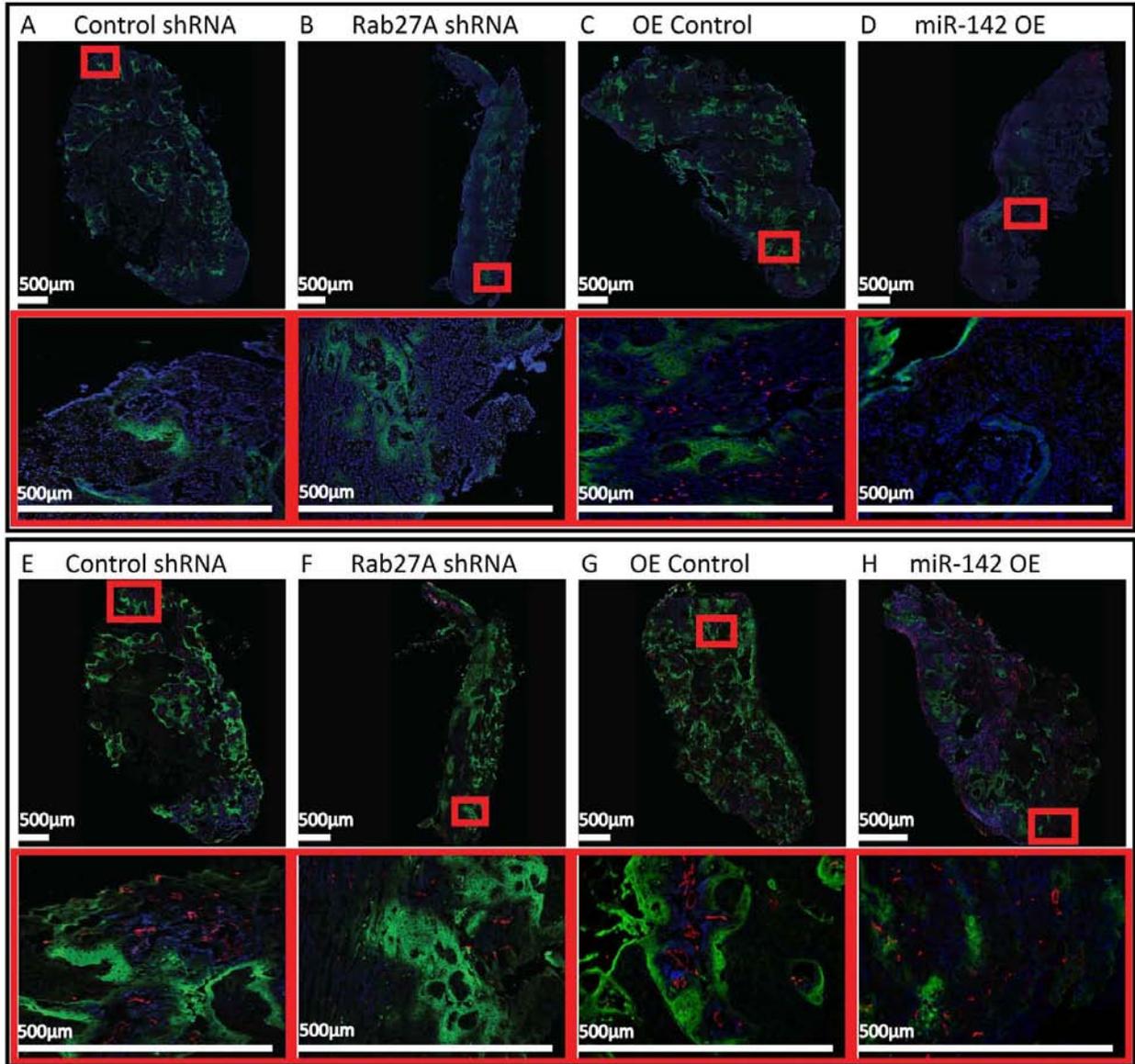
Figure 5.7 Tiling images of tumor cross sections. Images are shown with their associated higher magnification images in red boxes. Staining for all nuclei with DAPI (Blue), BRDU (Red), and Pimonidazole (Green) A-D; and Injected Hoechst (Blue), CD31 (Red) and Pimonidazole (Green) E-H. With Control shRNA (A,E), Rab27A shRNA (B,F) OE Control (C,G) and miR-142 OE (D,H) tumors.

To further elucidate the function of miR-142-3p *in vivo*, we analyzed the impact of miR-142-3p over-expression in mouse xenograft models of oral cancer. Mir-142-3p over-expression significantly decreased the growth rate of implanted tumors (Fig. 5.6A and B), consistent with our cell culture findings that indicated that miR-142-3p has an intracellular tumor suppressive effect. We were interested in determining if there was a difference in the proliferative fraction of cells in the primary tumor and therefore measured staining with BrDU which incorporates into cells in S-Phase. No differences were observed between treatment groups (Fig. 5.6C). Interestingly, miR-142-3p over-expressing tumor xenograft tissues also showed increased vascular density (Fig. 5.6D). The increased number of endothelial cells resulted in an increase in tissue perfusion, suggesting that the blood vessels were functional (Fig. 5.6E). Increased miR-142-3p also led to a decrease in tumor hypoxia (Fig. 5.6F), though hypoxia may be caused by either under-supply or over-consumption of O_2. This was determined using BrdU a synthetic analog of thymidine which incorporates into DNA that has been replicated in the 90 minutes between injection and euthanasia. No significant differences were observed, which suggests the observed difference in hypoxia was due to blood supply rather than O_2 consumption, however this assumes the cellular metabolic rate was otherwise similar. These data have shown an increase in functional blood vessels in tumors with over-expression of miR-142-3p but also a decrease in tumor growth.

5.4   Discussion

We sought to determine if SEV-mediated release of specific miRNAs could simultaneously drive malignant processes by multiple mechanisms. MiR-142-3p, miR-451a, miR-150-5p, and miR-223-3p were found to be consistently enriched in the SEVs of oral cancer

and dysplasia cell lines relative to their expression inside the donor cells, complementing previous work showing that miRNAs may be selectively packaged into SEVs in a cell state / cell type-specific manner (14,172,185,186). These miRNAs have predominantly been shown to be tumor suppressive in cancer cells (202,209-211), though this does not preclude an oncogenic role in other contexts. For example, SEV-mediated introduction of miR-223-3p and miR-150-5p to tumor stroma may facilitate evasion of immune responses (212,213).

Secretion of the above miRNAs has been associated with different malignancies: miR-451a has been reported as highly expressed in colon cancer SEVs (214), miR-451a and miR-223-3p have been reported as up-regulated in serum samples from esophageal cancer patients (215), and SEVs from monocytes containing miR-150-5p has been reported to promote angiogenesis (14). These earlier findings, combined with the knowledge that cancer cell lines secrete larger amounts of SEVs than non-cancerous lines (172,185), suggest that the SEV-mediated miRNA excretion plays a role in promoting the growth of the tumor cell itself, as well as the tumor stroma. These findings align with clinical data showing that high Rab27A expression, and the presumed increase in SEV release that follows, is a poor prognostic indicator in many cancer types (216-218). Selective retention of miR-502-5p by donor cells may be attributable to an as-yet-undetermined oncogenic function.

MiR-142-3p was selected for follow-up analysis in part because we saw the most consistent increase in its concentration due to shRNA-mediated SEV inhibition (Fig. 5.2C). Most other miRNA candidates exhibited varying increases in concentration due to Rab27A inhibition (Fig. 5.2C), with miR-451a appearing unaffected (a finding that suggests that this miRNA is excreted from the cell in a Rab27A-independent manner). ShRNA-mediated inhibition of Rab27A caused a 12-fold increase in the concentration of miR-142-3p in donor Cal27 cells,

while also reducing the amount of SEV-excreted miR-142-3p by approximately half. Since increased miR-142-3p expression in donor cells caused decreased growth (Fig. 5.3A and B), this suggests that increased SEV-mediated miR-142-3p secretion may be a means of removing this tumor suppressive effect, a finding that is similar to one reported for miR-23b-3p in bladder cancer cells (13).

Earlier reports have described SEV-secreted miR-150-5p and other miRNAs as pro-angiogenic factors that mediate cell-cell communication in cell models (14,16,187,188). We have reported SEV-secreted miR-142-3p as an additional pro-angiogenic factor based on our findings that show increase tube formation in endothelial cells (Fig. 5.4). Mouse model experiments showed that miR-142-3p over-expression led to increased functional blood vessel density and associated decreases in hypoxia. It remains a possibility that this phenotype could have been caused not only by angiogenesis, as suggested by *in vitro* analysis but also vasculogenesis and reduced loss of existing blood vessels. Future research on miR-142-3p's effect on these pathways would be illuminating. It seems as if the blood vessel density promoting effect of miR-142-3p was insufficient to rescue the proliferation decreasing effects of the miRNA, and raises the question of what would happen if only secreted miR-142-3p was increased with no effect on intercellular levels. It is interesting to examine the treatment implications of our results as it is generally expected that tumors with lower levels of hypoxia, are more sensitive to chemotherapy. In OSCC hypoxic tumors are resistant to frontline treatments with 5-Flurouracil and cisplatin. This is mediated by hypoxia induced cell cycle arrest as well as the activation of drug efflux pathways via HIF1a (219,220). Vascular density could also increase the availability of reactive oxygen species thereby increasing radiation sensitivity (220).

Significantly, we report that SEV-mediated release of miR-142-3p appears to facilitate multiple malignant processes at the same time; selective exclusion of miR-142-3p mitigates its tumor suppressive growth inhibitory effect in donor oral cancer cells, while also inducing pro-angiogenic activity in recipient cells in associated stroma. Both of these processes involve altered activation of TGFBR1, which mediates TGFB pathway signaling and has been reported to possess both oncogenic and tumor suppressive activity (207,221,222). TGFBR1 and the TGFB pathway in general are known to play a complex role in vascular homeostasis, with both pro- and anti-angiogenic effects. Knockout of TGFBR1 can lead to fragility and malformations in blood vessels while enzymatic inhibition can lead to angiogenesis (223-225). The angiogenic effects of TGFBR1 appear to be context specific which other researchers have noted increases the difficulty in understanding the pathway's molecular action (224,226). While this study examined tube formation *in vitro,* and changes in vascular density *in vivo* leading to decreased hypoxia, further work is needed to assess the complete role of TGFBR1 inhibition on the course or OSCC.

In vivo analysis on Rab27A inhibition (Fig. 5.6) demonstrates effects on the tumor stroma, opposing the effects of miR-142-3p over-expression. There is a decrease in functional vasculature suggesting that Rab27A plays a tumor promoting role. This is consistent with the hypothesis that the wild type level of secreted miR-142-3p causes increases in blood vessel density and this effect is removed upon Rab27A knockdown. Rab27A knock-down does not affect TGFBR1 levels within the cancer cell likely due to the miRNAs being sequestered from the cytosol. Therefore the decrease in growth seen in the Rab27A KD mice is likely due to the effects of decreased nutrient supply from the limited vascular density. While these results are consistent with a miR-142-3p centered affect, follow up analysis could elucidate an additional

role of other secreted miRNAs and proteins, as there are many other associated factors transferred to the stroma in a Rab27A dependant manor. Previous researchers have demonstrated a complementary tumor-promoting effect of Rab27A on metastasis (227,228). Future studies will demonstrate the mechanism by which Rab27A promotes vascular density, and tumor cell growth. We also predict there is a functional role of SEV signaling to endothelial cells in the formation of pre-metastatic niches, which would complement others' work on the topic (229).

In summary, we have found evidence of selective (rather than indiscriminate) SEV packaging of four miRNAs for exclusion from oral cancer and dysplasia cell lines, as well as selective retention of one miRNA by these same cells. Follow up analysis of one miRNA selectively excluded via SEVs, miR-142-3p, showed that its release leads to both increased growth in donor cells and enhanced tumor supporting potential in cells in associated stroma, both via altered expression of TGFBR1. Further studies building on this work are needed to characterize the machinery driving selective SEV packaging of miRNAs, and to identify the selective forces that alter the behavior of this machinery in the context of malignancy.

Chapter 6: Secretion of miR-142-3p in Lung Cancer Induces Angiogenesis and Fibroblast Activation

6.1 Introduction

In the previous chapters we have focused on OSCC which is the 8th most common cancer worldwide (86). We wished to determine if any of the information gained from the analysis of secreted miRNAs in HNSCC is applicable to other cancer types. Worldwide, the leading cause of cancer death is lung cancer, the majority of cases are non-small cell lung carcinomas (NSCLC) (86). The largest subgroup is adenocarcinoma which shares a similar risk profile with OSCC, notably both are highly linked to smoking (86).

Increasing attention has been paid to the study of secreted miRNAs in lung cancer. In a similar fashion to oral cancer there are a substantial number of miRNAs that have been identified as lung cancer biomarkers (230). Multiple groups have also examined the ability of lung cancer miRNAs secreted via SEVs to act as cell-to-cell communicators. Adenocarcinoma SEVs are capable of increasing the metastatic potential of otherwise poorly metastatic cell lines in lung tissue and lymph nodes by the action of miR-494-3p and miR-542-3p on the pre-metastatic stroma (18). Additionally, miR-21-5p and miR-29a-5p are capable of causing pro-inflammatory changes in immune cells through action on the toll-like receptor, TLR8 (231). This complements the work that researchers have done to examine the cancer to stroma communication ability of SEV miRNAs which have been shown to promote angiogenesis, and activate the growth promoting properties of fibroblasts (14,16,187,232,233). For example in breast cancer miR-9-5p can be transferred to normal fibroblasts to act upon E-cadherin, causing them to transform into

cancer associated fibroblasts (CAFs). This activates many genes involved in wound healing which can also support tumor growth (232), as well as chemoresistance (234).

Previous work in oral cancer has shown that SEV secretion allows for the removal of the inhibitory effect of miR-142-3p on TGFBR1 (Chapter 5), a protein known to promote cell growth in lung cancer cells (235). Oral cancer cells then transfer miR-142-3p to endothelial cells where there is a TGFBR1 mediated increase in angiogenesis (Chapter 5). In previous research, we have shown that in lung adenocarcinoma cell lines, miRNAs including miR-142-3p are selectively secreted from the cells via SEVs (citation pending). We theorize that the secretion of miR-142-3p from lung cancer cells also promotes the creation of an oncogenic tumor stroma. Determining the function of secreted miR-142-3p in lung adenocarcinoma will be important in order to determine the molecular mechanisms that drive this disease, and increase our knowledge of how SEV miRNAs assist in modifying the tumor microenvironment.

6.2   Materials and Methods

The Methods utilized were the same as those in Chapter 5 unless otherwise mentioned.

6.2.1   Cell Lines

Cell lines were obtained from ATCC, the lung adenocarcinoma cell lines H1437 and H2073 were cultured in RPMI 1640 media with 10% FBS, according to the supplier's guidelines. HMEC1, Wi-38 and 293T cells were cultured in DMEM media supplemented with 10% FBS.

6.2.2   SEV Isolation

SEVs were isolated as described in Chapter 5, with the use of 1% depleted FBS supplemented RPMI media for SEV collection in lung cancer cells.

6.2.3   Fibroblast Activation Experiment

Wi-38 cells were seeded in 96 well plates and after reaching 30% confluency SEVs isolated from 1, 15cm plate of H1437 or H2073 cells were added to the culture media per well. The media was replaced at 24, and 48 hours with additional SEV containing media. Protein and RNA extractions occurred at 72 hours after SEV addition.

6.2.4   Western Blotting

RIPA buffer with 1:100 phosphatase inhibitor cocktail I & II (Sigma-Aldrich) and protease inhibitor (Thermo Fisher Scientific) was used to lyse EVs and cells. Protein was quantified using a Pierce BCA kit (Thermo Fisher Scientific). 10µg of protein was run on a NuPAGE 4-12% Bis-Tris Gels (Thermo Fisher Scientific) and then transferred to PVDF membranes (Millipore). Membranes were blocked in 5% BSA, 1x TBS, and 0.1% Tween-20 for 1 hour at room temperature. Primary antibodies 1:1000 anti-TGFBR1 (AF3025, R&D Systems), 1:8000 anti-GAPDH (2118, Cell Signaling Technology), 1:2000 α-SMA (14968, Cell Signaling), 1:1000 Desmin (PA5 16705, Thermo Fisher Scientific), 1:1000 PDGFR-β (SC-432, Santa Cruz Biotechnology) were applied for 16 hours at 4°C. All antibodies were diluted in blocking buffer. Horseradish peroxidase conjugated secondary antibodies 1:2000 anti-mouse (NXA931, GE Healthcare) or 1:2000 anti-rabbit (7074, Cell Signaling Technology) were applied for 1 hour at

room temperature. Quantification was performed with normalization of TGFBR1 to GAPDH using the ImageJ 'gel analysis' function.

6.3   Results

6.3.1   miRNA is Transferred From Lung Cells to Endothelial Cells

In order to determine if SEVs from lung adenocarcinoma cells can be transferred to endothelial cells, SEVs from both H1437 OE Control and H2073 OE Control cells were collected and transferred to HMEC1 cells in 96 well plates, incubated for 48 hours, and then compared to cells receiving no additional SEVs. Measured using qRT-PCR, cells receiving SEVs had a 2.4 (H1437) or 2.3 (H2073) fold greater level of miR-142-3p then those receiving none (Fig. 6.1). To determine if this effect was caused by miRNA transfer and not an induction of local miRNA expression by way of some other SEV contained factor, this experiment was also performed using SEVs collected from H1437 and H2073 cells over-expressing miR-142-3p. SEVs collected from cell lines over expressing miR-142-3p had 3.4 and 5.1 times higher concentrations of miR-142-3p than OE Control SEVs from H1437 and H2073 cell lines respectively. The addition of these SEVs increased concentration of miR-142-3p in HMEC1 receiver cells by 8.7 and 9.5 fold for SEVs from H1437 and H2073 respectively (Fig. 6.1). The difference in miR-142-3p levels between cells receiving SEVs from H1437 and H2073 is likely explained by the increased concentration of miR-142-3p in the SEVs of H2073.
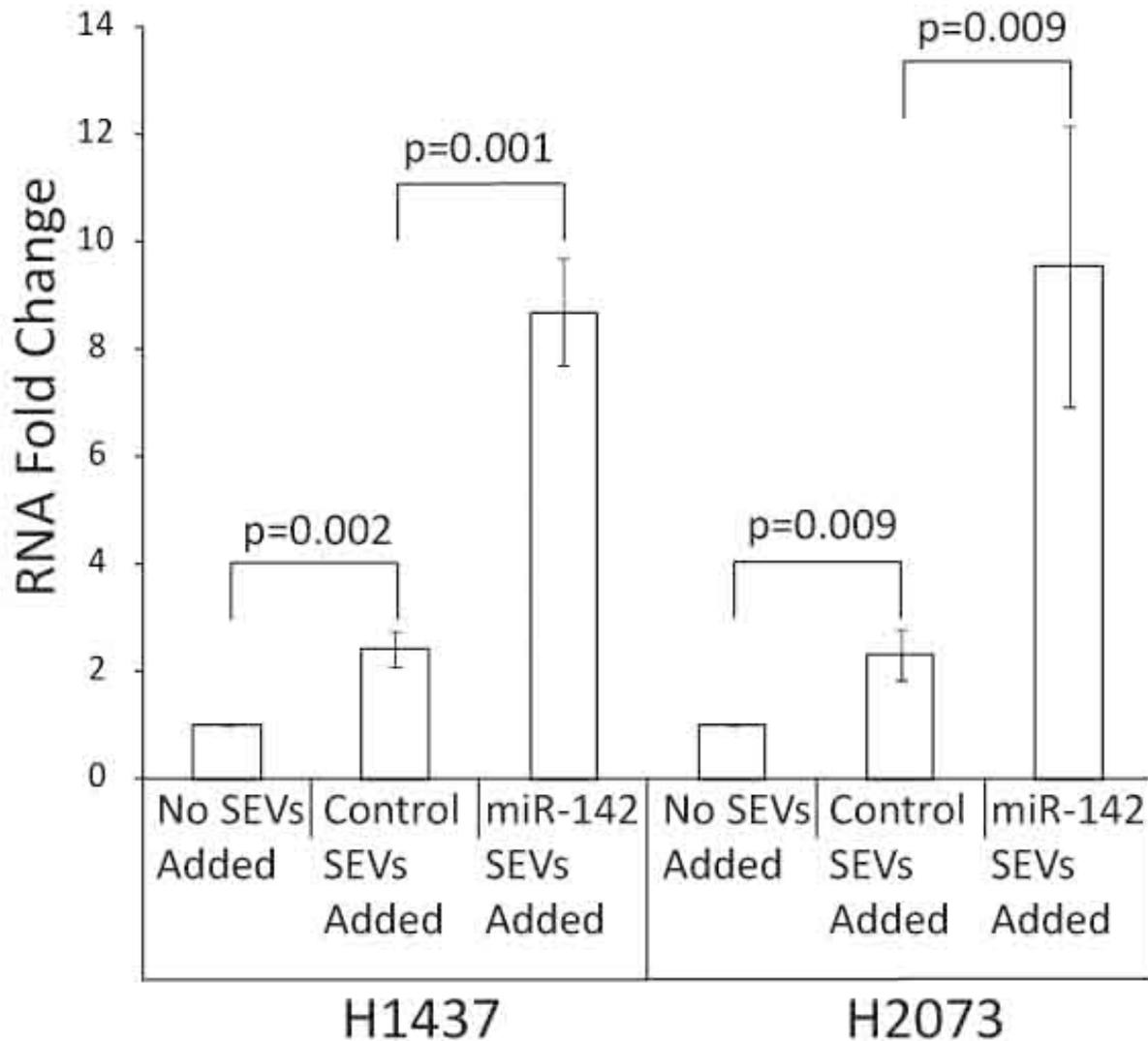
Figure 6.1 Transfer of miRNA to endothelial cells from lung cancer SEVs. Results of miR-142-3p qRT-PCR on HMEC1 cells after the addition of SEVs isolated from H1437 or H2073 cells infected with either miR-142-3p or control over-expression vectors. Levels of miR-142-3p were normalized to levels of U6 sno-RNA.

6.3.2 Secreted miR-142-3p Promotes Angiogenesis

To determine if secreted miR-142-3p was capable of promoting angiogenesis we performed a tube formation assay on HMEC1 endothelial cells. Endothelial cell cells were in three treatment groups, those receiving no SEVs, those receiving SEVs from OE Control cells and those receiving SEVs from miR-142 OE cells. This was performed with SEVs derived from both H1437 and H2073 cells. All treatments were capable of forming tubes (Fig 6.2 A-F, I) and the addition of OE Control SEVs increased tube formation by 9% (p=0.02), and 23% (p=0.04) for SEVs from H1437 and H2073 respectively. The addition of miR-142-3p OE SEVs increased tube formation by 37%, (p=0.001 H1437) and 40% (p=0.03 H2073) when compared to the HMEC1 cells with no SEVs added. This difference was 26% (H1437) and 22% (H2073) more when compared to the addition of OE Control SEVs. To confirm alterations in tube formation were a result of miR-142-3p, the tube formation assays were repeated with direct over expression of miR-142-3p (Fig 6.2 G-I). This caused a greater increase in tube formation (40%) than the addition of SEVs.
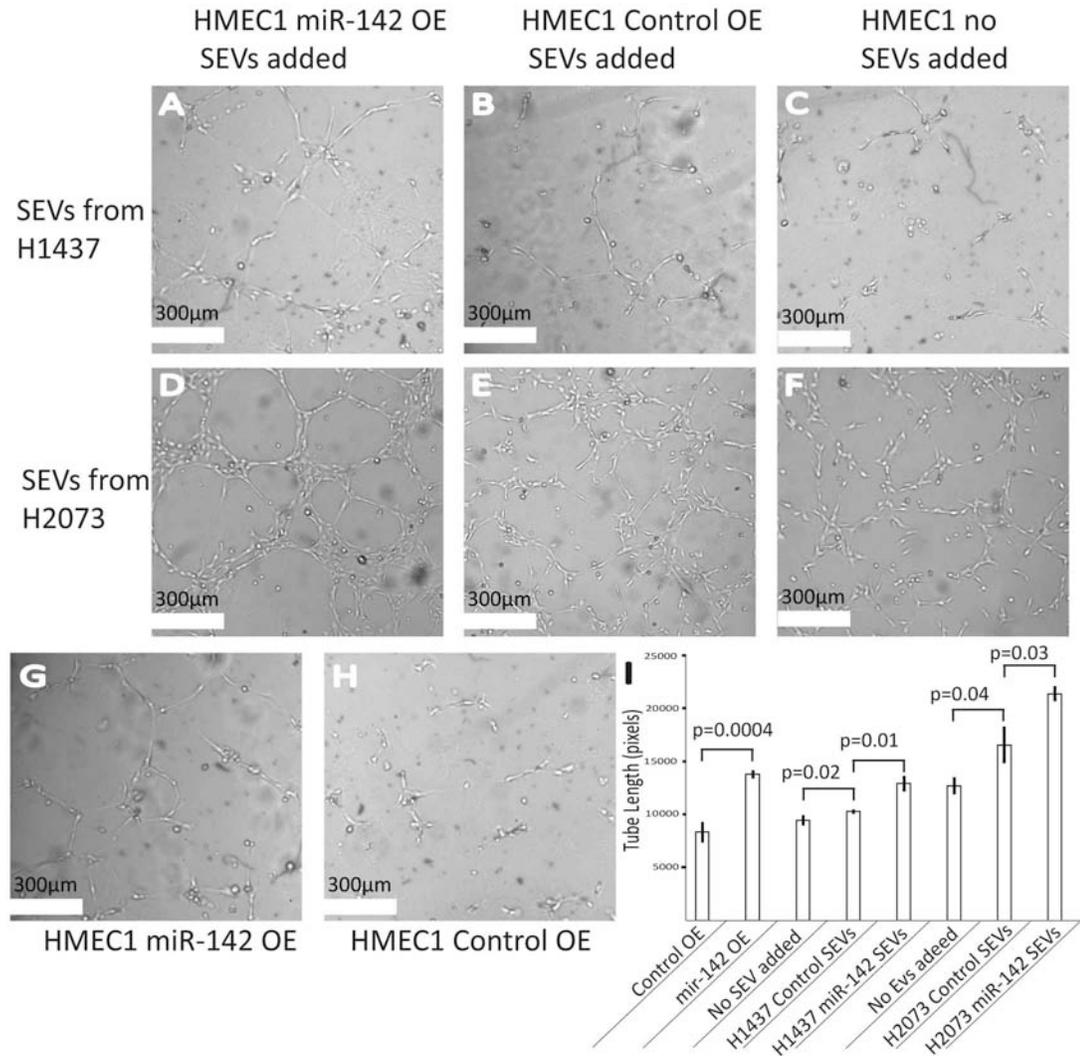
Figure 6.2 The effect of miR-142-3p on tube formation assays. Tube formation assays on HMEC1 cells with the addition of SEVs of H1437 or H2073 cells infected with a miR-142-3p (A,D) or control (B,E) over-expression vector compared to HMEC1 cells with no SEVs added (C,F). Tube formation assays comparing HMEC1 cells infected with miR-142-3p (G) or control (H) over-expression vectors. I: The average tube length across 3 wells. Error bars represent standard deviation and p values were calculated by 2 tailed equal variance t-test.

6.3.3   Secreted miR-142-3p Targets TGFBR1 in HMEC1s

We have previously shown that SEV transferred miR-142-3p can promote angiogenesis by acting upon the gene TGFBR1 (Chapter 5) in oral cancer, through interaction with the gene's 3'UTR (202,205). To establish the same pathway caused alterations in tube formation in lung adenocarcinoma, SEVs from H1437 cells or H2073 cells with mIR-142 OE or OE Control vectors were added to HMEC1 cells in 96 well plates. 48 hours after SEV addition, protein was extracted from these cells and compared to HMEC1 cells grown without the addition of SEVs. There was an observed decrease of TGFBR1 in HMEC1 cells receiving OE Control SEVs from H1437 cells of 66% and a decrease of 37% with OE Control SEVs from H2073 cells (Fig. 6.3). The decrease in TGFBR1 was larger when cells received SEVs from miR-142 OE cell lines. With SEVs isolated from H1437 cells, the decrease was 83% and with SEVs isolated from H2073 cells the decrease was 55% (Fig 6.3). To confirm that TGFBR1 was inhibited by miR-142-3p and not an alternate property of the SEVs, HMEC1 cells were directly infected with miR-142-3p, causing a decrease in TGFBR1 expression of 91%.
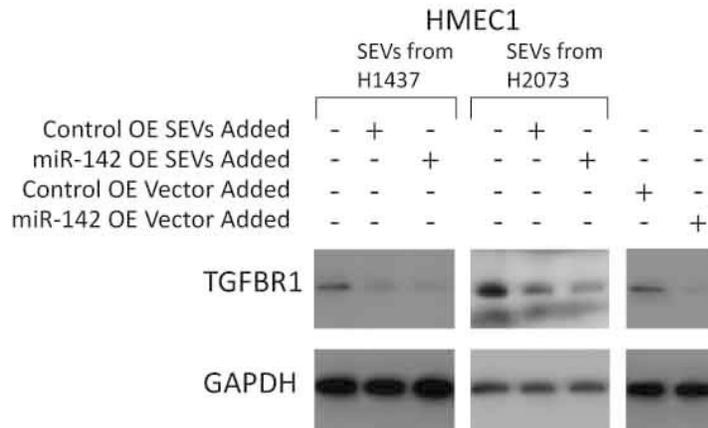
Figure 6.3 The effect of miR-142-3p on TGFBR1. Western blots on TGFBR1 on HMEC1 cells after the addition of SEVs from H1437 or H2073 cells infected with miR-142 OE or OE Control vectors. Also shown are western blots from HMEC1 cells infected directly with miR-142OE or OE Control vectors. GAPDH was used as a loading control.

These data are merely correlative and it is possible that the interaction between miR-142-3p and TGFBR1 is incidental to the finding of an alteration in tube formation. In order to rule out this possibility, we performed a phenotypic rescue experiment in HMEC1 cells, infected with a TGFBR1 ORF clone, which was insensitive to inhibition from miR-142-3p (Fig 6.4 A). This experiment showed that tube formation was decreased upon over-expression of TGFBR1 even with the addition of miR-142 OE SEVs, from H1437 or H2073. This caused a decrease in tube formation of 34 and 35% respectively (Fig 6.4 B-F).
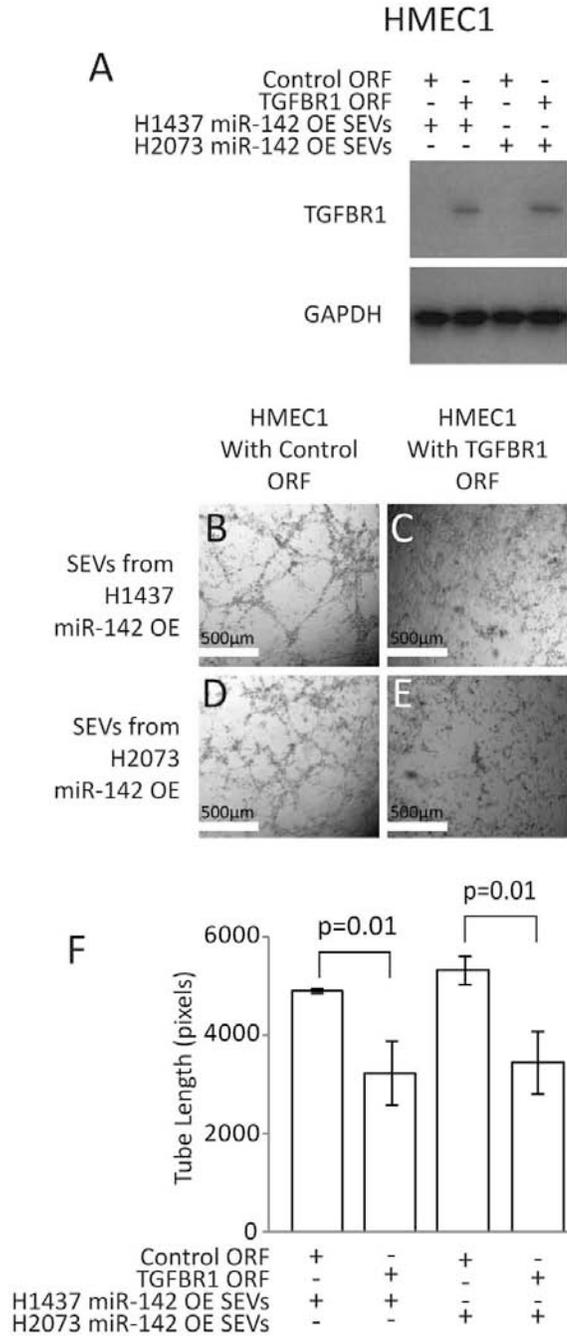
Figure 6.4 TGFBR1 rescue and its effect on tube formation. A: Western blot of TGFBR1 confirming rescue in HMEC1s, in the presence of miR-142-3p over-expressing cell lines. B-E: Representative images of tube formation assays in HMEC1s with TGFBR1 ORF (C, E) or Control ORF (B, D) vectors after the addition of SEVs from miR-142-3p over-expressing H1437 (B,C) and H2073 (D,E) cell lines. F: Average tube length determined using ImageJ macro 'Angiogenesis Analyzer across three wells. Error bars represent standard deviation and p values were calculated using students t-test.

6.3.4   Secreted miR-142-3p Promotes Cancer Associated Fibroblast Transformation

The most common cells in the tumor stroma are fibroblasts (236), and would therefore likely also receive a large proportion of tumor SEVs. In tumors, fibroblasts can be transformed into CAFs to play a pro-inflammatory role in a similar way to wound repairing myofibroblasts (236). To determine if SEV secreted miR-142-3p promotes the development of CAF markers, SEVs from H1437 and H2073 cells were added onto Wi-38 lung fibroblasts and replaced every day for 3 days. This addition of OE Control SEVs from H1437 and H2073 led to an increase of Wi-38 miR-142-3p concentration of 2.5 fold and 2.0 fold respectively. The addition of miR-142 OE SEVs from H1437 and H2073 cells led to an increase in miR-142-3p of 11.1 and 8.4 fold respectively (Fig 6.5 A). Western blots were performed on the proteins Desmin, α-SMA, and PDGFR-β (Fig 6.5 B) which are positively correlated with fibroblast activation and CAF transformation (234). There is a large increase in the concentration of α-SMA after the addition of SEVs, and a noticeable increase in the amount of PDGFR- β detected. Desmin which is highly expressed in cells that did not receive SEVs, did not have a change in expression. In contrast to endothelial cells the protein TGFBR1 showed only minor changes (Fig 6.5 C), suggesting that miR-142-3p causes fibroblast activation through another target.
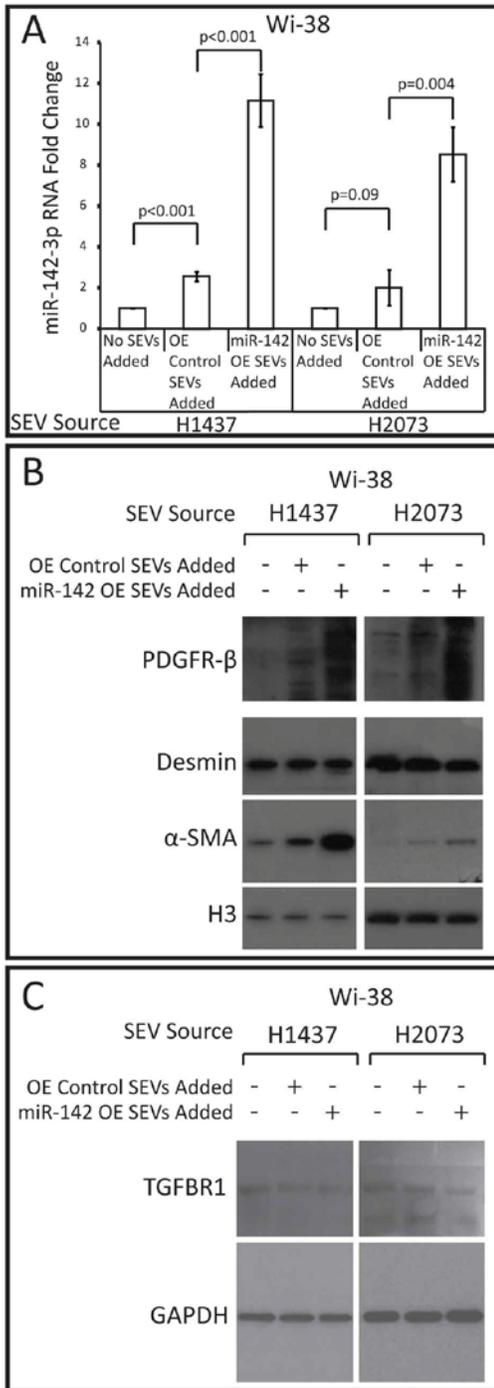
Figure 6.5 The effect of miR-142-3p SEVs on CAFs. A: qRT-PCR results for miR-142-3p in Wi-38 fibroblasts after the addition of SEVs from H1437 or H2073 cells, with or without the over-expression of miR-142-3p. B: Western blots for CAF markers, PDGFR-β, Desmin, α-SMA and the loading control Histone H3. Wi-38 fibroblasts were tested after the addition of SEVs from H1437 or H2073 cells containing OE Control or miR-142 OE vectors. C: Wi-38 cell western blots on TGFBR1 and the loading control GAPDH after the addition of SEVs from H1437 or H2073 cells infected with miR-142 OE or OE Control vectors.

6.4   Discussion

In NSCLC it appears that miR-142-3p is removed from the lung cells to eliminate its tumor suppressive effect (202,205,235), we show that it is then transferred to endothelial and fibroblast cells where it has an oncogenic effect. The idea that a miRNA may be selectively secreted as a means of disposal has been proposed with let-7 in gastric cancer and miR-23b-3p in bladder cancer (89). In oral cancer, miR-142-3p secretion has been shown to serve a dual role (Chapter 5). The miRNA which is growth suppressive locally can also induce angiogenesis through SEV transfer. We demonstrate the angiogenesis promoting effects of miR-142-3p transfer from lung cancer cells and additionally examine the ability of this miRNA to induce CAF transformation. Mir-142-3p's complex role in lung tumor initiation and growth could explain why a decrease in the expression of miR-142-3p isn't selected for as a means to reduce the growth inhibitory effects on cancer cells.

SEV transfer of miR-142-3p to fibroblasts induces increased expression in the CAF markers α-SMA and PDGFR-β but not Desmin. Other researchers detected Desmin in unaltered Wi-38 cells, with less noticeable increases upon activation when compared to α-SMA (237). Combined these markers have been associated with CAFs and myofibroblasts however future research will need to establish miR-142-3p's ability to induce the functional traits associated with CAFs. It is interesting that TGFBR1 appeared to only have minor alterations from miR-142-3p SEV addition. TGFB signaling in fibroblasts would be expected to increase CAF development, and a TGFBR1 reduction would decrease this (238). We speculate that there is some feedback mechanism to keep the expression of this gene high.

We have shown that the release of miR-142-3p from lung cancer cells via SEVs is capable of promoting angiogenesis by targeting the gene TGFBR1. TGFBR1 in endothelial cells

can cause apoptosis and its inhibition is capable of increasing proliferation (207). Previously miR-142-3p has been show to target TGFBR1 in NSCLC cells (202), however TGFBR1 has an unusual role in promoting cancer growth. It is known to play a tumor suppressive role early on in cancer initiation (239), and its absence leads to spontaneous squamous cell carcinoma formation (240). However in non-small lung cancer TGFBR1, plays an oncogenic role, with inhibition of TGFBR1 leading to increased growth and invasive potential of the cancer cells (241). Analysis of patient plasma samples have shown that high TGFB levels are a negative prognostic indicator in lung cancer suggesting that over-activation of the pathway at late stage increases cancer aggressiveness (242). Our work has examined the role of miR-142-3p with regards to TGFBR1, however miRNAs are known to be capable of targeting many mRNAs, for example HMGB1 is also targeted by miR-142-3p in NSCLC (243). It is therefore important to consider that miR-142-3p's action in promoting angiogenesis may additionally involve other targets.

The role of TGFBR1 in lung cancer patients seems to be related to the role of miR-142-3p. Examination of serum miRNA shows that miR-142-3p is a biomarker for increased aggressiveness in operable NSCLC (244). This same study showed lower levels of miR-142-3p in individuals with benign conditions and individuals with advanced stage disease (244). Advanced lung cancer is characterized by tumor necrosis due to insufficient neovascularization with a corresponding reduced ability to deliver blood and nutrients. This could partially be explained by the decreased blood concentration of the pro-angiogenic miR-142-3p (244). Other researchers however have demonstrated that in NSCLC the level of angiogenesis does not appear to be correlated with the level of necrosis (245). Additionally the levels of other pro-angiogenic factors such as VEGF tend to increase with progression of the disease (246), leading to the hypothesis that the demand for oxygen and nutrients is the determining factor in necrosis rather

than the supply. In NSCLC angiogenesis appears to be a negative prognostic indicator for both aggressiveness and survival (247-250). The more widely studied angiogenesis promoter VEGF has been shown to be targetable by the drug bevacizumab in NSCLC, causing modest improvements in survival (251). It is possible that in a similar fashion secreted miR-142-3p is a potential druggable target which would likely play a larger role in early stage, yet aggressive disease. The dual role of miR-142-3p in lung cancer increases the complexity of any potential therapy.

In summary we have shown that miR-142-3p secreted from lung cancer cells is capable of being trafficked to endothelial and fibroblast cells. In endothelial cells the miRNA targets the gene TGFBR1 in order to eliminate its anti-angiogenic effect. SEV transfer of mIR-142-3p is capable of inducing fibroblast activation, a phenotype associated with tumor supportive CAFs. We have demonstrated additional mechanisms by which cancer cells interact with the tumor stroma to create a favorable microenvironment.

Chapter 7: Discussion and Conclusion

7.1 Summary of Findings

Building upon the utility of the standard therapies: surgery, radiation and chemotherapy, recent developments in targeted therapy and tumor detection have had limited success in improving the approximately 50% survival rate of OSCC over 5 years. There remains a continuing need to develop new modalities for treating oral cancer. Current methods to diagnose OSCC have encountered difficulty especially when assessing disease recurrence, due to large scale alterations in the structural anatomy of the oral cavity that occurs following treatment with surgery and radiation. Improvements in detection can lead to an earlier application of existing and future treatments. The continued creation of novel OSCC treatments will require gaining an in-depth knowledge on OSCC biology to identify druggable targets in the tumor stroma as well as the cancer cells themselves. The work described in this thesis describes the creation of a secreted miRNA biomarker panel for oral cancer with the potential to differentiate individuals with OSCC/*CIS* from HCs. I have also completed an in depth examination on the functional role of miRNAs secreted from oral cancer cells. We have also demonstrated that the information gained here is also informative when studying lung adenocarcinoma, which shares many of the same miRNA alterations found in OSCC.

7.1.1 Biomarker Analysis of Individuals with OSCC and *CIS*

Chapter 3 of this thesis focuses on the investigation of a panel of miRNAs capable of differentiating between healthy individuals and patients with either OSCC or *CIS*. In this chapter 48 individuals with OSCC or *CIS* were compared to 51 healthy individuals on their expression of

a panel of 742 miRNAs by way of qRT-PCR. Logistic regression was used to create a subset

panel of 14 miRNAs in which to perform verification analysis at a higher throughput. These

miRNAs were assessed for their ability to remain informative when utilizing a different platform

and this ultimately led to the creation of a panel of 6 miRNAs (and one endogenous control)

comprised of miRNAs: miR-125b-5p, miR-342-3p, miR-23a-3p, miR-205-5p, miR-145-5p and

miR-33a-5p. MiR-23b-3b was selected as the endogenous control. While we predicted this panel

of miRNAs would have a sensitivity and specificity of approximately 0.87 and 0.92 respectively,

this represented an optimistic best case scenario. A validation of this miRNA panel on an

independent test set was used as conformation. As this test set did not influence the selection of

the miRNAs in the panel this is a better approximation of the clinical utility of the biomarker

test. In the independent test set we were capable of differentiating serum samples of individuals

with OSCC/*CIS* from those without, with a sensitivity and specificity of 0.45 and 0.96

respectively and an AUC of 0.90. This suggests that the statistical test has a validated ability to

separate OSCC/*CIS* samples from HCs but has an unreliable ability to make calls. There is an

unaccounted for bias towards the selection of fewer cancer samples in the group that tested

positive. The miRNA panel was assessed for its robustness to errors in the qRT-PCR platform

and it was found that simulated random errors were not the cause of the changes between

training and test sets.

7.1.2   Assessment of Cell lines and Their Ability to Act as an Oral Cancer Model

To complement previous researchers' work on commonly used oral cancer cell lines, in

Chapter 4 I examined a group of commonly used normal oral keratinocyte cells and assessed

them for molecular alterations which would not be expected in healthy tissue. These cells were

assessed for molecular alteration to DNA copy number as well as mRNA and miRNA expression. The main result of these experiments was a noticeable alteration in the expression of many commonly studied oncogenes, as well as alterations in DNA copy number. These mutations were more severe in cell lines that had been immortalized for extended growth in cell culture. The data were posted in an online database so that other researchers performing work with these cell lines will have a reference to determine which cell line is appropriate for their experiments. This is beneficial knowledge and provides a baseline for gene expression when comparing to cells under experimental conditions.

7.1.3 Functional Assessment of Secreted miRNAs

Another primary goal of my thesis was to determine what the functional role of secreted miRNAs were with regards to promoting carcinogenesis. This was first examined in Chapter 5 in oral cancer. An assessment of which miRNAs are selectively secreted from OSCC cell lines found no overlap with the miRNAs that are significantly altered in the serum of patients with oral cancer. The miRNAs: miR-150-5p, miR-142-3p, miR-451a and miR-223-3p were found to be enriched in SEVs when compared to the cells they originating from, implying that there was active selection for these molecules. Only miR-502-5p was found to be enriched within the cellular fraction suggesting that this miRNA was selectively excluded from SEVs.

Follow-up functional analysis was focused on miR-142-3p and it was determined to have a dual role. MiR-142-3p is secreted from oral cancer cell lines partially to remove its growth suppressive effect from within the cancer cells. As other researchers have shown with other miRNAs, miR-142-3p when secreted via SEVs has an ability to act in cell-to-cell communication targeting endothelial cells and inducing them to form 'tubes', one of the necessary steps in

angiogenesis. We also determined that these effects were mediated by the protein TGFBR1. TGFBR1 is a protein that has previously been described as having tumor suppressive and tumor promoting effects in an apparently context specific fashion.

Within cancer biology many observed phenomenon are common across multiple different cancer types especially within carcinomas. We wished to determine if the functional role of miR-142-3p was the same in the context of lung cancer. Examination of secreted miR-142-3p also showed a TGFBR1 mediated induction of endothelial tube formation. MiR-142-3p from lung cancer was also transferred via SEVs to fibroblasts where they were induced to undergo changes associated with CAFs, fibroblast activation and, wound healing.

7.2 Conclusions Regarding Hypotheses

For this thesis my hypotheses were: 1) There is a subset of serum miRNAs that are capable of differentiating between individuals with and without oral cancer or *CIS* 2) miRNAs are being selectively excluded from OSCC cells when doing so will confer a carcinogenic advantage. This can occur both by the removal of tumor suppressive miRNAs and also by promoting a supportive tumor microenvironment by the secretion of cell-to-cell communicating miRNAs. 3) The tumor promoting activity of these miRNAs will not be unique to OSCC but will also affect other cancer types including NSCLC.

Hypothesis 1 was examined in Chapter 3 and examination of miRNA expression in healthy patients and patients with OSCC or *CIS* demonstrated that it is possible to predict cancer status based of a subset of 6 serum miRNAs, however the method is vulnerable to systematic biases in sample classification.

Hypothesis 2 was examined in Chapter 5 and the results demonstrate that miR-142-3p is excluded from OSCC cells not only to remove its tumor suppressive effect but also to transfer a tumor promoting effect to endothelial cells. Therefore hypothesis 2 is supported and this research also leaves open the possibility there may be other effects of the miRNAs in question.

Hypothesis 3 was supported by the work shown in Chapter 6, demonstrating that miR-142-3p in lung cancer SEVs, shares the tumor promoting effects found in oral cancer, both through the already established pathway involving the promotion of angiogenesis but also through fibroblast activation.

7.3   Strengths and Limitations

The serum analysis described in this thesis has a number of strengths when compared to similar research performed by others. More individuals were included in this experiment than what is typical of circulating miRNA studies. This gives a greater confidence that the results were not merely an effect of sampling error (7,8). Additionally the statistical analysis performed is more robust then is common as many researchers assess miRNA differences using t-tests or ANOVAs rather than using regression or similar methods which are intended to offer a predictive value. Although the literature may be confusing as many researchers use the term 'validation', it is not always used in the statistical sense to describe studies where the participants are split into training, validation, and test sets. The term can be applied to functional validation instead. The inclusion of independent test sets is a major strength of this thesis. Unfortunately the statistical test is vulnerable to biases which affect making calls. The sensitivity of the serum miRNA study was 0.45 which is lower then what would be suitable for a test intended to screen

patients, and limits the future applications of the blood test to attempts to 'rule in' a diagnosis that is already suspected.

For the serum analysis there is room for improvement. Firstly the ratio of miRNAs being examined to patients in the study is not optimal, and the inclusion of additional patients would give more confidence. Furthermore to guard against unconscious but systematic bias, assessment of a statistical model is improved when a second blinded researcher performs data collection. It is not practical for a study of this scale; however, biomarker analysis is greatly improved when the patients being examined have an unknown cancer status, and are members of the same risk group in which the test would be applied to. For example if the long term application of this biomarker panel was to detect disease recurrence, the preferred test population would be individuals who have already completed initial treatment, to determine if the miRNA panel detects OSCC before it would otherwise have been evident.

Quantifying miRNAs secreted by oral cancer cell lines was strengthened by the previous characterization of these cell lines. This allowed for an assessment of the genes involved in SEV secretion, and allowed for research to proceed with the knowledge that certain pathways were down-regulated for example: SMPD3 dependant SEV secretion. It remains that these cell lines are not a perfect analog for whole tumors, as was made clear by my work and the work of others, and therefore this would be considered a weakness. Examination of miR-142-3p determined that the gene TGFBR1 was the target. While alterations to TGFBR1 were sufficient to explain the tumor promoting phenotype, this study is limited by the fact that other miR-142-3p/target interactions were not examined. An additional limitation of my research and the work of others is an inability to explain the context specific activity of TGFBR1 and the TGFB pathway, which can have different effects even within similar tissue types.

Mouse modeling was important in strengthening this work against the limitations of *in vitro* assays, and the use of immune-compromised mice allowed for the use of human tumor grafts. This allowed for the quantification of tumor growth to consider the growth and interactions of the tumor stroma. The xenograft model used was also limited by the inability to distinguish between the suspected pro-angiogenic effects of miR-142-3p and possible pro-vasculogenic effects, or other effects leading to increased blood vessel density. While useful a limitation of immune-compromised mice is that they are not able to give information about the cancer's interaction with immune cells which are known to play a major role in SEV and miRNA based communication.

Conformation that miR-142-3p's SEV mediated effects are not limited to the context of oral cancer greatly strengthens this research as OSCC remains an understudied cancer when compared to more common cancer types such as lung. Knowledge that the miR-142-3p /TGFBR1 pathway is relevant in multiple tissue types will assist with the visibility of this research. This may attract scientists wishing to utilize our data for the development of drug therapies as researchers will be driven by the greater number of patients which may benefit from the treatment.

7.4   Significance

The overall goal of this research was to gain a deeper understanding of miRNA secretion in the context of oral cancer. The statistical rigor, and increased sample size of this study can help us be confident that the results represent the underlying trends of the data and are not overly optimistic. This is a common pitfall to biomarker research with the majority of reported biomarkers never seeing diagnostic use, despite initially promising results.

The cell line analysis here will provide an easy to use source of information for researchers using oral cell lines for *in vitro* analysis. This will allow future research to be completed with increased speed as this resource will ease the selection of cell lines to analyze. This paper has already achieved this goal with regards to other researchers in our own group. Additionally, Chapter 4 provides a useful reminder of the differences between cell lines, and human tissue that should serve as a caution to researchers who may wish to over-extrapolate the significance of their work.

The detection of miR-142-3p's role in promoting carcinogenesis through a dual functionality gives a great deal of insight into the field of SEV research complementing previous discoveries in the field. An understanding of this aspect of tumor biology may yield to a wide variety of cancer therapies targeting tumor/stroma communication.

7.5   Future Directions

Future studies on serum miRNA biomarkers in OSCC will be needed before a product can be marketed to clinics. It is necessary to first demonstrate efficacy of a biomarker on a population where cancer status is unknown, and performance must be superior to existing methods. It may be easier to improve upon existing methods of detection when those methods have proven to be ineffective. For example it is currently more difficult to detect OSCC as a recurrence than as a primary disease using visual examination. It's possible a miRNA based biomarker may be superior. It is also possible that future work on serum miRNAs will be useful in predicting which pre-cancerous lesions will progress. The current method of predicting which dysplasias will progress is based off of the grade of the lesion. Only a fraction of dysplasias will progress, and it is possible that the secreted miRNA profile of these lesions may be more similar

to that of established cancers. This would preferably be tested in a prospective study examining individuals with pre-malignant diseases. The number of individuals needed in the study would be specific to which stage of pre-malignant lesion is examined, due to the number of patients who will progress, being lower with earlier stages. We can use the sensitivity and specificity in known cancers of 0.45 and 0.96 to predict the likely sensitivity and specificity of a miRNA test in dysplasia serum samples. If we intend to create a test used to 'rule in' malignant transformation and are willing to accept that many patients may be missed, we could tolerate a sensitivity and specificity of 0.25 and 0.85 respectively. Using the online tool 'powerandsamplesize' we performed a sample size calculation for a one sided proportion test with an alpha of 0.05 and a beta of 0.80. A future test would need to include 32 progressors and 47 non-progressors. Knowing that approximately 50% of severe dysplasia will progress (252) we can predict the number of patients we would need to include. This was calculated using the program SampSize with the prevalence feature determining that 111 individuals would need to be included to have a 95% confidence in enrolling at least 47 non-progressors (253,254). If testing individuals with moderate dysplasia where the conversion rate is approximately 30% (252) 134 individuals would need to be included to have a 95% confidence in testing 32 progressors. This would likely lead to more non-progressors being tested then is required, due to their over-representation in the test population. In one desired a biomarker capable of ruling out the possibility of dysplasia progression, they would likely need to search for biomarkers with a higher sensitivity.

One must keep in mind the lessons learned from notable research on mammography demonstrating that improved diagnosis may potentially lead to over treatment and overall worse

patient outcomes (255). It will therefore be important to test the efficacy of a biomarker in improving patient survival rates, rather than solely in lesion detection.

During analysis of miR-142-3p we noticed an incidental finding in xenograft tumors. When the cancer cells had decreased expression for the exosome secretion protein Rab27A there was a notable increase in tumor hypoxia. A further exploration of this effect, to examine interactions with endothelial cells in isolation would be informative. It would also be very interesting to see if SEVs secreted from OSCC or lung cancer cell lines were capable of acting distantly to prime pre-metastatic niches in a similar fashion to the alterations which occur in the tumor stroma. One would expect that there may be decreased transfer of SEV miRNAs to distant sites compared to local sites when examining mice. This could be tested using tracking of stained SEVs. It would be interesting to learn if any of these potential actions also occurred through action on the TGFB pathway. It is possible that these observed finding were due to the secretion of the other identified miRNAs miR-451a, miR-150-5p and miR-223-3p. Our study was unable to explain the sometimes opposing actions of the genes in this pathway and how they can be act as tumor suppressors or oncogenes in a context specific manner. To further explore the treatment implications of this research it would be illuminating to conduct research on drugs which target the TGFBR1 receptor which is responsible for angiogenesis related alterations, and to elucidate the drug's effect on survival.

References

1.   Ovalle WK, Nahirney PC. Netter's essential histology. Elsevier Health Sciences; 2013.
2.   Warnakulasuriya S, Reibel J, Bouquot J, Dabelsteen E. Oral epithelial dysplasia classification systems: predictive value, utility, weaknesses and scope for improvement. J Oral Pathol Med 2008;37(3):127-33.
3.   Torre LA, Bray F, Siegel RL, Ferlay J, Lortet-Tieulent J, Jemal A. Global cancer statistics, 2012. CA: a cancer journal for clinicians 2015;65(2):87-108.
4.   Marur S, Forastiere AA. Head and Neck Squamous Cell Carcinoma: Update on Epidemiology, Diagnosis, and Treatment. 2016. Elsevier. p 386-96.
5.   Dediol E, Sabol I, Virag M, Grce M, Muller D, Manojlović S. HPV prevalence and p16INKa overexpression in non-smoking non-drinking oral cavity cancer patients. Oral diseases 2016.
6.   Sankaranarayanan R, Sauvaget C, Ramadas K, Ngoma T, Teguete I, Muwonge R, et al. Clinical trials of cancer screening in the developing world and their impact on cancer healthcare. Annals of oncology 2011;22(Suppl 7):vii20-vii28.
7.   Lin S-C, Liu C-J, Lin J-A, Chiang W-F, Hung P-S, Chang K-W. miR-24 up-regulation in oral carcinoma: Positive association from clinical and in vitro analysis. Oral oncology 2010;46(3):204-08.
8.   MacLellan SA, Lawson J, Baik J, Guillaud M, Poh CFY, Garnis C. Differential expression of miRNAs in the serum of patients with high-risk oral lesions. Cancer medicine 2012;1(2):268-74.
9.   Pegtel DM, Cosmopoulos K, Thorley-Lawson DA, van Eijndhoven MA, Hopmans ES, Lindenberg JL, et al. Functional delivery of viral miRNAs via exosomes. Proceedings of the National Academy of Sciences 2010;107(14):6328-33.
10.   Gallo A, Tandon M, Alevizos I, Illei GG. The majority of microRNAs detectable in serum and saliva is concentrated in exosomes. PLoS One 2012;7(3):e30679.
11.   Arroyo JD, Chevillet JR, Kroh EM, Ruf IK, Pritchard CC, Gibson DF, et al. Argonaute2 complexes carry a population of circulating microRNAs independent of vesicles in human plasma. Proceedings of the National Academy of Sciences 2011;108(12):5003-08.
12.   Turchinovich A, Weiz L, Langheinz A, Burwinkel B. Characterization of extracellular circulating microRNA. Nucleic acids research 2011:gkr254.
13.   Ostenfeld MS, Jeppesen DK, Laurberg JR, Boysen AT, Bramsen JB, Primdal-Bengtson B, et al. Cellular disposal of miR23b by RAB27-dependent exosome release is linked to acquisition of metastatic properties. Cancer Research 2014;74(20):5758-71.
14.   Zhang Y, Liu D, Chen X, Li J, Li L, Bian Z, et al. Secreted monocytic miR-150 enhances targeted endothelial cell migration. Molecular cell 2010;39(1):133-44.
15.   Bartel DP. MicroRNAs: genomics, biogenesis, mechanism, and function. Cell 2004;116(2):281-97.
16.   Kosaka N, Iguchi H, Hagiwara K, Yoshioka Y, Takeshita F, Ochiya T. Neutral sphingomyelinase 2 (nSMase2)-dependent exosomal transfer of angiogenic microRNAs regulate cancer cell metastasis. Journal of Biological Chemistry 2013;288(15):10849-59.
17.   Ye S-b, Li Z-L, Luo D-h, Huang B-j, Chen Y-S, Zhang X-s, et al. Tumor-derived exosomes promote tumor progression and T-cell dysfunction through the regulation of enriched exosomal microRNAs in human nasopharyngeal carcinoma. Oncotarget 2014;5(14):5439-52.

18.   Rana S, Malinowska K, Zöller M. Exosomal tumor microRNA modulates premetastatic organ cells. Neoplasia 2013;15(3):281-IN31.

19.   Tsui NB, Ng EK, Lo YD. Stability of endogenous and added RNA in blood specimens, serum, and plasma. Clinical chemistry 2002;48(10):1647-53.

20.   Mitchell PS, Parkin RK, Kroh EM, Fritz BR, Wyman SK, Pogosova-Agadjanyan EL, et al. Circulating microRNAs as stable blood-based markers for cancer detection. Proceedings of the National Academy of Sciences 2008;105(30):10513-18.

21.   Wang L-g, Gu J. Serum microRNA-29a is a promising novel marker for early detection of colorectal liver metastasis. Cancer epidemiology 2012;36(1):e61-e67.

22.   Asaga S, Kuo C, Nguyen T, Terpenning M, Giuliano AE, Hoon DS. Direct serum assay for microRNA-21 concentrations in early and advanced breast cancer. Clinical chemistry 2011;57(1):84-91.

23.   Wang ZX, Bian HB, Wang JR, Cheng ZX, Wang KM, De W. Prognostic significance of serum miRNA-21 expression in human non-small cell lung cancer. Journal of surgical oncology 2011;104(7):847-51.

24.   Kim JW, Wieckowski E, Taylor DD, Reichert TE, Watkins S, Whiteside TL. Fas ligand–positive membranous vesicles isolated from sera of patients with oral cancer induce apoptosis of activated T lymphocytes. Clinical Cancer Research 2005;11(3):1010-20.

25.   Wieckowski EU, Visus C, Szajnik M, Szczepanski MJ, Storkus WJ, Whiteside TL. Tumor-derived microvesicles promote regulatory T cell expansion and induce apoptosis in tumor-reactive activated CD8+ T lymphocytes. The Journal of Immunology 2009;183(6):3720-30.

26.   Szajnik M, Czystowska M, Szczepanski MJ, Mandapathil M, Whiteside TL. Tumor-derived microvesicles induce, expand and up-regulate biological activities of human regulatory T cells (Treg). PloS one 2010;5(7):e11469.

27.   Rekker K, Saare M, Roost AM, Kubo A-L, Zarovni N, Chiesi A, et al. Comparison of serum exosome isolation methods for microRNA profiling. Clinical biochemistry 2014;47(1):135-38.

28.   Witwer KW, Buzas EI, Bemis LT, Bora A, Lässer C, Lötvall J, et al. Standardization of sample collection, isolation and analysis methods in extracellular vesicle research. Journal of extracellular vesicles 2013;2.

29.   Mráz M, Malinova K, Mayer J, Pospisilova S. MicroRNA isolation and stability in stored RNA samples. Biochemical and biophysical research communications 2009;390(1):1-4.

30.   Zampetaki A, Mayr M. Analytical challenges and technical limitations in assessing circulating miRNAs. Thrombosis and haemostasis 2012;108(4):592.

31.   Park NJ, Li Y, Yu T, Brinkman BM, Wong DT. Characterization of RNA in saliva. Clinical chemistry 2006;52(6):988-94.

32.   Wiklund ED, Gao S, Hulf T, Sibbritt T, Nair S, Costea DE, et al. MicroRNA alterations and associated aberrant DNA methylation patterns across multiple sample types in oral squamous cell carcinoma. PLoS One 2011;6(11):e27840.

33.   Lau CS, Wong DT. Breast cancer exosome-like microvesicles and salivary gland cells interplay alters salivary gland cell-derived exosome-like microvesicles in vitro. PloS one 2012;7(3):e33037.

34. Park NJ, Zhou H, Elashoff D, Henson BS, Kastratovic DA, Abemayor E, et al. Salivary microRNA: discovery, characterization, and clinical utility for oral cancer detection. Clinical Cancer Research 2009;15(17):5473-77.
35. Zahran F, Ghalwash D, Shaker O, Al-Johani K, Scully C. Salivary microRNAs in oral cancer. Oral diseases 2015;21(6):739-47.
36. Momen-Heravi F, Trachtenberg A, Kuo W, Cheng Y. Genomewide study of salivary microRNAs for detection of oral cancer. Journal of Dental Research 2014:0022034514531018.
37. Liu CJ, Lin SC, Yang CC, Cheng HW, Chang KW. Exploiting salivary miR-31 as a clinical biomarker of oral squamous cell carcinoma. Head & neck 2012;34(2):219-24.
38. Salazar C, Nagadia R, Pandit P, Cooper-White J, Banerjee N, Dimitrova N, et al. A novel saliva-based microRNA biomarker panel to detect head and neck cancers. Cellular Oncology 2014;37(5):331-38.
39. Al-Malkey MK, Abbas AA, Khalaf NF, Mubarak IA, Jasim IA. Expression Analysis of Salivary Microrna-31 in Oral Cancer Patients. Int J Curr Microbiol App Sci 2015;4(12):375-82.
40. Duz MB, Karatas OF, Guzel E, Turgut NF, Yilmaz M, Creighton CJ, et al. Identification of miR-139-5p as a saliva biomarker for tongue squamous cell carcinoma: A pilot study. Cellular Oncology 2016;39(2):187-93.
41. Liu X-G, Zhu W-Y, Huang Y-Y, Ma L-N, Zhou S-Q, Wang Y-K, et al. High expression of serum miR-21 and tumor miR-200c associated with poor prognosis in patients with lung cancer. Medical Oncology 2012;29(2):618-26.
42. Toiyama Y, Takahashi M, Hur K, Nagasaka T, Tanaka K, Inoue Y, et al. Serum miR-21 as a diagnostic and prognostic biomarker in colorectal cancer. Journal of the National Cancer Institute 2013;105(12):849-59.
43. Gao J, Zhang Q, Xu J, Guo L, Li X. Clinical significance of serum miR-21 in breast cancer compared with CA153 and CEA. Chinese Journal of Cancer Research 2013;25(6):743-48.
44. Liu CJ, Kao SY, Tu HF, Tsai MM, Chang KW, Lin SC. Increase of microRNA miR-31 level in plasma could be a potential marker of oral cancer. Oral diseases 2010;16(4):360-64.
45. Yang CC, Hung PS, Wang PW, Liu CJ, Chu TH, Cheng HW, et al. miR-181 as a putative biomarker for lymph-node metastasis of oral squamous cell carcinoma. Journal of oral pathology & medicine 2011;40(5):397-404.
46. Lu Y-C, Chen Y-J, Wang H-M, Tsai C-Y, Chen W-H, Huang Y-C, et al. Oncogenic function and early detection potential of miRNA-10b in oral cancer as identified by microRNA profiling. Cancer Prevention Research 2012;5(4):665-74.
47. Liu X, Luo H-N, Tian W-D, Lu J, Li G, Wang L, et al. Diagnostic and prognostic value of plasma microRNA deregulation in nasopharyngeal carcinoma. Cancer biology & therapy 2013;14(12):1133-42.
48. Lu Y-C, Chang JT-C, Huang Y-C, Huang C-C, Chen W-H, Lee L-Y, et al. Combined determination of circulating miR-196a and miR-196b levels produces high sensitivity and specificity for early detection of oral cancer. Clinical biochemistry 2015;48(3):115-21.
49. Ayaz L, Görür A, Yaroğlu HY, Özcan C, Tamer L. Differential expression of microRNAs in plasma of patients with laryngeal squamous cell carcinoma: potential

early-detection markers for laryngeal squamous cell carcinoma. Journal of cancer research and clinical oncology 2013;139(9):1499-506.

50. Zhang G, Zong J, Lin S, Verhoeven RJ, Tong S, Chen Y, et al. Circulating Epstein–Barr virus microRNAs miR-BART7 and miR-BART13 as biomarkers for nasopharyngeal carcinoma diagnosis and treatment. International Journal of Cancer 2015;136(5):E301-E12.

51. Tachibana H, Sho R, Takeda Y, Zhang X, Yoshida Y, Narimatsu H, et al. Circulating miR-223 in Oral Cancer: Its Potential as a Novel Diagnostic Biomarker and Therapeutic Target. PLoS One 2016;11(7):e0159693.

52. Hsu C-M, Lin P-M, Wang Y-M, Chen Z-J, Lin S-F, Yang M-Y. Circulating miRNA is a novel marker for head and neck squamous cell carcinoma. Tumor Biology 2012;33(6):1933-42.

53. Zeng X, Xiang J, Wu M, Xiong W, Tang H, Deng M, et al. Circulating miR-17, miR-20a, miR-29c, and miR-223 combined as non-invasive biomarkers in nasopharyngeal carcinoma. PLoS One 2012;7(10):e46367.

54. Heegaard NH, Schetter AJ, Welsh JA, Yoneda M, Bowman ED, Harris CC. Circulating micro-RNA expression profiles in early stage nonsmall cell lung cancer. International journal of cancer 2012;130(6):1378-86.

55. McDonald JS, Milosevic D, Reddi HV, Grebe SK, Algeciras-Schimnich A. Analysis of circulating microRNA: preanalytical and analytical challenges. Clinical chemistry 2011;57(6):833-40.

56. Ries J, Vairaktaris E, Agaimy A, Kintopp R, Baran C, Neukam FW, et al. miR-186, miR-3651 and miR-494: potential biomarkers for oral squamous cell carcinoma extracted from whole blood. Oncology reports 2014;31(3):1429-36.

57. Wong TS, Liu XB, Wong BYH, Ng RWM, Yuen APW, Wei WI. Mature miR-184 as potential oncogenic microRNA of squamous cell carcinoma of tongue. Clinical Cancer Research 2008;14(9):2588-92.

58. MacLellan SA, MacAulay C, Lam S, Garnis C. Pre-profiling factors influencing serum microRNA levels. BMC clinical pathology 2014;14(1):1.

59. Kirschner MB, Edelman JJB, Kao SC, Vallely MP, Van Zandwijk N, Reid G. The impact of hemolysis on cell-free microRNA biomarkers. The origin, function and diagnostic potential of extracellular microRNA in human body fluids 2014:53.

60. Pritchard CC, Kroh E, Wood B, Arroyo JD, Dougherty KJ, Miyaji MM, et al. Blood cell origin of circulating microRNAs: a cautionary note for cancer biomarker studies. Cancer Prevention Research 2012;5(3):492-97.

61. MacLellan SA, MacAulay C, Lam S, Garnis C. Pre-profiling factors influencing serum microRNA levels. BMC clinical pathology 2014;14(1):27.

62. Wang S, Xiang J, Li Z, Lu S, Hu J, Gao X, et al. A plasma microRNA panel for early detection of colorectal cancer. International Journal of Cancer 2015;136(1):152-61.

63. Maxwell JH, Ferris RL, Gooding W, Cunningham D, Mehta V, Kim S, et al. Extracapsular spread in head and neck carcinoma: impact of site and human papillomavirus status. Cancer 2013;119(18):3302-08.

64. Argiris A, Li S, Ghebremichael M, Egloff A, Wang L, Forastiere A, et al. Prognostic significance of human papillomavirus in recurrent or metastatic head and neck cancer: an

analysis of Eastern Cooperative Oncology Group trials. Annals of Oncology 2014;25(7):1410-16.

65. Yang Y, Li Y-x, Yang X, Jiang L, Zhou Z-j, Zhu Y-q. Progress risk assessment of oral premalignant lesions with saliva miRNA analysis. BMC cancer 2013;13(1):1.

66. Hou B, Ishinaga H, Midorikawa K, Shah SA, Nakamura S, Hiraku Y, et al. Circulating microRNAs as novel prognosis biomarkers for head and neck squamous cell carcinoma. Cancer biology & therapy 2015;16(7):1042-46.

67. Brito JA, Gomes CC, Pimenta FJ, Barbosa AA, Prado MA, Prado VF, et al. Reduced expression of mir15a in the blood of patients with oral squamous cell carcinoma is associated with tumor staging. Experimental and therapeutic medicine 2010;1(1):217-21.

68. Lerner C, Wemmert S, Bochen F, Kulas P, Linxweiler M, Hasenfus A, et al. Characterization of miR-146a and miR-155 in blood, tissue and cell lines of head and neck squamous cell carcinoma patients and their impact on cell proliferation and migration. Journal of cancer research and clinical oncology 2016;142(4):757-66.

69. Woolgar JA, Scott J, Vaughan E, Brown J, West C, Rogers S. Survival, metastasis and recurrence of oral cancer in relation to pathological features. Annals of the Royal College of Surgeons of England 1995;77(5):325.

70. Lynch DP. Oral cancer risk and detection. The importance of screening technology. RDH 2007;27(9):1010-112.

71. Taylor JM, Ankerst DP, Andridge RR. Validation of biomarker-based risk prediction models. Clinical Cancer Research 2008;14(19):5977-83.

72. Chen JJ, Lu T-P, Chen D-T, Wang S-J. Biomarker adaptive designs in clinical trials. Translational Cancer Research 2014;3(3):279-92.

73. Salín-Pascual RJ, Rosas M, Jimenez-Genchi A, Rivera-Meza BL. Antidepressant effect of transdermal nicotine patches in nonsmoking patients with major depression. Journal of Clinical Psychiatry 1996.

74. Takahashi K, Yokota S-i, Tatsumi N, Fukami T, Yokoi T, Nakajima M. Cigarette smoking substantially alters plasma microRNA profiles in healthy subjects. Toxicology and applied pharmacology 2013;272(1):154-60.

75. Tosar JP, Gámbaro F, Sanguinetti J, Bonilla B, Witwer KW, Cayota A. Assessment of small RNA sorting into different extracellular fractions revealed by high-throughput sequencing of breast cell lines. Nucleic acids research 2015:gkv432.

76. Valadi H, Ekström K, Bossios A, Sjöstrand M, Lee JJ, Lötvall JO. Exosome-mediated transfer of mRNAs and microRNAs is a novel mechanism of genetic exchange between cells. Nat Cell Biol 2007;9(6):654-59.

77. Lässer C, Alikhani VS, Ekström K, Eldh M, Paredes PT, Bossios A, et al. Human saliva, plasma and breast milk exosomes contain RNA: uptake by macrophages. Journal of translational medicine 2011;9(1):9.

78. Aucher A, Rudnicka D, Davis DM. MicroRNAs transfer from human macrophages to hepato-carcinoma cells and inhibit proliferation. The Journal of Immunology 2013;191(12):6250-60.

79. Canitano A, Venturi G, Borghi M, Ammendolia MG, Fais S. Exosomes released in vitro from Epstein–Barr virus (EBV)-infected cells contain EBV-encoded latent phase mRNAs. Cancer letters 2013;337(2):193-99.

80. Gourzones C, Gelin A, Bombik I, Klibi J, Vérillaud B, Guigay J, et al. Extra-cellular release and blood diffusion of BART viral micro-RNAs produced by EBV-infected nasopharyngeal carcinoma cells. Virol J 2010;7(271):1-12.

81. Meckes DG, Shair KH, Marquitz AR, Kung C-P, Edwards RH, Raab-Traub N. Human tumor virus utilizes exosomes for intercellular communication. Proceedings of the National Academy of Sciences 2010;107(47):20370-75.

82. Wong AMG, Kong KL, Tsang JWH, Kwong DLW, Guan XY. Profiling of Epstein-Barr virus-encoded microRNAs in nasopharyngeal carcinoma reveals potential biomarkers and oncomirs. Cancer 2012;118(3):698-710.

83. Ramachandran I, Thavathiru E, Ramalingam S, Natarajan G, Mills W, Benbrook DM, et al. Wnt inhibitory factor 1 induces apoptosis and inhibits cervical cancer growth, invasion and angiogenesis in vivo. Oncogene 2012;31(22):2725-37.

84. Xia T, O'Hara A, Araujo I, Barreto J, Carvalho E, Sapucaia JB, et al. EBV microRNAs in primary lymphomas and targeting of CXCL-11 by ebv-mir-BHRF1-3. Cancer research 2008;68(5):1436-42.

85. Cole KE, Strick CA, Paradis TJ, Ogborne KT, Loetscher M, Gladue RP, et al. Interferon–inducible T cell alpha chemoattractant (I-TAC): a novel Non-ELR CXC Chemokine with potent activity on activated T cells through selective high affinity binding to CXCR3. The Journal of experimental medicine 1998;187(12):2009-21.

86. Stewart BW, Kleihues P. World Cancer Report. Stewart BW, Kleihues P, editors. Lyon: WHO International Agency for Research on Cancer; 2003.

87. Warnakulasuriya S. Global epidemiology of oral and oropharyngeal cancer. Oral oncology 2009;45(4):309-16.

88. Komatsu S, Ichikawa D, Takeshita H, Tsujiura M, Morimura R, Nagata H, et al. Circulating microRNAs in plasma of patients with oesophageal squamous cell carcinoma. British journal of cancer 2011;105(1):104-11.

89. Ohshima K, Inoue K, Fujiwara A, Hatakeyama K, Kanto K, Watanabe Y, et al. Let-7 microRNA family is selectively secreted into the extracellular environment via exosomes in a metastatic gastric cancer cell line. PLoS One 2010;5(10):e13247.

90. Kirschner MB, Kao SC, Edelman JJ, Armstrong NJ, Vallely MP, van Zandwijk N, et al. Haemolysis during sample preparation alters microRNA content of plasma. PLoS One 2011;6(9):e24145.

91. Liu C-J, Lin J-S, Cheng H-W, Hsu Y-H, Cheng C-Y, Lin S-C. Plasma miR-187* is a potential biomarker for oral carcinoma. Clinical Oral Investigations 2016:1-8.

92. Hayward J, Regezi J. Oral dysplasia and in situ carcinoma: clinicopathologic correlations of eight patients. Journal of oral surgery (American Dental Association: 1965) 1977;35(9):756-62.

93. Amagasa T, Yokoo E, Sato K, Tanaka N, Shioda S, Takagi M. A study of the clinical characteristics and treatment of oral carcinoma in situ. Oral surgery, oral medicine, oral pathology 1985;60(1):50-55.

94. Poh CF, Anderson DW, Durham JS, Chen J, Berean KW, MacAulay CE, et al. Fluorescence Visualization–Guided Surgery for Early-Stage Oral Cancer. JAMA Otolaryngology–Head & Neck Surgery 2016;142(3):209-16.

95.   Vandesompele J, De Preter K, Pattyn F, Poppe B, Van Roy N, De Paepe A, et al. Accurate normalization of real-time quantitative RT-PCR data by geometric averaging of multiple internal control genes. Genome biology 2002;3(7):research0034.

96.   Harrell Jr FE, Lee KL, Matchar DB, Reichert TA. Regression models for prognostic prediction: advantages, problems, and suggested solutions. Cancer treatment reports 1985;69(10):1071-77.

97.   Tibshirani R. Regression shrinkage and selection via the lasso. Journal of the Royal Statistical Society Series B (Methodological) 1996:267-88.

98.   Goossens N, Nakagawa S, Sun X, Hoshida Y. Cancer biomarker discovery and validation. Translational cancer research 2015;4(3):256.

99.   Maxim LD, Niebo R, Utell MJ. Screening tests: a review with examples. Inhal Toxicol 2014;26(13):811-28.

100.   Tian X, Chen Z, Shi S, Wang X, Wang W, Li N, et al. Clinical Diagnostic Implications of Body Fluid MiRNA in Oral Squamous Cell Carcinoma: A Meta-Analysis. Medicine 2015;94(37).

101.   Horowitz A. Perform a death defying act-The 90-second oral cancer examination. Journal of the American Dental Association 2001;132:36S-40S.

102.   Fayyad-Kazan H, Bitar N, Najar M, Lewalle P, Fayyad-Kazan M, Badran R, et al. Circulating miR-150 and miR-342 in plasma are novel potential biomarkers for acute myeloid leukemia. Journal of translational medicine 2013;11(1):1.

103.   Wang H, Tan G, Dong L, Cheng L, Li K, Wang Z, et al. Circulating MiR-125b as a marker predicting chemoresistance in breast cancer. PLoS One 2012;7(4):e34210.

104.   Yuxia M, Zhennan T, Wei Z. Circulating miR-125b is a novel biomarker for screening non-small-cell lung cancer and predicts poor prognosis. Journal of cancer research and clinical oncology 2012;138(12):2045-50.

105.   Henson BJ, Bhattacharjee S, O'Dee DM, Feingold E, Gollin SM. Decreased expression of miR-125b and miR-100 in oral cancer cells contributes to malignancy. Genes, Chromosomes and Cancer 2009;48(7):569-82.

106.   Feng Z, Jiang B, Chandra J, Ghannoum M, Nelson S, Weinberg A. Human beta-defensins: differential activity against candidal species and regulation by Candida albicans. Journal of Dental Research 2005;84(5):445-50.

107.   Smith IM, Glazer CA, Mithani SK, Ochs MF, Sun W, Bhan S, et al. Coordinated activation of candidate proto-oncogenes and cancer testes antigens via promoter demethylation in head and neck cancer and lung cancer. PLoS One 2009;4(3):e4961.

108.   Alawi F, Lin P, Ziober B, Patel R. Dyskerin expression correlates with active proliferation independently of telomerase. Head & neck 2011;33(7):1041.

109.   Jabr-Milane LS, van Vlerken LE, Yadav S, Amiji MM. Multi-functional nanocarriers to overcome tumor drug resistance. Cancer treatment reviews 2008;34(7):592-602.

110.   Ha PK, Benoit NE, Yochem R, Sciubba J, Zahurak M, Sidransky D, et al. A transcriptional progression model for head and neck cancer. Clinical Cancer Research 2003;9(8):3058-64.

111.   Tsui IF, Garnis C. Integrative molecular characterization of head and neck cancer cell model genomes. Head & neck 2010;32(9):1143-60.

112. Sharma SV, Lee DY, Li B, Quinlan MP, Takahashi F, Maheswaran S, et al. A chromatin-mediated reversible drug-tolerant state in cancer cell subpopulations. Cell 2010;141(1):69-80.

113. Kozaki K-i, Imoto I, Mogi S, Omura K, Inazawa J. Exploration of tumor-suppressive microRNAs silenced by DNA hypermethylation in oral cancer. Cancer Research 2008;68(7):2094-105.

114. Järvinen AK, Autio R, Kilpinen S, Saarela M, Leivo I, Grénman R, et al. High-resolution copy number and gene expression microarray analyses of head and neck squamous cell carcinoma cell lines of tongue and larynx. Genes, Chromosomes and Cancer 2008;47(6):500-09.

115. Lin SC, Liu CJ, Chiu CP, Chang SM, Lu SY, Chen YJ. Establishment of OC3 oral carcinoma cell line and identification of NF-κB activation responses to areca nut extract. Journal of oral pathology & medicine 2004;33(2):79-86.

116. McGregor F, Muntoni A, Fleming J, Brown J, Felix DH, MacDonald DG, et al. Molecular Changes Associated with Oral Dysplasia Progression and Acquisition of Immortality Potential for Its Reversal by 5-Azacytidine. Cancer Research 2002;62(16):4757-66.

117. Hunter KD, Thurlow JK, Fleming J, Drake PJ, Vass JK, Kalna G, et al. Divergent routes to oral cancer. Cancer Research 2006;66(15):7405-13.

118. Califano J, van der Riet P, Westra W, Nawroz H, Clayman G, Piantadosi S, et al. Genetic progression model for head and neck cancer: implications for field cancerization. Cancer Research 1996;56(11):2488-92.

119. Hayflick L, Moorhead PS. The serial cultivation of human diploid cell strains. Experimental cell research 1961;25(3):585-621.

120. Sato M, Vaughan MB, Girard L, Peyton M, Lee W, Shames DS, et al. Multiple oncogenic changes (K-RASV12, p53 knockdown, mutant EGFRs, p16 bypass, telomerase) are not sufficient to confer a full malignant phenotype on human bronchial epithelial cells. Cancer Research 2006;66(4):2116-28.

121. Westerman KA, Leboulch P. Reversible immortalization of mammalian cells mediated by retroviral transfer and site-specific recombination. Proceedings of the National Academy of Sciences 1996;93(17):8971-76.

122. Halbert C, Demers G, Galloway D. The E7 gene of human papillomavirus type 16 is sufficient for immortalization of human epithelial cells. Journal of virology 1991;65(1):473-78.

123. Bodnar AG, Ouellette M, Frolkis M, Holt SE, Chiu C-P, Morin GB, et al. Extension of life-span by introduction of telomerase into normal human cells. Science 1998;279(5349):349-52.

124. Kim J, Ji M, DiDonato JA, Rackley RR, Kuang M, Sadhukhan PC, et al. An hTERT-immortalized human urothelial cell line that responds to anti-proliferative factor. In Vitro Cellular & Developmental Biology-Animal 2011;47(1):2-9.

125. Tsao S-W, Mok SC, Fey EG, Fletcher JA, Wan TS, Chew E-C, et al. Characterization of human ovarian surface epithelial cells immortalized by human papilloma viral oncogenes (HPV-E6E7 ORFs). Experimental cell research 1995;218(2):499-507.

126. Rheinwald JG, Hahn WC, Ramsey MR, Wu JY, Guo Z, Tsao H, et al. A two-stage, p16INK4A-and p53-dependent keratinocyte senescence mechanism that limits replicative

potential independent of telomere status. Molecular and cellular biology 2002;22(14):5157-72.

127. Dickson MA, Hahn WC, Ino Y, Ronfard V, Wu JY, Weinberg RA, et al. Human keratinocytes that express hTERT and also bypass a p16INK4a-enforced mechanism that limits life span become immortal yet retain normal growth and differentiation characteristics. Molecular and cellular biology 2000;20(4):1436-47.

128. Burns J, Clark L, Yeudall W, Mitchell R, Mackenzie K, Chang S, et al. The p53 status of cultured human premalignant oral keratinocytes. British journal of cancer 1994;70(4):591.

129. Munro J, Stott FJ, Vousden KH, Peters G, Parkinson EK. Role of the alternative INK4A proteins in human keratinocyte senescence: evidence for the specific inactivation of p16INK4A upon immortalization. Cancer Research 1999;59(11):2516-21.

130. Chomczynski P, Sacchi N. Single-step method of RNA isolation by acid guanidinium thiocyanate-phenol-chloroform extraction. Analytical biochemistry 1987;162(1):156-9.

131. Towle R, Truong D, Hogg K, Robinson WP, Poh CF, Garnis C. Global analysis of DNA methylation changes during progression of oral cancer. Oral oncology 2013;49(11):1033-42.

132. Ishkanian AS, Malloff CA, Watson SK, J deLeeuw R, Chi B, Coe BP, et al. A tiling resolution DNA microarray with complete coverage of the human genome. Nature genetics 2004;36(3):299-303.

133. Wong KK, DeLeeuw RJ, Dosanjh NS, Kimm LR, Cheng Z, Horsman DE, et al. A comprehensive analysis of common copy-number variations in the human genome. The American Journal of Human Genetics 2007;80(1):91-104.

134. Lockwood W, Chari R, Coe B, Girard L, Macaulay C, Lam S, et al. DNA amplification is a ubiquitous mechanism of oncogene activation in lung and other cancers. Oncogene 2008;27(33):4615-24.

135. Tsui IFL, Rosin MP, Zhang L, Ng RT, Lam WL. Multiple aberrations of chromosome 3p detected in oral premalignant lesions. Cancer Prevention Research 2008;1(6):424-29.

136. Khojasteh M, Lam WL, Ward RK, MacAulay C. A stepwise framework for the normalization of array CGH data. BMC bioinformatics 2005;6(1):274.

137. Chi B, J deLeeuw R, Coe BP, Ng RT, MacAulay C, Lam WL. MD-SeeGH: a platform for integrative analysis of multi-dimensional genomic data. BMC bioinformatics 2008;9(1):243.

138. Carro A, Rico D, Rueda OM, Díaz-Uriarte R, Pisano DG. waviCGH: a web application for the analysis and visualization of genomic copy number alterations. Nucleic acids research 2010;38(suppl 2):W182-W87.

139. Kanehisa M, Goto S. KEGG: kyoto encyclopedia of genes and genomes. Nucleic acids research 2000;28(1):27-30.

140. Smoot ME, Ono K, Ruscheinski J, Wang P-L, Ideker T. Cytoscape 2.8: new features for data integration and network visualization. Bioinformatics 2011;27(3):431-32.

141. Bindea G, Mlecnik B, Hackl H, Charoentong P, Tosolini M, Kirilovsky A, et al. ClueGO: a Cytoscape plug-in to decipher functionally grouped gene ontology and pathway annotation networks. Bioinformatics 2009;25(8):1091-93.

142. Gorenchtein M, Towle R, Dickman C, Zhu Y, Poh CF, Garnis C. Dysregulation of microRNAs across oral cancer fields in non-smokers. Oral Oncology (Submitted)2013.

143. Mestdagh P, Van Vlierberghe P, De Weer A, Muth D, Westermann F, Speleman F, et al. A novel and universal method for microRNA RT-qPCR data normalization. Genome Biol 2009;10(6):R64.

144. Chang DD, Park N-H, Denny CT, Nelson SF, Pe M. Characterization of transformation related genes in oral cancer cells. Oncogene 1998;16(15):1921.

145. Hawley-Nelson P, Vousden KH, Hubbert NL, Lowy DR, Schiller JT. HPV16 E6 and E7 proteins cooperate to immortalize human foreskin keratinocytes. The EMBO journal 1989;8(12):3905.

146. Scheffner M, Werness BA, Huibregtse JM, Levine AJ, Howley PM. The E6 oncoprotein encoded by human papillomavirus types 16 and 18 promotes the degradation of p53. Cell 1990;63(6):1129.

147. Pickering CR, Zhang J, Yoo S-Y, Bengtsson L, Moorthy S, Neskey DM, et al. Integrative genomic characterization of oral squamous cell carcinoma identifies frequent somatic drivers. Cancer Discovery 2013.

148. Gjoerup OV, Wu J, Chandler-Militello D, Williams GL, Zhao J, Schaffhausen B, et al. Surveillance mechanism linking Bub1 loss to the p53 pathway. Proceedings of the National Academy of Sciences 2007;104(20):8334-39.

149. Chang T-C, Wentzel EA, Kent OA, Ramachandran K, Mullendore M, Lee KH, et al. Transactivation of miR-34a by p53 broadly influences gene expression and promotes apoptosis. Molecular cell 2007;26(5):745-52.

150. Scapoli L, Palmieri A, Lo ML, Pezzetti F, Rubini C, Girardi A, et al. MicroRNA expression profiling of oral carcinoma identifies new markers of tumor progression. International journal of immunopathology and pharmacology 2010;23(4):1229.

151. Kumar M, Lu Z, Takwi AAL, Chen W, Callander NS, Ramos KS, et al. Negative regulation of the tumor suppressor p53 gene by microRNAs. Oncogene 2010;30(7):843-53.

152. Shay J, Bacchetti S. A survey of telomerase activity in human cancer. European Journal of Cancer 1997;33(5):787-91.

153. Tabori U, Nanda S, Druker H, Lees J, Malkin D. Younger age of cancer initiation is associated with shorter telomere length in Li-Fraumeni syndrome. Cancer Research 2007;67(4):1415-18.

154. Edington KG, Loughran OP, Berry IJ, Parkinson EK. Cellular immortality: a late event in the progression of human squamous cell carcinoma of the head and neck associated with p53 alteration and a high frequency of allele loss. Molecular carcinogenesis 1995;13(4):254-65.

155. Stewart SA, Hahn WC, O'Connor BF, Banner EN, Lundberg AS, Modha P, et al. Telomerase contributes to tumorigenesis by a telomere length-independent mechanism. Proceedings of the National Academy of Sciences 2002;99(20):12606-11.

156. Chapman EJ, Kelly G, Knowles MA. Genes involved in differentiation, stem cell renewal, and tumorigenesis are modulated in telomerase-immortalized human urothelial cells. Molecular Cancer Research 2008;6(7):1154-68.

157. Fuchs E, Green H. Regulation of terminal differentiation of cultured human keratinocytes by vitamin A. Cell 1981;25(3):617-25.

158. Kopan R, Traska G, Fuchs E. Retinoids as important regulators of terminal differentiation: examining keratin expression in individual epidermal cells at various stages of keratinization. The Journal of Cell Biology 1987;105(1):427-40.

159. Sdek P, Zhang Z, Cao J, Pan H, Chen W, Zheng J. Alteration of cell-cycle regulatory proteins in human oral epithelial cells immortalized by HPV16 E6 and E7. International journal of oral and maxillofacial surgery 2006;35(7):653-57.

160. Boldrup L, Coates PJ, Laurell G, Nylander K. Differences in p63 expression in SCCHN tumours of different sub-sites within the oral cavity. Oral oncology 2011;47(9):861-65.

161. Krump M, Ehrmann J. Differences in CD44s expression in HNSCC tumours of different areas within the oral cavity. Biomedical Papers 2013;157(4):280-83.

162. Severino P, Alvares AM, Michaluart P, Okamoto OK, Nunes FD, Moreira-Filho CA, et al. Global gene expression profiling of oral cavity cancers suggests molecular heterogeneity within anatomic subsites. BMC research notes 2008;1(1):113.

163. Boldrup L, Coates PJ, Wahlgren M, Laurell G, Nylander K. Subsite-based alterations in miR-21, miR-125b, and miR-203 in squamous cell carcinoma of the oral cavity and correlation to important target proteins. Journal of carcinogenesis 2012;11(1):18.

164. Di Vizio D, Kim J, Hager MH, Morello M, Yang W, Lafargue CJ, et al. Oncosome formation in prostate cancer: association with a region of frequent chromosomal deletion in metastatic disease. Cancer Research 2009;69(13):5601-09.

165. Théry C, Amigorena S, Raposo G, Clayton A. Isolation and characterization of exosomes from cell culture supernatants and biological fluids. Current protocols in cell biology 2006:3.22. 1-3.22. 29.

166. Colombo M, Raposo G, Théry C. Biogenesis, secretion, and intercellular interactions of exosomes and other extracellular vesicles. Annual review of cell and developmental biology 2014;30:255-89.

167. Kowal J, Arras G, Colombo M, Jouve M, Morath JP, Primdal-Bengtson B, et al. Proteomic comparison defines novel markers to characterize heterogeneous populations of extracellular vesicle subtypes. Proceedings of the National Academy of Sciences 2016;113(8):E968-E77.

168. Minciacchi VR, Freeman MR, Di Vizio D. Extracellular vesicles in cancer: exosomes, microvesicles and the emerging role of large oncosomes. 2015. Elsevier. p 41-51.

169. Gorenchtein M, Poh C, Saini R, Garnis C. MicroRNAs in an oral cancer context–from basic biology to clinical utility. Journal of Dental Research 2012;91(5):440-46.

170. Towle R, Gorenchtein M, Garnis C, Dickman C, Zhu Y. Dysregulation of microRNAs across oral squamous cell carcinoma fields in non-smokers. J Interdiscipl Med Dent Sci 2014;2(131):2.

171. Yu F, Yao H, Zhu P, Zhang X, Pan Q, Gong C, et al. let-7 regulates self renewal and tumorigenicity of breast cancer cells. Cell 2007;131(6):1109-23.

172. Taylor DD, Gercel-Taylor C. MicroRNA signatures of tumor-derived exosomes as diagnostic biomarkers of ovarian cancer. Gynecologic oncology 2008;110(1):13-21.

173. Logozzi M, De Milito A, Lugini L, Borghi M, Calabrò L, Spada M, et al. High levels of exosomes expressing CD63 and caveolin-1 in plasma of melanoma patients. PLoS One 2009;4(4):e5219.

174. Llorente A, Skotland T, Sylvänne T, Kauhanen D, Róg T, Orłowski A, et al. Molecular lipidomics of exosomes released by PC-3 prostate cancer cells. Biochimica et Biophysica Acta (BBA)-Molecular and Cell Biology of Lipids 2013;1831(7):1302-09.

175. Marleau AM, Chen C-S, Joyce JA, Tullis RH. Exosome removal as a therapeutic adjuvant in cancer. J Transl Med 2012;10(1):134.

176. Ohno S-i, Takanashi M, Sudo K, Ueda S, Ishikawa A, Matsuyama N, et al. Systemically injected exosomes targeted to EGFR deliver antitumor microRNA to breast cancer cells. Molecular Therapy 2013;21(1):185-91.

177. Hood JL, San RS, Wickline SA. Exosomes released by melanoma cells prepare sentinel lymph nodes for tumor metastasis. Cancer Research 2011;71(11):3792-801.

178. Grange C, Tapparo M, Collino F, Vitillo L, Damasco C, Deregibus MC, et al. Microvesicles released from human renal cancer stem cells stimulate angiogenesis and formation of lung premetastatic niche. Cancer Research 2011;71(15):5346-56.

179. Gibbings DJ, Ciaudo C, Erhardt M, Voinnet O. Multivesicular bodies associate with components of miRNA effector complexes and modulate miRNA activity. Nature cell biology 2009;11(9):1143-49.

180. Skog J, Würdinger T, van Rijn S, Meijer DH, Gainche L, Curry WT, et al. Glioblastoma microvesicles transport RNA and proteins that promote tumour growth and provide diagnostic biomarkers. Nature cell biology 2008;10(12):1470-76.

181. Villarroya-Beltri C, Gutiérrez-Vázquez C, Sánchez-Cabo F, Pérez-Hernández D, Vázquez J, Martin-Cofreces N, et al. Sumoylated hnRNPA2B1 controls the sorting of miRNAs into exosomes through binding to specific motifs. Nature communications 2013;4.

182. Guduric-Fuchs J, O'Connor A, Camp B, O'Neill CL, Medina RJ, Simpson DA. Selective extracellular vesicle-mediated export of an overlapping set of microRNAs from multiple cell types. BMC genomics 2012;13(1):1.

183. Villarroya-Beltri C, Baixauli F, Gutiérrez-Vázquez C, Sánchez-Madrid F, Mittelbrunn M. Sorting it out: regulation of exosome loading. 2014. Elsevier. p 3-13.

184. Batagov AO, Kuznetsov VA, Kurochkin IV. Identification of nucleotide patterns enriched in secreted RNAs as putative cis-acting elements targeting them to exosome nano-vesicles. BMC genomics 2011;12(Suppl 3):S18.

185. Rabinowits G, Gerçel-Taylor C, Day JM, Taylor DD, Kloecker GH. Exosomal microRNA: a diagnostic marker for lung cancer. Clinical lung cancer 2009;10(1):42-46.

186. Michael A, Bajracharya SD, Yuen PS, Zhou H, Star RA, Illei GG, et al. Exosomes from human saliva as a source of microRNA biomarkers. Oral diseases 2010;16(1):34-38.

187. Umezu T, Ohyashiki K, Kuroda M, Ohyashiki J. Leukemia cell to endothelial cell communication via exosomal miRNAs. Oncogene 2013;32(22):2747-55.

188. van Balkom BW, De Jong OG, Smits M, Brummelman J, den Ouden K, de Bree PM, et al. Endothelial cells require miR-214 to secrete exosomes that suppress senescence and induce angiogenesis in human and mouse endothelial cells. Blood 2013;121(19):3997-4006.

189. Zhou Q, Gallagher R, Ufret-Vincenty R, Li X, Olson EN, Wang S. Regulation of angiogenesis and choroidal neovascularization by members of microRNA-23~ 27~ 24 clusters. Proceedings of the National Academy of Sciences 2011;108(20):8287-92.

190. Kuehbacher A, Urbich C, Zeiher AM, Dimmeler S. Role of Dicer and Drosha for endothelial microRNA expression and angiogenesis. Circulation research 2007;101(1):59-68.

191. Rani S, O'Brien K, Kelleher FC, Corcoran C, Germano S, Radomski MW, et al. Isolation of exosomes for subsequent mRNA, MicroRNA, and protein profiling. Gene Expression Profiling: Springer; 2011. p 181-95.

192. Wei Z, Batagov AO, Carter DR, Krichevsky AM. Fetal Bovine Serum RNA Interferes with the Cell Culture derived Extracellular RNA. Scientific Reports 2016;6.

193. Shelke GV, Lässer C, Gho YS, Lötvall J. Importance of exosome depletion protocols to eliminate functional and RNA-containing extracellular vesicles from fetal bovine serum. Journal of extracellular vesicles 2014;3.

194. Dickman CT, Towle R, Saini R, Garnis C. Molecular characterization of immortalized normal and dysplastic oral cell lines. Journal of oral pathology & medicine 2014.

195. Towle R, Tsui IF, Zhu Y, MacLellan S, Poh CF, Garnis C. Recurring DNA copy number gain at chromosome 9p13 plays a role in the activation of multiple candidate oncogenes in progressing oral premalignant lesions. Cancer medicine 2014;3(5):1170-84.

196. Halvorsen E, Hamilton M, Young A, Wadsworth B, LePard N, Lee H, et al. Maraviroc decreases CCL8-mediated migration of CCR5+ regulatory T cells and reduces metastatic tumour growth in the lungs. OncoImmunology 2016(just-accepted):00-00.

197. Mathivanan S, Simpson RJ. ExoCarta: A compendium of exosomal proteins and RNA. Proteomics 2009;9(21):4997-5000.

198. Gould SJ, Raposo G. As we wait: coping with an imperfect nomenclature for extracellular vesicles. Journal of extracellular vesicles 2013;2.

199. Trajkovic K, Hsu C, Chiantia S, Rajendran L, Wenzel D, Wieland F, et al. Ceramide triggers budding of exosome vesicles into multivesicular endosomes. Science 2008;319(5867):1244-47.

200. Ostrowski M, Carmo NB, Krumeich S, Fanget I, Raposo G, Savina A, et al. Rab27a and Rab27b control different steps of the exosome secretion pathway. Nature cell biology 2010;12(1):19-30.

201. Mitchell JA, Aronson AR, Mork JG, Folk LC, Humphrey SM, Ward JM. Gene indexing: characterization and analysis of NLM's GeneRIFs. 2003. American Medical Informatics Association. p 460.

202. Lei Z, Xu G, Wang L, Yang H, Liu X, Zhao J, et al. MiR-142-3p represses TGF-β-induced growth inhibition through repression of TGFβR1 in non-small cell lung cancer. The FASEB Journal 2014;28(6):2696-704.

203. Network CGAR. Integrated genomic analyses of ovarian carcinoma. Nature 2011;474(7353):609-15.

204. Yamano Y, Uzawa K, Shinozuka K, Fushimi K, Ishigami T, Nomura H, et al. Hyaluronan-mediated motility: a target in oral squamous cell carcinoma. International journal of oncology 2008;32(5):1001-09.

205. Xu S, Wei J, Wang F, Kong L-Y, Ling X-Y, Nduom E, et al. Effect of miR-142-3p on the M2 macrophage and therapeutic efficacy against murine glioblastoma. Journal of the National Cancer Institute 2014;106(8):dju162.

206. Bourguignon LY, Singleton PA, Zhu H, Zhou B. Hyaluronan promotes signaling interaction between CD44 and the transforming growth factor β receptor I in metastatic breast tumor cells. J Biol Chem 2002;277(42):39703-12.

207. Ota T, Fujii M, Sugizaki T, Ishii M, Miyazawa K, Aburatani H, et al. Targets of transcriptional regulation by two distinct type I receptors for transforming growth factor-β in human umbilical vein endothelial cells. Journal of cellular physiology 2002;193(3):299-318.

208. Arnaoutova I, George J, Kleinman HK, Benton G. The endothelial cell tube formation assay on basement membrane turns 20: state of the science and the art. Angiogenesis 2009;12(3):267-74.

209. Zhang T, Sun Q, Liu T, Chen J, Du S, Ren C, et al. MiR-451 increases radiosensitivity of nasopharyngeal carcinoma cells by targeting ras-related protein 14 (RAB14). Tumor Biol 2014;35(12):12593-99.

210. Feng J, Yang Y, Zhang P, Wang F, Ma Y, Qin H, et al. miR-150 functions as a tumour suppressor in human colorectal cancer by targeting c-Myb. Journal of cellular and molecular medicine 2014;18(10):2125-34.

211. Pinatel EM, Orso F, Penna E, Cimino D, Elia AR, Circosta P, et al. miR-223 Is a Coordinator of Breast Cancer Progression as Revealed by Bioinformatics Predictions. PLoS ONE 2014;9(1).

212. Tsitsiou E, Lindsay MA. microRNAs and the immune response. Current opinion in pharmacology 2009;9(4):514-20.

213. Chen Q, Wang H, Liu Y, Song Y, Lai L, Han Q, et al. Inducible microRNA-223 down-regulation promotes TLR-triggered IL-6 and IL-1beta production in macrophages by targeting STAT3. PLoS One 2012;7(8):e42971.

214. Ji H, Chen M, Greening DW, He W, Rai A, Zhang W, et al. Deep sequencing of RNA from three different extracellular vesicle (EV) subtypes released from the human LIM1863 colon cancer cell line uncovers distinct miRNA-enrichment signatures. 2014.

215. Wu C, Li M, Hu C, Duan H. Clinical significance of serum miR-223, miR-25 and miR-375 in patients with esophageal squamous cell carcinoma. Molecular biology reports 2014;41(3):1257-66.

216. Wang J-S, Wang F-B, Zhang Q-G, Shen Z-Z, Shao Z-M. Enhanced expression of Rab27A gene by breast cancer cells promoting invasiveness and the metastasis potential by secretion of insulin-like growth factor-II. Molecular Cancer Research 2008;6(3):372-82.

217. Wang Q, Ni Q, Wang X, Zhu H, Wang Z, Huang J. High expression of RAB27A and TP53 in pancreatic cancer predicts poor survival. Medical Oncology 2015;32(1):1-9.

218. Wang H, Zhao Y, Zhang C, Li M, Jiang C, Li Y. Rab27a was identified as a prognostic biomaker by mRNA profiling, correlated with malignant progression and subtype preference in gliomas. PLoS One 2014;9(2).

219. Yoshiba S, Ito D, Nagumo T, Shirota T, Hatori M, Shintani S. Hypoxia induces resistance to 5-fluorouracil in oral cancer cells via G 1 phase cell cycle arrest. Oral oncology 2009;45(2):109-15.

220. Sasabe E, Zhou X, Li D, Oku N, Yamamoto T, Osaki T. The involvement of hypoxia-inducible factor-1α in the susceptibility to γ-rays and chemotherapeutic drugs of oral squamous cell carcinoma cells. International Journal of Cancer 2007;120(2):268-77.

221. Soufla G, Sifakis S, Baritaki S, Zafiropoulos A, Koumantakis E, Spandidos DA. VEGF, FGF2, TGFB1 and TGFBR1 mRNA expression levels correlate with the malignant transformation of the uterine cervix. Cancer letters 2005;221(1):105-18.

222. Languino LR, Singh A, Prisco M, Inman GJ, Luginbuhl A, Curry JM, et al. Exosome-mediated transfer from the tumor microenvironment increases TGFβ signaling in squamous cell carcinoma. Am J Transl Res 2016;8(5):2432-37.

223. ten Dijke P, Arthur HM. Extracellular control of TGFβ signalling in vascular development and disease. Nature reviews Molecular cell biology 2007;8(11):857-69.

224. Pardali E, Goumans M-J, ten Dijke P. Signaling by members of the TGF-β family in vascular morphogenesis and disease. Trends Cell Biol 2010;20(9):556-67.

225. Liu Z, Kobayashi K, van Dinther M, van Heiningen SH, Valdimarsdottir G, van Laar T, et al. VEGF and inhibitors of TGFβ type-I receptor kinase synergistically promote blood-vessel formation by inducing α5-integrin expression. Journal of cell science 2009;122(18):3294-302.

226. Carmeliet P, Jain RK. Molecular mechanisms and clinical applications of angiogenesis. nature 2011;473(7347):298-307.

227. Bobrie A, Colombo M, Krumeich S, Raposo G, Théry C. Diverse subpopulations of vesicles secreted by different intracellular mechanisms are present in exosome preparations obtained by differential ultracentrifugation. Journal of extracellular vesicles 2012;1.

228. Peinado H, Alečković M, Lavotshkin S, Matei I, Costa-Silva B, Moreno-Bueno G, et al. Melanoma exosomes educate bone marrow progenitor cells toward a pro-metastatic phenotype through MET. Nature medicine 2012;18(6):883-91.

229. Hoshino A, Costa-Silva B, Shen T-L, Rodrigues G, Hashimoto A, Mark MT, et al. Tumour exosome integrins determine organotropic metastasis. nature 2015;527(7578):329-35.

230. Hou J, Meng F, Chan LW, Cho WC, Wong SC. Circulating Plasma MicroRNAs As Diagnostic Markers for NSCLC. Frontiers in Genetics 2016;7.

231. Fabbri M, Paone A, Calore F, Galli R, Gaudio E, Santhanam R, et al. MicroRNAs bind to Toll-like receptors to induce prometastatic inflammatory response. Proceedings of the National Academy of Sciences 2012;109(31):E2110-E16.

232. Baroni S, Romero-Cordoba S, Plantamura I, Dugo M, D'Ippolito E, Cataldo A, et al. Exosome-mediated delivery of miR-9 induces cancer-associated fibroblast-like properties in human breast fibroblasts. Cell Death & Disease 2016;7(7):e2312.

233. Zhang L, Zhang S, Yao J, Lowery FJ, Zhang Q, Huang W-C, et al. Microenvironment-induced PTEN loss by exosomal microRNA primes brain metastasis outgrowth. nature 2015;527(7576):100-04.

234. Shiga K, Hara M, Nagasaki T, Sato T, Takahashi H, Takeyama H. Cancer-associated fibroblasts: their characteristics and their roles in tumor growth. Cancers 2015;7(4):2443-58.

235. Kim W, Kim E, Lee S, Kim D, Chun J, Park KH, et al. TFAP2C-mediated upregulation of TGFBR1 promotes lung tumorigenesis and epithelial–mesenchymal transition. Experimental & Molecular Medicine 2016;48(11):e273.

236. Li H, Fan X, Houghton J. Tumor microenvironment: the role of the tumor stroma in cancer. Journal of cellular biochemistry 2007;101(4):805-15.

237. Laplante P, Raymond M-A, Gagnon G, Vigneault N, Sasseville AM-J, Langelier Y, et al. Novel fibrogenic pathways are activated in response to endothelial apoptosis: implications in the pathophysiology of systemic sclerosis. The Journal of Immunology 2005;174(9):5740-49.

238. Bhowmick NA, Chytil A, Plieth D, Gorska AE, Dumont N, Shappell S, et al. TGF-ß signaling in fibroblasts modulates the oncogenic potential of adjacent epithelia. Science 2004;303(5659):848-51.

239. Santibañez JF, Quintanilla M, Bernabeu C. TGF-β/TGF-β receptor system and its role in physiological and pathological conditions. Clinical science 2011;121(6):233-51.

240. Honjo Y, Bian Y, Kawakam K, Molinolo A, Longenecker G, Boppana R, et al. TGFβ Receptor I Conditional Knockout Mice Develop Spontaneous Squamous Cell Carcinoma. Cell Cycle 2007;6(11):1360-66.

241. Wang L-K, Hsiao T-H, Hong T-M, Chen H-Y, Kao S-H, Wang W-L, et al. MicroRNA-133a suppresses multiple oncogenic membrane receptors and cell invasion in non-small cell lung carcinoma. PLoS One 2014;9(5):e96765.

242. Zhao L, Sheldon K, Chen M, Yin MS, Hayman JA, Kalemkerian GP, et al. The predictive role of plasma TGF-β1 during radiation therapy for radiation-induced lung toxicity deserves further study in patients with non-small cell lung cancer. Lung Cancer 2008;59(2):232-39.

243. Xiao P, Liu W-L. MiR-142-3p functions as a potential tumor suppressor directly targeting HMGB1 in non-small-cell lung carcinoma. International journal of clinical and experimental pathology 2015;8(9):10800.

244. Kaduthanam S, Gade S, Meister M, Brase JC, Johannes M, Dienemann H, et al. Serum miR-142-3p is associated with early relapse in operable lung adenocarcinoma patients. Lung Cancer 2013;80(2):223-27.

245. Swinson DE, Jones JL, Richardson D, Cox G, Edwards JG, O'Byrne KJ. Tumour necrosis is an independent prognostic marker in non-small cell lung cancer: correlation with biological variables. Lung Cancer 2002;37(3):235-40.

246. Matsuyama W, Hashiguchi T, Mizoguchi A, Iwami F, Kawabata M, Arimura K, et al. Serum levels of vascular endothelial growth factor dependent on the stage progression of lung cancer. CHEST Journal 2000;118(4):948-51.

247. Macchiarini P, Fontanini G, Squartini F, Angeletti C, Hardin M. Relation of neovascularisation to metastasis of non-small-cell lung cancer. The Lancet 1992;340(8812):145-46.

248. Yano T, Tanikawa S, Fujie T, Masutani M, Horie T. Vascular endothelial growth factor expression and neovascularisation in non-small cell lung cancer. European Journal of Cancer 2000;36(5):601-09.

249. Bremnes RM, Camps C, Sirera R. Angiogenesis in non-small cell lung cancer: the prognostic impact of neoangiogenesis and the cytokines VEGF and bFGF in tumours and blood. Lung Cancer 2006;51(2):143-58.

250. Offersen BV, Pfeiffer P, Hamilton-Dutoit S, Overgaard J. Patterns of angiogenesis in nonsmall-cell lung carcinoma. Cancer 2001;91(8):1500-09.

251. Reck M, von Pawel J, Zatloukal P, Ramlau R, Gorbounova V, Hirsh V, et al. Phase III trial of cisplatin plus gemcitabine with either placebo or bevacizumab as first-line therapy

for nonsquamous non–small-cell lung cancer: AVAiL. Journal of Clinical Oncology 2009;27(8):1227-34.

252. Speight PM. Update on oral epithelial dysplasia and progression to cancer. Head and neck pathology 2007;1(1):61-66.

253. Sakpal TV. Sample size estimation in clinical trial. Perspectives in clinical research 2010;1(2):67.

254. Glaziou P. Sampsize calculator. SourceForgeNet 2005.

255. Miller AB, Wall C, Baines CJ, Sun P, To T, Narod SA. Twenty five year follow-up for breast cancer incidence and mortality of the Canadian National Breast Screening Study: randomised screening trial. 2014.

Appendix A

Table A.1 Genes that show 2-fold difference in expression between immortalized and non-immortalized lines.

Genes Up-regulated in Immortalized Cell lines	Genes Down-regulated in Immortalized Cell lines
ARHGAP11A	ABCC13
ARNTL2	APOF
ARPP-19	C10orf10
ASCC3	C10orf136
ASPM	C4orf18
ATF3	C8orf17
B2M	CBR4
BIRC5	CXCL14
BRCA1	DCC
BUB1	ELAVL4
BXDC1	EPN3
BXDC2	FBXO32
C1orf112	FN1
C1orf163	FTMT
C20orf199	GPR98
C6orf159	HERC3
C6orf173	HES1
CCNB1	IQUB
CCNB2	KHDRBS2
CCT2	KNG1
CDC2	KRT15
CDCA2	KRT16
CDCA5	LOC284232
CEBPZ	LOC645904
CENPN	LOC647107
CEP55	LOC651721
CKLF	LRRC2
CKS1B	MN1
CKS2	NOTCH1
CSRP2	OR2H1
DEPDC1	OVOL1
DIAPH3	PCDHB19P
DNAJC9	PSG3
EPSTI1	RORC
FABP5	RPH3A
FANCD2	SDK2
FANCI	SEMG2
FBXO5	SP5
GGH	SYT16
Genes Up-regulated in	**Genes Down-regulated in**

Immortalized Cell lines	Immortalized Cell lines
GNL3	TAAR6
H2AFZ	TANC2
HAT1	TCF7L2
HIST2H2AC	TGFB2
HMGCS1	THSD7A
HSP90AA1	TMEM26
IFIT2	TNFAIP8L3
KIAA0101	TNFRSF19
KRR1	TTTY11
LHX6	UBE2U
LSM3	ULK1
MCM10	UNC5B
MCM6	VIPR1
MCM8	WNT5A
MLF1IP	ZNF319
NCAPG	
NDC80	
NEFH	
NMI	
NT5C3	
NUDCD1	
OIP5	
PARP14	
PBK	
PMAIP1	
PRC1	
PTTG1	
RAB3B	
RACGAP1	
RCC1	
RNF138	
RPL39L	
RPS4Y1	
RPS4Y2	
SFRS3	
SFRS7	
SHCBP1	
SMC4	
SNRPD1	
TDG	
TIMELESS	

Genes Up-regulated in	Genes Down-regulated in

Immortalized Cell lines	Immortalized Cell lines
TIPIN	
TK1	
TNFRSF8	
TTK	
TWISTNB	
UBE2T	
VRK1	
ZNF121	
ZNF708	
ZWINT	

Table A.2 Genomic gains and losses in the 8 tested cell lines.

Cell Line	Gain/ Loss	Chromosome	First Clone	First Base Pair	Last Clone	Last Base Pair
OKF6	GAIN	2	N0111B23	54,135,756	N0254O14	54,360,912
TERT2	LOSS	2	F0598F07	89,558,527	N0168J01	91,694,559
	GAIN	3	N0489M05	112,460,495	N0795F24	113,210,064
	LOSS	4	N0749B10	48,910,988	N0604G23	52,788,367
	GAIN	5	N0262P03	130,350,388	N0182E22	180,844,590
	LOSS	8	N0509F16	86,213,371	M2067O20	86,655,436
	LOSS	9	N0104D19	42,297,099	N0211E19	64,605,023
	LOSS	14	N0284A08	104,335,297	M2011A05	105,202,688
	LOSS	15	N0207G06	18,268,506	N0644M04	18,539,773
	LOSS	21	N0777J19	37,639,783	N0457P07	46,959,990
POE9n	LOSS	1	N0069P10	140,919,966	N0464H08	142,002,328
TERT	GAIN	2	N0438O12	120,819,666	N0598J08	121,824,272
	GAIN	8	N0509F16	86,213,371	N0050N04	86,545,470
	LOSS	9	N0113D07	506,206	N0020A20	24,625,768
	GAIN	9	N0088I18	64,543,669	N0035I18	134,368,271
	GAIN	10	N0140A10	133,798,920	N0106C07	135,345,809
	GAIN	15	N0644M04	18,349,327	N0603B24	19,964,521
	GAIN	19	M2509P17	8,397,601	N0014H08	8,769,001
	GAIN	20	N0103O09	45,038,571	N0552L23	45,928,807
OKP7	GAIN	1	N0376P08	29,473,834	N0638H12	30,092,544
bmi1	GAIN	1	N0010P20	119,021,392	N0754O09	119,798,563
TERT	GAIN	5	N0434D20	69,116,796	N0350A19	71,005,823
	LOSS	12	N0607F06	66,751,757	N0528M24	67,158,273
	GAIN	15	N0494O02	29,870,754	M2205B01	30,593,680
	GAIN	16	N0432C09	28,160,013	N0264B17	29,027,705
OKF4	GAIN	3	N0775L22	159,424,706	N0230B20	159,971,533
TERT	GAIN	4	N0756P18	133,963,367	N0348O12	134,651,835
	GAIN	5		Whole Chromosome		
	GAIN	6	N0421D20	100,574,264	N0641G10	101,265,454
	GAIN	7	N0030C10	16,380,007	N0594C23	17,193,701
	GAIN	7	N0193J02	25,480,612	N0216K12	25,978,905
	GAIN	8	N0651O22	42,650,430	N0691F16	46,731,375
	GAIN	11	F0586N11	10,504,905	M2107O23	10,824,435
	GAIN	13	N0113B23	87,267,747	N0160C14	88,049,817
	GAIN	15	N0494O02	29,870,754	N0732H03	30,389,184
	GAIN	15	F0529J15	39,512,578	M2295I07	40,401,165
	LOSS	19	N0282G19	8,649,994	N0203K06	8,817,056

Cell Line	Gain/ Loss	Chromosome	First Clone	First Base Pair	Last Clone	Last Base Pair
OKF6	LOSS	2	F0598F07	89,558,527	N0168J01	91,694,559
E6E7	LOSS	4	N0749B10	48,910,988	N0604G23	52,788,367
	GAIN	5		Whole q arm		
	LOSS	7	N0155G14	127,510,471	N0683N08	127,852,019
	LOSS	8	N0509F16	86,213,371	M2067O20	86,655,436
	LOSS	9	N0104D19	42,297,099	N0211E19	64,605,023
	LOSS	15	N0207G06	18,268,506	N0644M04	18,539,773
	LOSS	15	N0354M13	89,279,290	N0450F18	90,708,919
	LOSS	21	N0777J19	37,639,783	N0457P07	46,959,990
DOK	LOSS	1	M2025H04	118,986,907	N0464H08	142,002,328
	LOSS	1	N0115G11	145,225,900	N0338I16	146,530,015
	LOSS	2	N0433P11	88,871,537	N0168J01	91,694,559
	LOSS	3	N0473O09	74,851,892	N0666K17	75,702,371
	LOSS	4	N0193D10	9,058,652	N0640C20	9,921,137
	LOSS	4	N0620D19	48,915,531	N0047D08	52,908,129
	LOSS	4	N0321G19	191,015,114	M2011O21	191,485,234
	LOSS	6	N0788K02	160,352,109	N0090D23	161,084,214
	LOSS	7	N0009F15	0	M2036F06	258,633
	LOSS	8	F0586C17	110,607	N0404N21	1,763,129
	LOSS	8	N0447A06	7,080,263	N0556O05	8,046,057
	LOSS	8	N0743F19	11,862,350	N0683E21	12,461,849
	LOSS	8	N0509F16	86,213,371	M2067O20	86,655,436
	GAIN	9	N0390F02	34,968,240	N0312A20	36,033,506
	LOSS	9	N0614D12	42,728,872	N0211E19	64,605,023
	LOSS	9	N0242L09	70,187,367	N0488P04	70,537,808
	LOSS	11	N0306J02	67,708,597	N0134F13	68,068,197
	LOSS	12	N0500M09	8,079,853	N0215F23	9,448,272
	GAIN	12	N0039O12	107,928,324	N0027M06	108,409,469
	LOSS	15	N0207G06	18,268,506	N0644M04	18,539,773
	LOSS	18	N0713D15	14,121,673	N0223M07	15,294,624
	LOSS	19	N0282G19	8,649,994	N0203K06	8,817,056
	LOSS	19	N0653D16	47,768,276	N0160A19	48,610,383
	GAIN	20		Whole Chromosome		
OKF4	GAIN	1	N0580L22	141,733,089	N0649M01	143,178,669
E6E7	GAIN	16	N0242N20	51,259,884	N0802E09	52,260,176
OKF6	LOSS	3	N0075E19	44,512,112	N0219A11	44,991,832
TERT1	LOSS	4	N0011A02	39,342,966	N0395I06	40,124,840
	GAIN	5		Whole Chromosome		
	LOSS	6	N0667J10	14,956,946	M2155H10	15,323,835
	LOSS	10	N0155A04	74,218,648	N0429F01	74,871,237
	GAIN	11	N0328D19	60,756,022	N0724D01	61,762,444
	GAIN	14	N0166L02	20,965,676	N0310A23	21,256,288

Cell Line	Gain/ Loss	Chromosome	First Clone	First Base Pair	Last Clone	Last Base Pair
OKF6	GAIN	15	F0529J15	39,512,578	N0383M08	40,144,104
TERT1	GAIN	15	N0731O08	65,941,593	N0096C21	68,440,572
	LOSS	17	N0113K01	57,071,847	N0302J21	57,611,053
	LOSS	19	N0282G19	8,649,994	N0478A23	9,010,779

Genomic locations are relative to GRCh37/hg19, the 2009 assembly of the human genome
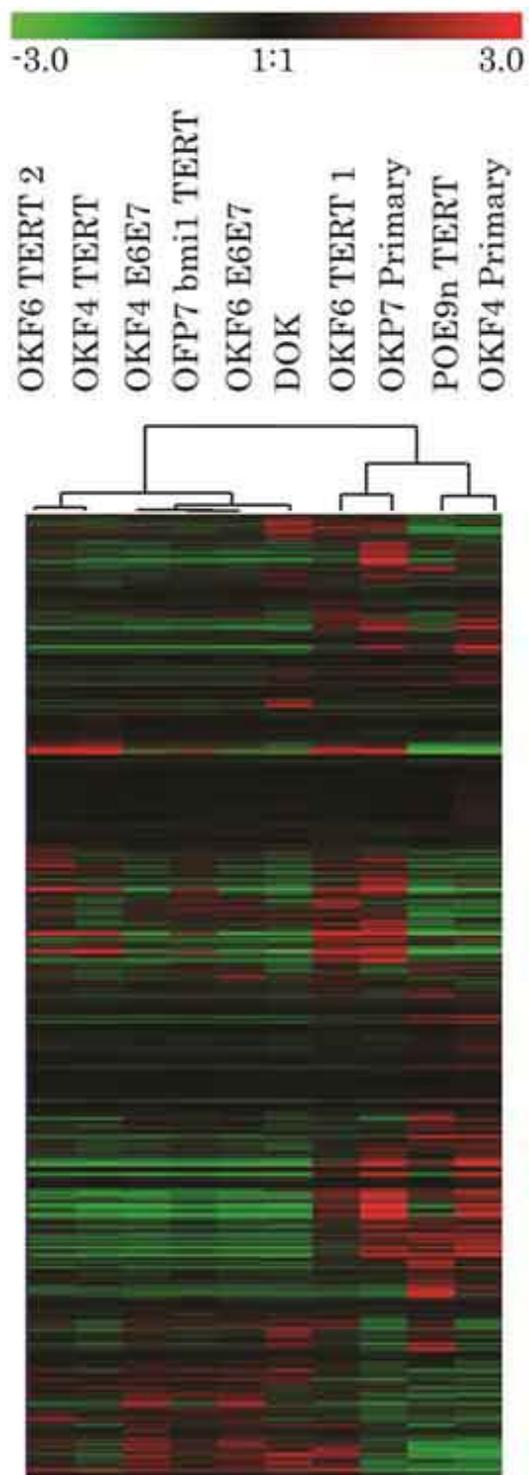
Figure A.1 Heat map for mRNA expression. The figure was created using the data for the 40 999 mRNAs that were expressed in at least 8 of the 10 cell lines tested.
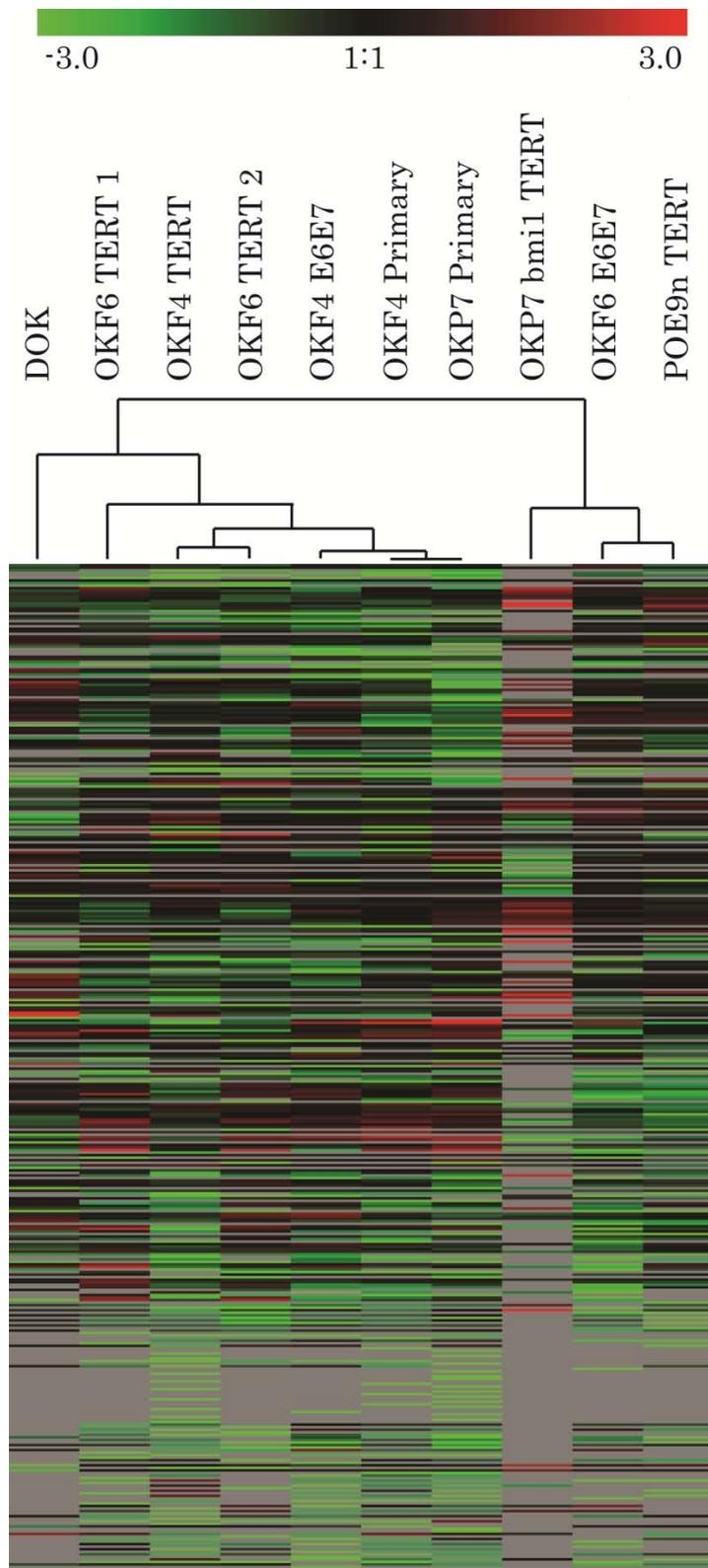
Figure A.2 Heat map for miRNA expression. The figure was created using the 396 miRNAs expressed in at least one sample.
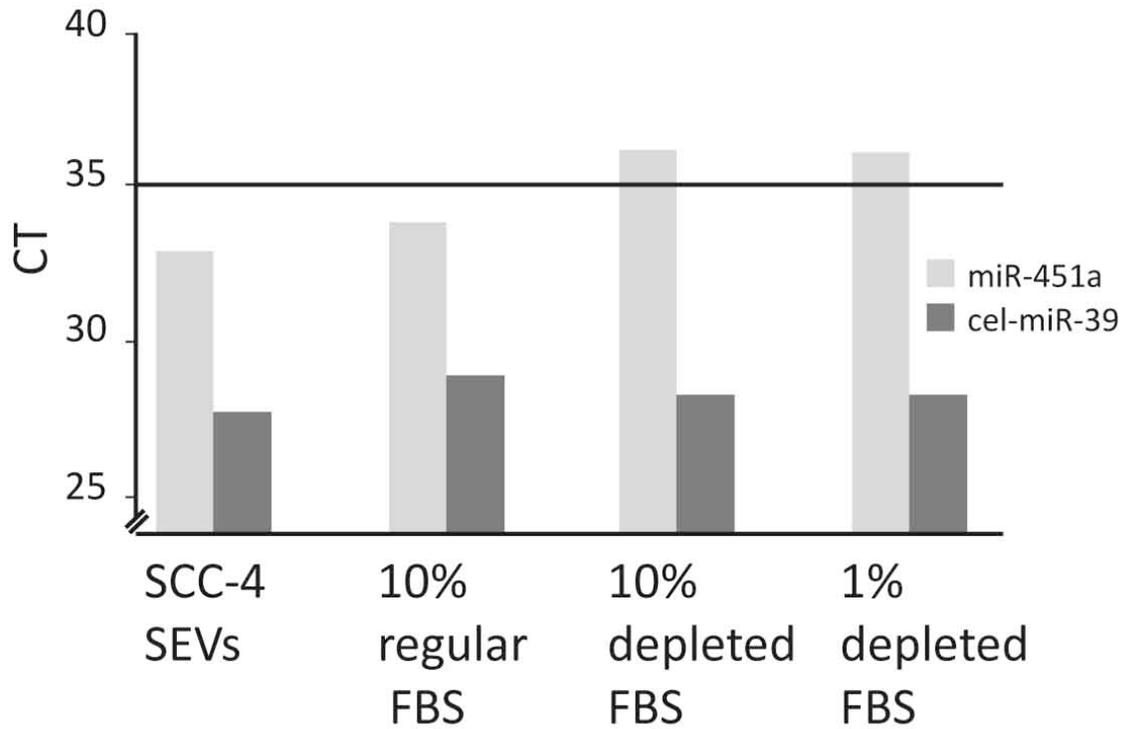
Figure A.3 Effects of SEV depletion of FBS. qRT-PCR results of RNA isolated from SCC-4 SEVs and blank media supplemented with 10% regular FBS, 10% depleted FBS or 1% depleted FBS. MiR-451a was tested along with the spike in cel-miR-39. The black bar represents the threshold of detection above which there may be no template control amplification. Equal volumes of miRNA were run using TaqMan qRT-PCR.
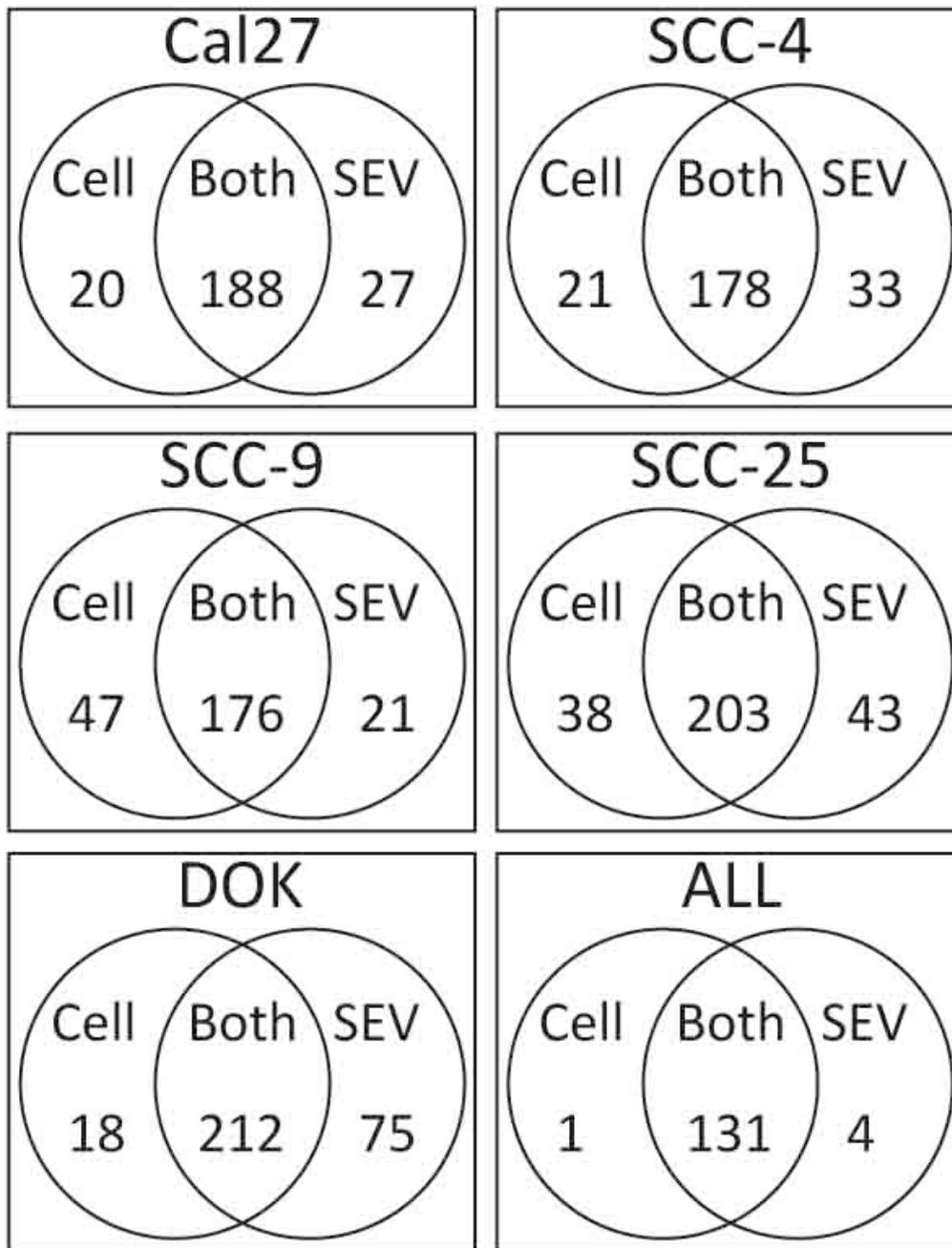
Figure A.4 Venn diagrams showing the number of miRNAs detected below a CT of 35, for each cell line by qRT-PCR, and the fraction in which the miRNAs were detected.
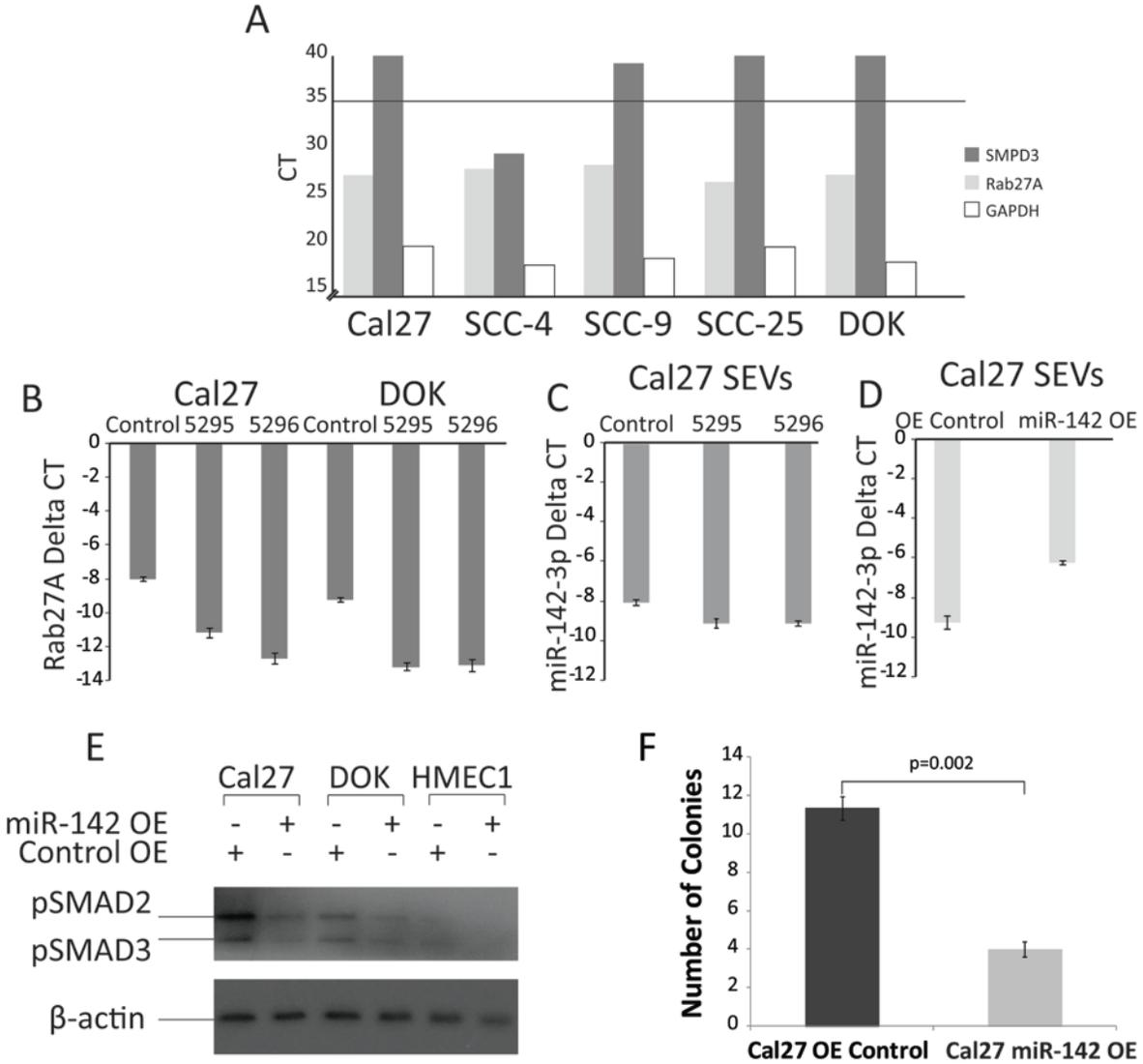
Figure A.5 Analysis of knockdown and over-expression cell lines. A: shows qRT-PCR CT values of the endogenous quantities of the SMPD3 and Rab27A, The black line represents our threshold of detection above which there may be amplification in no template controls. B: shows the knockdown efficiency of Rab27A shRNAs in Cal27 and DOK. GAPDH was used to normalize C: The amount of miR-142-3p secreted from the cells after SEV release was inhibited by Rab27A, Equal volumes of RNA were loaded and normalized to cel-miR-39 spike-in. D: shows the amount of miR-142-3p over-expression after lenti-infection in the SEVs collected from Cal27 cells. Spike-in cel-miR-39 was used to normalize. E: Western blot of pSMAD2/3 on cell lines with miR-142-3p over-expression. F: Colony formation assay on Cal27 OE Control and Cal27 miR-142 OE cells. P values were calculated using Student's t-test. All error bars represent the standard deviation over three replicates.